FERMION MASSES AND NEW SYMMETRIES BEYOND THE STANDARD MODEL

By

BENJAMIN NATHANIAL GROSSMANN

Bachelor of Science in Physics
Montana State University
Bozeman, Montana, USA
2003

Submitted to the Faculty of the
Graduate College of
Oklahoma State University
in partial fulfillment of
the requirements for
the Degree of
DOCTOR OF PHILOSOPHY
December, 2010

FERMION MASSES AND NEW SYMMETRIES BEYOND THE STANDARD MODEL

Dissertation Approved:

Dr. Satyanarayan Nandi

Dissertation Advisor

Dr. Kaladi S. Babu

Dr. Birne Binegar

Dr. Jacques H. H. Perk

Dr. Mark E. Payton

Dean of the Graduate College

ACKNOWLEDGMENTS

I extend my sincere appreciation to my advisor Dr. S. Nandi for his enthusiasm, guidance, and putting up with me after all these years.

Also, I want to thank him, along with my collaborators Z. Murdock, S. K. Rai, and B. McElrath for their contributions to our work, especially their efforts in calculating values related to various decays and backgounds.

I appreciate the willingness of my committee members—K. S. Babu, B. Binegar, and J. H. H. Perk—to take time out of their busy schedules.

I'd also like to thank the Oklahoma State University Physics Department and the United States Department of Energy for providing part of my financial support over the past years.

TABLE OF CONTENTS

LIST OF TABLES

LIST OF FIGURES

CHAPTER 1

INTRODUCTION

Modern physics categorizes all physical interaction into four fundamental forces: the strong force among the quarks and gluons; the weak force among the quarks, leptons, and weak gauge bosons; electromagnetism; and gravitation. All of these forces except gravitation have been gathered together into a theory known as the Standard Model of particle physics, and it has been remarkably successful.

1.1 Review of the Standard Model

The Standard Model (SM) is a local gauge theory that uses representations and interactions of fields allowed by the direct product group

$$SU(3)_C \times SU(2)_L \times U(1)_Y. \tag{1.1}$$

The group $SU(3)_C$ describes the quantum chromodynamics of the strong force. The direct product group $SU(2)_L \times U(1)_Y$ describes the electroweak force, a unification of electromagnetism and the weak force. The electric charge Q_{EM} of each field is related by

$$Q_{\text{EM}} = I_3 + \tfrac{1}{2}Y, \tag{1.2}$$

where I_3 the third isospin generator from $SU(2)_L$, and Y is the hypercharge of the field under $U(1)_Y$.

As a gauge invariant theory, the SM requires the Lagrangian to be unchanged when a gauge transformation occurs. The transformation under a gauge group can

Table 1.1: Charge assignments of the SM fields, grouped according to spin. The superscript i is the generation index for the fermions. Indices over the gauge groups are suppressed.

Spin $\frac{1}{2}$	$SU(3)_C$	$SU(2)_L$	$U(1)_Y$	Spin 1	$SU(3)_C$	$SU(2)_L$	$U(1)_Y$
q_L^i	3	2	$\frac{1}{3}$	G_μ	8	1	0
u_R^i	3	1	$\frac{4}{3}$	W_μ	1	3	0
d_R^i	3	1	$-\frac{2}{3}$	B_μ	1	1	0
l_L^i	1	2	-1	Spin 0			
e_R^i	1	1	-2	H	1	2	1

be described by the unitary matrix $V = \exp(-i\theta^a T_a)$, where each θ^a is a spacetime dependent parameter, and each T_a is a hermitian generator of the gauge group. The generators also depend on the representation of the field being transformed; thus V is also representation dependent. In general, the transformation rules for fermions ψ and scalar bosons ϕ belonging to the fundamental representation of a group, and the vector bosons A_μ belonging to the adjoint representation of a group are

$$\psi \mapsto V\psi, \qquad \phi \mapsto V\phi, \qquad A_\mu \mapsto VA_\mu V^\dagger - \frac{i}{g}(\partial_\mu V)V^\dagger. \tag{1.3}$$

where $A_\mu = T_a A_\mu^a$ and g is the gauge coupling of the group. The transformation matrix is equivalent to the identity, $V = I$, for the fields belonging to the singlet representation of a group. The Lagrangian contains products of these fields, along with the covariant derivative

$$\mathcal{D}_\mu = \partial_\mu - igA_\mu, \tag{1.4}$$

such that after a transformation, none of the transformation matrices remain, and the result is the same as the original Lagrangian.

The representations of the elementary fields of the SM shown in Table 1.1. Their

allowed interactions are determined by these representations. A very important (and surprising) feature is that the left and right chiral components of the fermions belong to different representations of the weak group $SU(2)_L$. The left chiral fields are doublets under $SU(2)_L$,

$$q_L^i = \begin{pmatrix} u_L^i \\ d_L^i \end{pmatrix}, \qquad\qquad l_L^i = \begin{pmatrix} \nu_L^i \\ e_L^i \end{pmatrix}, \tag{1.5}$$

while the right chiral fields are singlets.

One important aspect of this distinction between left and right components is the prevention of the Lagrangian from containing an explicit mass term for the fermions. A generic mass term for a fermion ψ would be

$$m\overline{\psi}\psi = m(\overline{\psi_L}\psi_R + \overline{\psi_R}\psi_L). \tag{1.6}$$

However, when a gauge transformation is applied:

$$m(\overline{\psi_L}\psi_R + \overline{\psi_R}\psi_L) \mapsto m(\overline{\psi_L}V_L^\dagger V_R\psi_R + \overline{\psi_R}V_R^\dagger V_L\psi_L). \tag{1.7}$$

In any model where the left and right components are in different representations, $V_L^\dagger V_R \neq I$. Thus the Lagrangian cannot contain any of these explicit fermion mass terms if it is to be gauge invariant.

Mass terms for gauge bosons also have problems appearing in the Lagrangian. An explicit mass term for the gauge bosons would appear and transform as

$$\begin{aligned} \frac{m^2}{2}A^\mu A_\mu &\mapsto \frac{m^2}{2}\left(VA^\mu V^\dagger - \frac{i}{g}(\partial^\mu V)V^\dagger\right)\left(VA_\mu V^\dagger - \frac{i}{g}(\partial_\mu V)V^\dagger\right) \\ &= \frac{m^2}{2}\left(VA^\mu A_\mu V^\dagger - \frac{i}{g}(\partial^\mu V)A_\mu V^\dagger + \frac{i}{g}VA^\mu(\partial_\mu V^\dagger) + \frac{1}{g^2}(\partial^\mu V)(\partial_\mu V^\dagger)\right). \end{aligned} \tag{1.8}$$

The form of the transformed term is not the same as the original, thus the gauge bosons also cannot have explicit mass terms in the Lagrangian. This isn't a problem for the massless photon and gluons, but the massive $W^\pm$ and Z need mass terms

to come from somewhere (historically, the prediction of massive gauge bosons came before their discovery, and is a consequence of the material covered in the next several paragraphs).

To get around this apparent lack of mass in the theory, the SM takes advantage of spontaneous symmetry breaking with the Higgs mechanism. By introducing a complex spin zero field, the Higgs boson H, the Lagrangian can now contain a potential described by[1]

$$\mathcal{V}(H) = -\mu^2 H^\dagger H + \lambda (H^\dagger H)^2. \tag{1.9}$$

Although the Higgs boson has transformation properties similar to the fermions (Eq. 1.3), it's not plagued by the problem of left and right chiral fields.

$$\begin{aligned} -\mu^2 H^\dagger H + \lambda (H^\dagger H)^2 &\mapsto -\mu^2 H^\dagger V^\dagger V H + \lambda (H^\dagger V^\dagger V H)^2 \\ &= -\mu^2 H^\dagger H + \lambda (H^\dagger H)^2. \end{aligned} \tag{1.10}$$

The potential must be bounded from below ($\lambda > 0$). When $\mu^2 < 0$, then it has a minimum at the origin. However, if $\mu^2 > 0$, then it has minima at

$$\langle H \rangle = \pm \sqrt{\frac{\mu^2}{2\lambda}} = \pm \frac{v}{\sqrt{2}}, \tag{1.11}$$

where v is called the vacuum expectation value (vev).

The Higgs field can then be shifted to a minimum of the potential. In the unitary gauge, this is expressed in terms of the real field h_0.

$$H = \begin{pmatrix} H^+ \\ H_0 \end{pmatrix} \mapsto \frac{1}{\sqrt{2}} \begin{pmatrix} 0 \\ h_0 + v \end{pmatrix}. \tag{1.12}$$

The shifted Higgs field can then be used in the kinetic terms of the Higgs field.

$$|\mathcal{D}_\mu H|^2 = \left| (\partial_\mu - igW_\mu - ig' \frac{1}{2} B_\mu) H \right|^2. \tag{1.13}$$

[1]Many texts reverse the sign on the quadratic term so $\mathcal{V}(H) = \mu^2 H^\dagger H + \lambda (H^\dagger H)^2$. This will reverse the inequalities for μ^2 for determining the minima of the potential.

Expanding this out, mass terms for the $W^{\pm}$, Z, and photon yield

$$m_W = \frac{gv}{2}, \qquad m_Z = \frac{v\sqrt{g^2+g'^2}}{2} = \frac{m_W}{\cos\theta_W}, \qquad m_A = 0, \tag{1.14}$$

where Z_μ and A_μ are the mass eigenstates of W^3_μ and B_μ, and the mixing angle between them is related to the gauge couplings by $\tan\theta_W = g'/g$. The symmetry under which all the gauge bosons are massless has been broken by the Higgs mechanism. In terms of the symmetry groups,

$$SU(2)_L \times U(1)_Y \xrightarrow{\text{broken to}} U(1)_{\text{EM}}. \tag{1.15}$$

The photon is the gauge boson of the leftover electromagnetic symmetry $U(1)_{\text{EM}}$.

Although explicit mass terms for fermions cannot be written down, interactions between fermions and a Higgs boson can be written down. Since the Higgs boson and the left-chiral fermions of the SM are all doublets under $SU(2)_L$, they have the same transformation properties. In contrast, the right-chiral singlets have an identity transformation. The gauge invariance for these types of fields under $SU(2)_L$ can easily be shown by

$$f\overline{\psi_L}H\psi_R \mapsto f\overline{\psi_L}V_L^\dagger V_L H\psi_R = f\overline{\psi_L}H\psi_R, \tag{1.16}$$

where f is the dimensionless Yukawa coupling. The product of the doublets should be worked out and the vev of the Higgs boson taken into account. For the Higgs-lepton couplings in the SM, it is

$$\begin{aligned} f^e_{ij}\overline{l^i_L}He^j_R &= f^e_{ij}\begin{pmatrix}\overline{\nu^i_L} & \overline{e^i_L}\end{pmatrix}\begin{pmatrix}0\\ \frac{1}{\sqrt{2}}(h_0+v)\end{pmatrix}e^j_R = \frac{f^e_{ij}}{\sqrt{2}}\overline{e^i_L}\,(h_0+v)\,e^j_R \\ &= \frac{f^e_{ij}}{\sqrt{2}}\overline{e^i_L}e^j_R h_0 + \frac{f^e_{ij}v}{\sqrt{2}}\overline{e^i_L}e^j_R, \end{aligned} \tag{1.17}$$

where i, j are the generation indices. The first term describes the coupling of the Higgs boson with the charged leptons. The last term has the form of a mass term, with a mass $f^e_{ij}v/\sqrt{2}$.

Specifically, the SM Yukawa terms in the Lagrangian are

$$f^u_{ij}\overline{q^i_L}\widetilde{H}u^j_R + f^d_{ij}\overline{q^i_L}Hd^j_R + f^e_{ij}\overline{l^i_L}He^j_R + h.c., \tag{1.18}$$

where $\widetilde{H} = i\sigma_2 H^*$, and $\sigma_2 = \left(\begin{smallmatrix} 0 & -i \\ i & 0 \end{smallmatrix}\right)$, the second Pauli matrix. From this, the mass matrices spanning the generations of the SM are

$$M^u_{ij} = f^u_{ij}\frac{v}{\sqrt{2}}, \qquad M^d_{ij} = f^d_{ij}\frac{v}{\sqrt{2}}, \qquad M^e_{ij} = f^e_{ij}\frac{v}{\sqrt{2}}. \tag{1.19}$$

Noticeably, Eq. 1.19 does not have a mass matrix for the neutrinos. In the SM, the neutrinos don't have right-handed components ν^i_R. Consequently, the neutrinos don't acquire masses from the Higgs Mechanism in the SM, and they remain massless.

1.2 Problems with fermion mass predictions

The mass relations from Eq. 1.14 were first published in late 1960s [1, 2]. More than a decade later, the W and Z bosons were discovered, and the relationships held. Once the gauge couplings and gauge boson masses are known, it is easy to determine $v/\sqrt{2} \simeq 174$ GeV. This is conveniently the same factor that relates the Yukawa matrices to the mass matrices in the SM.

This means in the diagonalized mass eigenbasis, the top quark (with a mass of 171.3 GeV) has a Yukawa coupling close to one. However, the up quark (2.33×10^{-3} GeV) has a Yukawa coupling five orders of magnitude smaller. In f^d_{ij} and f^e_{ij}, the range of orders of magnitudes is only marginally smaller. When all three matrices are taken as a whole, the Yukawa couplings span over five orders of magnitude.

Experimentally, the values of each Yukawa matrix (f^u_{ij}, f^d_{ij}, f^e_{ij}) can be found in the diagonalized mass basis. However, the three generations of fermions are not regulated by any known symmetry, so three mass eigenvalues are not enough to determine the nine Yukawa couplings within each matrix. With three matrices, this means there are 27 undetermined Yukawa couplings spanning five orders of magnitude. This wide range of so many parameters has no explanation in the SM.

In contrast to the seemingly arbitrary and unpredictable masses of the charged fermions, the SM requires all the neutrinos to be massless. However, experiments show evidence of neutrino flavor oscillations. These oscillations directly imply the neutrinos have tiny non-zero masses, contradicting the SM.

These issues are just a few among the list of shortcomings in the SM. Many models have been put forward in an attempt to explain, circumvent, or eliminate these problems. Some researchers have embedded the fields into larger symmetry groups that break down to the SM. Others have imposed additional symmetries onto the SM. In almost all cases, there are new and exotic fields. And they bring along new interactions that can yield physics that has the potential to be observed.

This dissertation will address the issues described above by using symmetries in addition to the SM. Even though the symmetry groups will be small, $U(1)$ and Z_2, these symmetries can easily be found in the literature and where they are used in a variety of ways. Frequently these symmetries, especially $U(1)$, are not imposed uniformly on the existing fields. Chapters 2–5 will examine the use of $U(1)$ symmetries and additional fields to address the issue of the quark mass hierarchy and Yukawa couplings in the SM. This will be contrasted in Chapters 6 and 7 where the effects of one of the additional fields will be examined. The issue of neutrino masses will be treated in Chapter 8 with a departure from the mechanism used for the charged fermion masses. A discrete Z_2 symmetry will be used instead of a $U(1)$ symmetry.

1.3 Note on the inclusion of published material

The contents of this dissertation were done as works of collaboration with other authors. These works have been published in a couple different journals.

Material from Chapters 3–5 was done in collaboration with Z. Murdock and S. Nandi and is expected to be submitted for publication in the near future [3].

The contents of Chapters 6 and 7 were done in collaboration with B. McElrath,

S. Nandi, and S. K. Rai and appears in *Physical Review D* [4].

Chapter 2 is material common to both of these works and has been expanded.

Chapter 8 covers material done in collaboration with Z. Murdock and S. Nandi and appears in *Physics Letters B* [5].

The publishers of both journals (APS for *Physical Review D* and Elsevier for *Physics Letters B*) hold the respective copyrights for the published articles. However, both journals state that a journal author retains the right to include his/her own articles, in whole or in part, within a thesis or dissertation without obtaining specific permission from the journal.

CHAPTER 2

THE HIGGS AND GAUGE BOSONS

2.1 The use of extra symmetries

The SM has withstood remarkable testing. No experiment has produced a result directly negating the SM. However, there still remains a number of shortcomings and curiosities. It is generally believed not to be a final and complete theory. There are many varied models proposed to extend the SM to solve and explain these noticeable features.

Attempts are made to incorporate gravity into a model of particle physics by considering compact extra dimensions in addition to the usual four spacetime dimensions [6, 7], or more recently by a gauge/gravity duality [8]. The three gauge couplings are similar when run up to a high energy scale ($\sim 10^{16}$ GeV), so Grand Unified Theories (GUTs) try to unify them into one coupling of a single group. The gauge hierarchy problem can be addressed by using Supersymmetry (SUSY) to extend the SM. Some SUSY models also provide candidates for the enigmatic dark matter, although there are contenders that rely on other mechanisms, such as adding an electroweak singlet Higgs boson with a Z_2 symmetry to the SM [9]. Even combining methods has been used, such as SUSY with extra dimensions to unify Higgs and gauge bosons to relate Yukawa couplings with the gauge couplings [10]. This is just a very short list of different approaches to extending the SM, but many extensions include extra particles and extra interactions related to a new symmetry group.

Many models with only an additional $U(1)$ symmetry have been considered. These include leptophobic models, hadrophobic models, a symmetry group only coupling

with third generation fermions, and extra symmetries to address the issue of anomalous magnetic moments [11]. Other models attempt to embed the SM into larger symmetry groups and lead to an extra $U(1)$ when they are broken down to the SM. Some of these attempts have lead to using $SO(10)$ or E_6 GUTs, superstring E_6 [12, 13], top-flavor models [14, 15, 16], and Left-Right symmetry models [17], and string-inspired supersymmetric models [18].

By whichever means a $U(1)$ symmetry enters these models, some care has to be taken so the new fields don't push theoretical predictions of the known fields outside the bounds of established experimental certainty. Two methods of doing this are relatively straightforward. If the new fields are charged under the SM, then they should be more massive than the SM fields. Otherwise, the new fields need to be neutral under the SM gauge symmetry, and the SM fields need to be neutral under the new symmetry group. In either case there would necessarily need to be new "intermediate" fields in this model to communicate to the SM fields the presence of this hidden $U(1)$ sector.

A hidden symmetry sector can provide some tools to explain the smallness and hierarchy of the Yukawa couplings in the SM.

One possible approach, using radiative corrections, uses scalar leptoquarks at the TeV mass scale and has them couple with the top quark and the SM leptons. A hierarchy of fermion masses are then related to powers of a loop factor when calculating radiative corrections [19, 20, 21, 22].

Another approach is to use higher dimensional operators of Higgs bosons that yield the effective four dimensional couplings of the SM [23, 24, 25]. In turn, these higher dimensional operators can themselves be effective operators from a symmetry sector at a high energy scale by using a Froggatt-Nielsen [26] type mechanism. This can be done whether the higher dimensional operators are built from the Higgs doublet of the SM, or if new Higgs bosons are added to the model.

The work done in Ref. [25] can be expanded and generalized to an entire class of models that also encompasses the work done in Refs. [23, 24]. The different models all have similarities, yet can be grouped by some distinguishing differences. Although the generalization is only performed on the quark sector, the charged lepton sector can be treated in a similar fashion.

The generalization of Ref. [25] continues to use a new SM single Higgs boson S and an accompanying local extra symmetry. The new local gauge symmetry is

$$SU(3)_C \times SU(2)_L \times U(1)_Y \times U(1)_S. \tag{2.1}$$

The new Higgs boson S is completely neutral under the SM; it is a colorless electroweak singlet. However, it is charged under the new local symmetry $U(1)_S$. The SM particles are all neutral under this new symmetry. Before exploring the fermion sector under this new symmetry, the interactions of this new Higgs boson with the SM Higgs field is examined.

2.2 The Higgs potential

As a Higgs boson, the S can contribute to the Higgs potential. The potential already has two terms coming from the Higgs doublet H. As a singlet, S cannot directly have a scalar product with the doublet. However, a quartic field coupling with a product of scalar products is allowed. The Higgs potential with H and S is

$$\begin{aligned}\mathcal{V}(H,S) = &-\mu_H^2(H^\dagger H) + \lambda_H(H^\dagger H)^2 \\ &- \mu_S^2(S^\dagger S) + \lambda_S(S^\dagger S)^2 \\ &+ \lambda_{HS}(H^\dagger H)(S^\dagger S).\end{aligned} \tag{2.2}$$

The parameters in the potential are assumed to have values such that both H and S have vevs in the electroweak (EW) scale. The complex fields H and S can be written

in terms of real fields h_0 and s_0 in the unitary gauge as

$$H \mapsto \frac{1}{\sqrt{2}} \begin{pmatrix} 0 \\ v_H + h_0 \end{pmatrix}, \qquad S \mapsto \frac{1}{\sqrt{2}} (v_S + s_0), \tag{2.3}$$

where v_H is the vev of H, and v_S is the vev of S. From the minimization of the Higgs potential, the parameters μ_H^2 and μ_S^2 can easily be expressible in terms of the vevs and the λ-parameters:

$$\mu_H^2 = v_H^2 \lambda_H + \frac{1}{2} v_S^2 \lambda_{HS}, \qquad \mu_S^2 = v_S^2 \lambda_S + \frac{1}{2} v_H^2 \lambda_{HS}. \tag{2.4}$$

If so inclined, expressions for the vevs can be obtained in terms of the parameters of the potential:

$$v_H^2 = \frac{\mu_H^2 - \frac{\lambda_{HS}}{2\lambda_S}\mu_S^2}{\lambda_H - \frac{\lambda_{HS}^2}{4\lambda_S}}, \qquad v_S^2 = \frac{\mu_S^2 - \frac{\lambda_{HS}}{2\lambda_H}\mu_H^2}{\lambda_S - \frac{\lambda_{HS}^2}{4\lambda_H}}. \tag{2.5}$$

After applying the unitary gauge of the Higgs fields and substituting the expressions for the μ^2 parameters, the potential can then be written into a manageable form, and separated by the powers of the Higgs fields with

$$\mathcal{V} = \mathcal{V}^{(0)} + \mathcal{V}^{(1)} + \mathcal{V}^{(2)} + \mathcal{V}^{(3)} + \mathcal{V}^{(4)}. \tag{2.6}$$

In the (h_0, s_0) basis, the terms of the potential are

$$\mathcal{V}^{(0)}(h_0, s_0) = -\frac{1}{4}\left(\lambda_H v_H^4 + \lambda_S v_S^4 + \lambda_{HS} v_H^2 v_S^2\right), \tag{2.7a}$$

$$\mathcal{V}^{(1)}(h_0, s_0) = 0, \tag{2.7b}$$

$$\mathcal{V}^{(2)}(h_0, s_0) = \lambda_H v_H^2 h_0^2 + \lambda_{HS} v_H v_S h_0 s_0 + \lambda_S v_S^2 s_0^2, \tag{2.7c}$$

$$\mathcal{V}^{(3)}(h_0, s_0) = \lambda_H v_H h_0^3 + \frac{1}{2}\lambda_{HS}(v_S h_0^2 s_0 + v_H h_0 s_0^2) + \lambda_S v_S s_0^3, \tag{2.7d}$$

$$\mathcal{V}^{(4)}(h_0, s_0) = \frac{1}{4}(\lambda_H h_0^4 + \lambda_{HS} h_0^2 s_0^2 + \lambda_S s_0^4). \tag{2.7e}$$

From $V^{(2)}(h_0, s_0)$, the mass-squared matrix of the Higgs fields in the (h_0, s_0) basis is found to be

$$\mathcal{M}^2_{h_0,s_0} = \begin{pmatrix} 2\lambda_H\, v_H^2 & \lambda_{HS}\, v_H\, v_S \\ \lambda_{HS}\, v_H\, v_S & 2\lambda_S\, v_S^2 \end{pmatrix}. \tag{2.8}$$

Since the matrix is not diagonal, the fields h_0 and s_0 cannot be mass eigenstates. To find the mass eigenstates, an orthogonal rotation can be performed. The fields in the mass eigenbasis are ϕ_H and ϕ_S and are related to the fields in the unitary gauge by

$$\begin{aligned} h_0 &= \phi_H \cos\vartheta + \phi_S \sin\vartheta, \\ s_0 &= -\phi_H \sin\vartheta + \phi_S \cos\vartheta. \end{aligned} \tag{2.9}$$

The rotation angle ϑ is given by

$$\tan 2\vartheta = \frac{\lambda_{HS} v_H v_S}{\lambda_S v_S^2 - \lambda_H v_H^2}, \tag{2.10a}$$

or, without the double angle, as

$$\tan\vartheta = \frac{\lambda_{HS} v_H v_S}{(\lambda_S v_S^2 - \lambda_H v_H^2) + \sqrt{(\lambda_S v_S^2 - \lambda_H v_H^2)^2 + \lambda_{HS}^2 v_H^2 v_S^2}} \,. \tag{2.10b}$$

The physical squared masses at the tree level are

$$m^2_{\phi_H,\phi_S} = \left(\lambda_S v_S^2 + \lambda_H v_H^2\right) \mp \sqrt{(\lambda_S v_S^2 - \lambda_H v_H^2)^2 + \lambda_{HS}^2 v_H^2 v_S^2} \,. \tag{2.11}$$

where ϕ_H is taken to be the lighter mass eigenstate, and ϕ_S is the heavier state. All these relationships can be used to rewrite the potential in terms of the physical Higgs fields. The terms that change are given by

$$\mathcal{V}^{(2)}(\phi_H, \phi_S) = m^2_{\phi_H}\phi_H^2 + m^2_{\phi_S}\phi_S^2, \tag{2.12a}$$

$$\begin{aligned} \mathcal{V}^{(3)}(\phi_H, \phi_S) = {} & \frac{1}{8}\phi_H^3 \left(v_H(6\lambda_H + \lambda_{HS})\cos\vartheta + v_H(2\lambda_H - \lambda_{HS})\cos 3\vartheta \right. \\ & \qquad \left. - v_S(\lambda_{HS} + 6\lambda_S)\sin\vartheta - v_S(\lambda_{HS} - 2\lambda_S)\sin 3\vartheta\right) \\ & + \frac{1}{8}\phi_H^2\phi_S \left(v_S(\lambda_{HS} + 6\lambda_S)\cos\vartheta + v_S(3\lambda_{HS} - 6\lambda_S)\cos 3\vartheta \right. \\ & \qquad \left. + v_H(6\lambda_H + \lambda_{HS})\sin\vartheta + v_H(6\lambda_H - 3\lambda_{HS})\sin 3\vartheta\right) \\ & + \frac{1}{8}\phi_H\phi_S^2 \left(v_H(6\lambda_H + \lambda_{HS})\cos\vartheta - v_H(6\lambda_H - 3\lambda_{HS})\cos 3\vartheta \right. \\ & \qquad \left. - v_S(\lambda_{HS} + 6\lambda_S)\sin\vartheta + v_S(3\lambda_{HS} - 6\lambda_S)\sin 3\vartheta\right) \\ & + \frac{1}{8}\phi_S^3 \left(v_S(\lambda_{HS} + 6\lambda_S)\cos\vartheta - v_S(\lambda_{HS} - 2\lambda_S)\cos 3\vartheta \right. \\ & \qquad \left. + v_H(6\lambda_H + \lambda_{HS})\sin\vartheta - v_H(2\lambda_H - \lambda_{HS})\sin 3\vartheta\right), \end{aligned} \tag{2.12b}$$

$$
\begin{aligned}
\mathcal{V}^{(4)}(\phi_H,\phi_S) = &\frac{1}{4}\phi_H^4\left(\lambda_H\cos^4\vartheta + \lambda_{HS}\cos^2\vartheta\sin^2\vartheta + \lambda_S\sin^4\vartheta\right)\\
&+\frac{1}{4}\phi_H^3\phi_S\left(\lambda_H - \lambda_S + (\lambda_H - \lambda_{HS} + \lambda_S)\cos 2\vartheta\right)\sin 2\vartheta\\
&+\frac{1}{16}\phi_H^2\phi_S^2\left(3\lambda_H + \lambda_{HS} + 3\lambda_S - 3(\lambda_H - \lambda_{HS} + \lambda_S)\cos 4\vartheta\right)\\
&+\frac{1}{4}\phi_H\phi_S^3\left(\lambda_H - \lambda_S - (\lambda_H - \lambda_{HS} + \lambda_S)\cos 2\vartheta\right)\sin 2\vartheta\\
&+\frac{1}{4}\phi_S^4\left(\lambda_S\cos^4\vartheta + \lambda_{HS}\cos^2\vartheta\sin^2\vartheta + \lambda_H\sin^4\vartheta\right).
\end{aligned}
\tag{2.12c}
$$

In these equations, the interaction of the two physical Higgs fields occurs in the cubic and quartic terms of the potential. The degree of interaction is regulated by λ_{HS} and ϑ (which is also regulated by λ_{HS}). If mixing is zero, then ϕ_H is exactly the same as in the SM.

2.3 Kinetic terms and gauge bosons

The Higgs fields also have kinetic terms. These terms provide mass to some of the gauge bosons when the electroweak symmetry is broken. The Higgs doublet H has the same terms as in the SM,

$$
\begin{aligned}
|\mathcal{D}_\mu H|^2 &= \left|(\partial_\mu - igW_\mu - ig'\frac{1}{2}B_\mu)H\right|^2\\
&\mapsto \frac{1}{2}\left|\partial_\mu h_0\right|^2 + \left(\frac{1}{8}\left|g'B_\mu - gW_\mu^3\right|^2 + \frac{1}{4}g^2W^{-\mu}W_\mu^+\right)(v_H + h_0)^2.
\end{aligned}
\tag{2.13}
$$

The mixing of the B_μ and W_μ^3 follows the standard procedure:

$$
\begin{aligned}
W_\mu^3 &= Z_\mu\cos\theta_W + A_\mu\sin\theta_W,\\
B_\mu &= -Z_\mu\sin\theta_W + A_\mu\cos\theta_W,
\end{aligned}
\tag{2.14}
$$

where the Weinberg angle θ_W is related to the gauge couplings by

$$
\cos\theta_W = \frac{g}{\sqrt{g^2+g'^2}}, \qquad \sin\theta_W = \frac{g'}{\sqrt{g^2+g'^2}}. \tag{2.15}
$$

The squared masses of the $W^\pm$, Z, and the photon are

$$
m_{W^\pm}^2 = \frac{g^2v_H^2}{4}, \qquad m_Z^2 = \frac{v_H^2}{4}(g^2+g'^2), \qquad m_A^2 = 0. \tag{2.16}
$$

This will effectively reduce Eq. (2.13) to

$$\begin{aligned}|\mathcal{D}_\mu H|^2 \mapsto \frac{1}{2}\left|\partial_\mu h_0\right|^2 + \frac{m_Z^2}{2} Z^\mu Z_\mu + m_{W^\pm}^2 W^{-\mu} W_\mu^+ \\ + \left(\frac{m_Z^2}{v_H} Z^\mu Z_\mu + 2\frac{m_{W^\pm}^2}{v_H} W^{-\mu} W_\mu^+\right) h_0 \\ + \left(\frac{m_Z^2}{2v_H^2} Z^\mu Z_\mu + \frac{m_{W^\pm}^2}{v_H^2} W^{-\mu} W_\mu^+\right) h_0^2.\end{aligned} \tag{2.17}$$

The new Higgs singlet S can be treated similarly. The S is charged under the extra $U(1)_S$ symmetry with a charge Y_S, so its covariant derivative contains the real field Z'_μ, the gauge field of the $U(1)_S$ symmetry. However, since S is a neutral singlet under the SM, it does not have any other gauge fields in its covariant derivative, thus

$$|\mathcal{D}_\mu S|^2 = \left|(\partial_\mu - i g_S \frac{1}{2} Y_S Z'_\mu) S\right|^2 \mapsto \frac{1}{2}\left|\partial_\mu s_0\right|^2 + \frac{g_S^2 Y_S^2}{8} Z'^\mu Z'_\mu (v_S^2 + 2 v_S s_0 + s_0^2). \tag{2.18}$$

The Z' gauge boson gets its mass from the pseudoscalar component of S when the $U(1)_S$ symmetry is broken. The mass of the Z' at tree level is

$$m_{Z'}^2 = \frac{g_S^2 Y_S^2 v_S^2}{4}. \tag{2.19}$$

The vev v_S is assumed to be on the order of the EW scale, similar to v_H. At this point, S is the only field charged under $U(1)_S$, so its charge can be normalized so that $Y_S = 1$ (effectively absorbing any deviation from 1 into g_S). If $g_S \sim \mathcal{O}(1)$, then the mass of the Z' should also be expected to be near the EW scale. However, since g_S isn't determined, the mass may be dramatically different.

In terms of the Z' mass, the kinetic term of the S is

$$|\mathcal{D}_\mu S|^2 \mapsto \frac{1}{2}\left|\partial_\mu s_0\right|^2 + \frac{m_{Z'}^2}{2} Z'^\mu Z'_\mu + \frac{m_{Z'}^2}{v_S} Z'^\mu Z'_\mu s_0 + \frac{m_{Z'}^2}{2v_S^2} Z'^\mu Z'_\mu s_0^2. \tag{2.20}$$

The kinetic terms in Eqs. (2.17) and (2.20) are in the gauge basis of the Higgs.

Rotating their sum into the mass physical basis yields

$$\begin{aligned}
|\mathcal{D}_\mu H|^2 + |\mathcal{D}_\mu S|^2 \mapsto & \frac{1}{2}\left|\partial_\mu \phi_H\right|^2 + \frac{1}{2}\left|\partial_\mu \phi_S\right|^2 \\
& + \frac{m_Z^2}{2} Z^\mu Z_\mu + m_{W^\pm}^2 W^{-\mu} W_\mu^+ + \frac{m_{Z'}^2}{2} Z'^\mu Z'_\mu \\
& + \left(\frac{m_Z^2}{v_H} Z^\mu Z_\mu + 2\frac{m_{W^\pm}^2}{v_H} W^{-\mu} W_\mu^+\right)(\phi_H \cos\vartheta + \phi_S \sin\vartheta) \\
& + \frac{m_{Z'}^2}{v_S} Z'^\mu Z'_\mu(-\phi_H \sin\vartheta + \phi_S \cos\vartheta) \\
& + \left(\frac{m_Z^2}{2v_H^2} Z^\mu Z_\mu + \frac{m_{W^\pm}^2}{v_H^2} W^{-\mu} W_\mu^+\right)(\phi_H \cos\vartheta + \phi_S \sin\vartheta)^2 \\
& + \frac{m_{Z'}^2}{2v_S^2} Z'^\mu Z'_\mu(-\phi_H \sin\vartheta + \phi_S \cos\vartheta)^2.
\end{aligned} \tag{2.21}$$

From this expression, the interactions of the ϕ_S with the SM gauge bosons can be picked out. The interactions, however, are suppressed by $\sin\vartheta$. Similarly, the ϕ_H has interactions with the Z' suppressed by $\sin\vartheta$. If the Higgs boson of the SM is found in the near future, but not a singlet Higgs or Z', this is suggestive of ϑ being very small or that S and Z' are very heavy. This is especially true for the Z' of this model.

Since the Z' does not couple to SM fields directly, its presence can only be determined from interactions with new fields and kinetic mixing with the Z. Kinetic mixing can occur through the term

$$\frac{\chi}{2g'g_S} F^{\mu\nu} F'_{\mu\nu} = \frac{\chi}{2g'g_S}\left(\partial^\mu B^\nu - \partial^\nu B^\mu\right)\left(\partial_\mu Z'_\nu - \partial_\nu Z'_\mu\right). \tag{2.22}$$

This is allowed because the gauge field B_μ, like the Z', is neutral under all the gauge groups of the SM, including the group it mediates, $U(1)_Y$. However, the coefficient χ can be small to suppress this effect. Mixing can also occur from higher order loop effects. Measurements of the Z properties at LEP1 constrain the mixing to be $\lesssim 10^{-3}$ [27, 28]. For the purposes of this dissertation, the kinetic mixing is assumed to be insignificant (i.e. $\chi = 0$).

CHAPTER 3

YUKAWA COUPLINGS OF THE CHARGED FERMIONS

The most massive elementary fermion in the SM is the top quark. In the SM, the top mass comes from the diagonalization of

$$M^u = f^u \frac{v}{\sqrt{2}}. \tag{3.1}$$

Using the values of the top mass and the vev of the Higgs, a quick estimate of f^u_{33} can be done:

$$\begin{aligned} m_t &\sim f^u_{33} \frac{v}{\sqrt{2}}, \\ (171 \text{ GeV}) &\sim f^u_{33} (174 \text{ GeV}). \end{aligned} \tag{3.2}$$

This shows $f^u_{33} \sim \mathcal{O}(1)$. Naïvely, all the other Yukawa couplings would be expected to be of similar magnitude. However, they are orders of magnitude smaller. The mechanism presented here will explain their smallness as effective Yukawa couplings.

First, the use of higher dimensional operators will be examined as a mechanism for generating the effective Yukawa coupling. Then in Chapter 4, the origins of these operators will be explored as extra symmetries are used to extend the SM to include exotic fields and interaction.

3.1 Operators with Higgs doublets: the $H^\dagger H$ model

The higher dimensional operators in the Yukawa couplings make the terms non-renormalizable. However, this is only an effective theory below a scale M, the mass scale where new vector-like quarks exist, and will be described in Chapter 4. The

operators in [23] rely on the SM Higgs doublet H, and are of the form

$$\left(\frac{H^\dagger H}{M^2}\right)^n y^u_{ij}\overline{q^i_L}u^j_R\widetilde{H}, \qquad\qquad \left(\frac{H^\dagger H}{M^2}\right)^n y^d_{ij}\overline{q^i_L}d^j_R H, \tag{3.3}$$

where $\widetilde{H} = i\sigma_2 H^*$. The exponent n is a non-negative integer that may have a different value for each pair of generation indices i, j (i.e. n is flavor dependent). The values of the coupling coefficients y^u, y^d are taken to be $\sim \mathcal{O}(1)$. The quark doublet q^i_L and quark singlets u^j_R, d^j_R are the SM quarks.

Since the Yukawa coupling $f^u_{33} \sim \mathcal{O}(1)$ in the SM, the exponent n is set to zero and the relevant term from Eq.(3.3) is

$$y^u_{33}\overline{q^3_L}u^3_R\widetilde{H}, \tag{3.4}$$

which corresponds directly with the SM. Thus the identification $f^u_{33} = y^u_{33}$ can be made right away. The remaining Yukawa couplings can be determined after the Higgs doublet H acquires a vev. The parametrization is the same as in Eq. (2.3). Substitution into the higher dimensional operators is straight forward, thus

$$\frac{(v_H + h_0)^{2n}}{2^n M^{2n}} y^u_{ij}\overline{u^i_L}u^j_R\frac{(v_H + h_0)}{\sqrt{2}}. \tag{3.5}$$

The mass terms and Yukawa terms can be picked out after performing a binomial expansion. The mass terms will have no Higgs field h_0, and the Yukawa terms will be linear in h_0. Examining only the binomials,

$$\begin{aligned}(v_H + h_0)^{2n}(v_H + h_0) &= (v_H^{2n} + 2nv_H^{2n-1}h_0 + \cdots)(v_H + h_0) \\ &= v_H^{2n+1} + (2n+1)v_H^{2n}h_0 + 2nv_H^{2n-1}h_0^2 + \cdots .\end{aligned} \tag{3.6}$$

The fieldless term from the expansion provides the mass terms of the form

$$M^u_{ij}\overline{u^i_L}u^j_R = \left(\frac{v_H^{2n}}{2^n M^{2n}} y^u_{ij}\frac{v_H}{\sqrt{2}}\right)\overline{u^i_L}u^j_R, \tag{3.7}$$

and the term linear in the field h_0 yields the Yukawa couplings of the form

$$f^u_{ij}\overline{u^i_L}u^j_R\frac{h_0}{\sqrt{2}} = \left((2n+1)\frac{v_H^{2n}}{2^n M^{2n}} y^u_{ij}\right)\overline{u^i_L}u^j_R\frac{h_0}{\sqrt{2}}. \tag{3.8}$$

These can be reduced to a less cumbersome expression by introducing a dimensionless parameter ϵ so that

$$\epsilon = \frac{v_H}{M\sqrt{2}}, \tag{3.9}$$

$$M^u_{ij} = \epsilon^{2n} y^u_{ij} \frac{v_H}{\sqrt{2}}, \qquad M^d_{ij} = \epsilon^{2n} y^d_{ij} \frac{v_H}{\sqrt{2}}, \tag{3.10}$$

$$f^u_{ij} = (2n+1)\epsilon^{2n} y^u_{ij}, \qquad f^d_{ij} = (2n+1)\epsilon^{2n} y^d_{ij}. \tag{3.11}$$

Again, n may have a different value for each pair of indices i, j. This is important to keep in mind. In the SM, the mass and Yukawa matrices are proportional,

$$M^u = f^u \frac{v_H}{\sqrt{2}}. \qquad \text{(Standard Model)} \tag{3.12}$$

However, in this model the $(2n+1)$ factor is potentially different for each element of the effective Yukawa matrix. This extra factor means the mass and Yukawa matrices are *not* proportional.

So far, two parameters ϵ, M have been introduced whose values are completely unknown. The value of M was assumed to be at a higher scale than the electroweak scale. However, knowing $v_H/\sqrt{2} \simeq 174$ GeV, its scale can be shown by examining M^u_{ij}.

Since y^u, $y^d \sim \mathcal{O}(1)$, the power of ϵ required for each matrix element must reduce that matrix element by an appropriate order of magnitude below the top mass (the largest matrix element). By comparing masses of the top and bottom quarks with the smallest allowed non-zero choice for the exponent ($n = 1$) of the bottom quark, an estimate on the value of ϵ can be established:

$$\begin{aligned} \frac{m_b}{m_t} \sim \frac{M^d_{33}}{M^u_{33}} &= \frac{\epsilon^2 y^d_{33} v_H/\sqrt{2}}{y^u_{33} v_H/\sqrt{2}}, \\ \mathcal{O}(10^{-2}) &\sim \epsilon^2, \end{aligned} \tag{3.13}$$

and consequently M is around the range of 1 to 2 TeV [23, 24].

Knowing the experimentally determined quark masses, and the order of magnitude of ϵ^2, the mass matrices can be written down by choosing appropriate values for n. Assuming the powers of ϵ within the mass matrices are symmetric, then

$$M^u = \begin{pmatrix} y^u_{11}\epsilon^6 & y^u_{12}\epsilon^4 & y^u_{13}\epsilon^4 \\ y^u_{21}\epsilon^4 & y^u_{22}\epsilon^2 & y^u_{23}\epsilon^2 \\ y^u_{31}\epsilon^4 & y^u_{32}\epsilon^2 & y^u_{33} \end{pmatrix} \frac{v_H}{\sqrt{2}}, \qquad M^d = \begin{pmatrix} y^d_{11}\epsilon^6 & y^d_{12}\epsilon^6 & y^d_{13}\epsilon^6 \\ y^d_{21}\epsilon^6 & y^d_{22}\epsilon^4 & y^d_{23}\epsilon^4 \\ y^d_{31}\epsilon^6 & y^d_{32}\epsilon^4 & y^d_{33}\epsilon^2 \end{pmatrix} \frac{v_H}{\sqrt{2}}. \tag{3.14}$$

The magnitudes of the off-diagonal elements were also chosen to be of similar magnitudes of the relevant diagonal elements. This appears to be reasonable since the quark mixing angles are of the order of the respective masses.

Once the powers of ϵ have been determined for the mass matrices, the $(2n+1)$ factor of the Yukawa matrices can be easily determined.

$$f^u = \begin{pmatrix} 7y^u_{11}\epsilon^6 & 5y^u_{12}\epsilon^4 & 5y^u_{13}\epsilon^4 \\ 5y^u_{21}\epsilon^4 & 3y^u_{22}\epsilon^2 & 3y^u_{23}\epsilon^2 \\ 5y^u_{31}\epsilon^4 & 3y^u_{32}\epsilon^2 & y^u_{33} \end{pmatrix}, \qquad f^d = \begin{pmatrix} 7y^d_{11}\epsilon^6 & 7y^d_{12}\epsilon^6 & 7y^d_{13}\epsilon^6 \\ 7y^d_{21}\epsilon^6 & 5y^d_{22}\epsilon^4 & 5y^d_{23}\epsilon^4 \\ 7y^d_{31}\epsilon^6 & 5y^d_{32}\epsilon^4 & 3y^d_{33}\epsilon^2 \end{pmatrix}. \tag{3.15}$$

3.2 Operators with Higgs singlets: the $S^\dagger S$ model

In contrast to the preceding model, the higher dimensional operators in Ref. [25] were made by replacing the doublet operator $H^\dagger H$ with the singlet operator $S^\dagger S$, so terms are of the form

$$\left(\frac{S^\dagger S}{M^2}\right)^n y^u_{ij}\overline{q^i_L}u^j_R\widetilde{H}, \qquad\qquad \left(\frac{S^\dagger S}{M^2}\right)^n y^d_{ij}\overline{q^i_L}d^j_R H. \tag{3.16}$$

As before, the parametrization of the Higgs fields will be in the unitary gauge shown in Eq. (2.3). The doublet H and the singlet S are written in terms of the real fields h_0 and s_0. Again, a substitution shows the binomials to be expanded:

$$\frac{(v_S+s_0)^{2n}}{2^n M^{2n}} y^u_{ij}\overline{u^i_L}u^j_R\frac{(v_H+h_0)}{\sqrt{2}}. \tag{3.17}$$

The difference from before is now there are two vevs and two fields that contribute. Examining the binomials,

$$\begin{aligned}(v_S + s_0)^{2n}(v_H + h_0) &= (v_S^{2n} + 2nv_S^{2n-1}s_0 + \cdots)(v_H + h_0) \\ &= v_S^{2n}v_H + 2nv_S^{2n-1}v_H s_0 + v_S^{2n}h_0 + 2nv_S^{2n-1}s_0 h_0 + \cdots .\end{aligned} \tag{3.18}$$

Mass terms are of the form

$$M_{ij}^u \overline{u_L^i} u_R^j = \left(\frac{v_S^{2n}}{2^n M^{2n}} y_{ij}^u \frac{v_H}{\sqrt{2}}\right) \overline{u_L^i} u_R^j, \tag{3.19}$$

Now, there are two types of Yukawa couplings. The couplings with h_0 and couplings with s_0 are

$$f_{ij}^{hu} \overline{u_L^i} u_R^j \frac{h_0}{\sqrt{2}} = \left(\frac{v_S^{2n}}{2^n M^{2n}} y_{ij}^u\right) \overline{u_L^i} u_R^j \frac{h_0}{\sqrt{2}}, \tag{3.20}$$

$$f_{ij}^{su} \overline{u_L^i} u_R^j \frac{s_0}{\sqrt{2}} = \left(2n \frac{v_S^{2n-1} v_H}{2^n M^{2n}} y_{ij}^u\right) \overline{u_L^i} u_R^j \frac{s_0}{\sqrt{2}}. \tag{3.21}$$

The same dimensionless parameter ϵ can be used to create more manageable expressions. However, because v_S is new to the terms, a second dimensionless parameter α can also be introduced to assist in simplifying the expressions, so that

$$\epsilon = \frac{v_H}{M\sqrt{2}}, \qquad \alpha = \frac{v_S}{v_H}, \qquad \alpha\epsilon = \frac{v_S}{M\sqrt{2}}. \tag{3.22}$$

Thus the mass matrices and Yukawa couplings are

$$M_{ij}^u = (\alpha\epsilon)^{2n} y_{ij}^u \frac{v_H}{\sqrt{2}}, \qquad M_{ij}^d = (\alpha\epsilon)^{2n} y_{ij}^d \frac{v_H}{\sqrt{2}}, \tag{3.23}$$

$$f_{ij}^{hu} = (\alpha\epsilon)^{2n} y_{ij}^u, \qquad f_{ij}^{hd} = (\alpha\epsilon)^{2n} y_{ij}^d, \tag{3.24}$$

$$f_{ij}^{su} = 2n(\alpha\epsilon)^{2n}\alpha^{-1} y_{ij}^u, \qquad f_{ij}^{sd} = 2n(\alpha\epsilon)^{2n}\alpha^{-1} y_{ij}^d. \tag{3.25}$$

The full mass matrices can be written out. Simply make the replacement $\epsilon^{2n} \mapsto (\alpha\epsilon)^{2n}$

for each element of Eq. (3.14), and the mass matrices are

$$
\begin{aligned}
M^u &= \begin{pmatrix} y^u_{11}(\alpha\epsilon)^6 & y^u_{12}(\alpha\epsilon)^4 & y^u_{13}(\alpha\epsilon)^4 \\ y^u_{21}(\alpha\epsilon)^4 & y^u_{22}(\alpha\epsilon)^2 & y^u_{23}(\alpha\epsilon)^2 \\ y^u_{31}(\alpha\epsilon)^4 & y^u_{32}(\alpha\epsilon)^2 & y^u_{33} \end{pmatrix} \frac{v_H}{\sqrt{2}}, \\
M^d &= \begin{pmatrix} y^d_{11}(\alpha\epsilon)^6 & y^d_{12}(\alpha\epsilon)^6 & y^d_{13}(\alpha\epsilon)^6 \\ y^d_{21}(\alpha\epsilon)^6 & y^d_{22}(\alpha\epsilon)^4 & y^d_{23}(\alpha\epsilon)^4 \\ y^d_{31}(\alpha\epsilon)^6 & y^d_{32}(\alpha\epsilon)^4 & y^d_{33}(\alpha\epsilon)^2 \end{pmatrix} \frac{v_H}{\sqrt{2}}.
\end{aligned}
\tag{3.26}
$$

With this specific model, the mass matrices and the Yukawa-h matrices are proportional in both the up and down sectors, the same as in the SM. The Yukawa-h matrices are

$$
\begin{aligned}
f^{hu} &= \begin{pmatrix} y^u_{11}(\alpha\epsilon)^6 & y^u_{12}(\alpha\epsilon)^4 & y^u_{13}(\alpha\epsilon)^4 \\ y^u_{21}(\alpha\epsilon)^4 & y^u_{22}(\alpha\epsilon)^2 & y^u_{23}(\alpha\epsilon)^2 \\ y^u_{31}(\alpha\epsilon)^4 & y^u_{32}(\alpha\epsilon)^2 & y^u_{33} \end{pmatrix}, \\
f^{hd} &= \begin{pmatrix} y^d_{11}(\alpha\epsilon)^6 & y^d_{12}(\alpha\epsilon)^6 & y^d_{13}(\alpha\epsilon)^6 \\ y^d_{21}(\alpha\epsilon)^6 & y^d_{22}(\alpha\epsilon)^4 & y^d_{23}(\alpha\epsilon)^4 \\ y^d_{31}(\alpha\epsilon)^6 & y^d_{32}(\alpha\epsilon)^4 & y^d_{33}(\alpha\epsilon)^2 \end{pmatrix}.
\end{aligned}
\tag{3.27}
$$

However, the Yukawa-s matrices are not proportional to the mass matrices, as it has the extra factor $2n$ associated with each element. These matrices are

$$
\begin{aligned}
f^{su} &= \begin{pmatrix} 6y^u_{11}\alpha^5\epsilon^6 & 4y^u_{12}\alpha^3\epsilon^4 & 4y^u_{13}\alpha^3\epsilon^4 \\ 4y^u_{21}\alpha^3\epsilon^4 & 2y^u_{22}\alpha\epsilon^2 & 2y^u_{23}\alpha\epsilon^2 \\ 4y^u_{31}\alpha^3\epsilon^4 & 2y^u_{32}\alpha\epsilon^2 & 0 \end{pmatrix}, \\
f^{sd} &= \begin{pmatrix} 6y^d_{11}\alpha^5\epsilon^6 & 6y^d_{12}\alpha^5\epsilon^6 & 6y^d_{13}\alpha^5\epsilon^6 \\ 6y^d_{21}\alpha^5\epsilon^6 & 4y^d_{22}\alpha^3\epsilon^4 & 4y^d_{23}\alpha^3\epsilon^4 \\ 6y^d_{31}\alpha^5\epsilon^6 & 4y^d_{32}\alpha^3\epsilon^4 & 2y^d_{33}\alpha\epsilon^2 \end{pmatrix}.
\end{aligned}
\tag{3.28}
$$

3.3 Operators with Higgs doublets and singlets

The preceding two models take the higher dimensional operators to be purely composed of only Higgs doublets or only Higgs singlets. But now consider the possibility of operators built from products of the doublet operator and singlet operator such as

$$\left(\frac{H^\dagger H}{M^2}\right)^{n_H}\left(\frac{S^\dagger S}{M^2}\right)^{n_S} y^u_{ij}\overline{q^i_L}u^j_R\widetilde{H}, \tag{3.29}$$

where n_H and n_S are non-negative integers that may have different values for each pair of generation indices i, j, just like n from the previous sections.

Again, a substitution reveals binomials in need of expansion with

$$\frac{(v_H+h_0)^{2n_H}(v_S+s_0)^{2n_S}}{2^{n_H+n_S}M^{2n_H+2n_S}} y^u_{ij}\overline{u^i_L}u^j_R\frac{(v_H+h_0)}{\sqrt{2}}. \tag{3.30}$$

Focusing on the relevant terms, the expansion proceeds by

$$\begin{aligned}
&(v_H+h_0)^{2n_H}(v_S+s_0)^{2n_S}(v_H+h_0)\\
&\quad=(v_H^{2n_H}+2n_Hv_H^{2n_H-1}h_0+\cdots)(v_S^{2n_S}+2n_Sv_S^{2n_S-1}s_0+\cdots)(v_H+h_0)\\
&\quad=(v_H^{2n_H}v_S^{2n_S}+2n_Hv_H^{2n_H-1}v_S^{2n_S}h_0+2n_Sv_H^{2n_H}v_S^{2n_S-1}s_0+\cdots)(v_H+h_0)\\
&\quad=v_H^{2n_H+1}v_S^{2n_S}+(2n_H+1)v_H^{2n_H}v_S^{2n_S}h_0+2n_Sv_H^{2n_H+1}v_S^{2n_S-1}s_0+\cdots.
\end{aligned} \tag{3.31}$$

Mass terms are of the form

$$M^u_{ij}\overline{u^i_L}u^j_R=\left(\frac{v_H^{2n_H}v_S^{2n_S}}{2^{n_H+n_S}M^{2n_H+2n_S}}y^u_{ij}\frac{v_H}{\sqrt{2}}\right)\overline{u^i_L}u^j_R. \tag{3.32}$$

The Yukawa terms are of the form

$$f^{hu}_{ij}\overline{u^i_L}u^j_R\frac{h_0}{\sqrt{2}}=\left((2n_H+1)\frac{v_H^{2n_H}v_S^{2n_S}}{2^{n_H+n_S}M^{2n_H+2n_S}}y^u_{ij}\right)\overline{u^i_L}u^j_R\frac{h_0}{\sqrt{2}}, \tag{3.33}$$

$$f^{su}_{ij}\overline{u^i_L}u^j_R\frac{s_0}{\sqrt{2}}=\left(2n_S\frac{v_H^{2n_H+1}v_S^{2n_S-1}}{2^{n_H+n_S}M^{2n_H+2n_S}}y^u_{ij}\right)\overline{u^i_L}u^j_R\frac{s_0}{\sqrt{2}}. \tag{3.34}$$

Again, the dimensionless parameters α and ϵ can be used to simplify the expressions. Also, an additional relation for the operator exponents can be added so that

$$\epsilon=\frac{v_H}{M\sqrt{2}},\qquad \alpha=\frac{v_S}{v_H},\qquad \alpha\epsilon=\frac{v_S}{M\sqrt{2}},\qquad n_H=n-n_S. \tag{3.35}$$

The mass and Yukawa matrices are then given by

$$M^u_{ij} = \alpha^{2n_S}\epsilon^{2n} y^u_{ij}\frac{v_H}{\sqrt{2}}, \qquad M^d_{ij} = \alpha^{2n_S}\epsilon^{2n} y^d_{ij}\frac{v_H}{\sqrt{2}}, \tag{3.36}$$

$$f^{hu}_{ij} = (2(n-n_S)+1)\alpha^{2n_S}\epsilon^{2n} y^u_{ij}, \qquad f^{hd}_{ij} = (2(n-n_S)+1)\alpha^{2n_S}\epsilon^{2n} y^d_{ij}, \tag{3.37}$$

$$f^{su}_{ij} = 2n_S\alpha^{2n_S-1}\epsilon^{2n} y^u_{ij}, \qquad f^{sd}_{ij} = 2n_S\alpha^{2n_S-1}\epsilon^{2n} y^d_{ij}. \tag{3.38}$$

Since ϵ regulates the order of magnitude for the mass matrices, it is reasonable to keep the same ϵ-texture as in Eq. (3.14). This fixes the value of n that will be used for each matrix element. However, this does not restrict the value of n_S. Within the mass matrices M^u and M^d, there are 17 matrix elements that may have varying values for the integer n_S, only restricted by $0 \leq n_S \leq n$.

For a mass term with a factor of ϵ^{2n}, the allowed powers of α are the even numbers ranging from zero to $2n$. Inspection of the mass matrices shows there are four mass terms with ϵ^2 (two allowed powers of α), seven with ϵ^4 (three allowed powers of α), and six with ϵ^6 (four allowed powers of α). Allowing powers of α to be independent for matrix elements with the same power of ϵ means there can be $2^4 3^7 4^6 = 143\ 327\ 232$ possible Lagrangians.

To simplify the situation, all matrix elements that have the same power of ϵ are restricted to have a common power of α. For example, the mass terms M^u_{22} and M^u_{23} are both proportional to ϵ^2. They are restricted to be both proportional to α^0 or both be proportional to α^2. They are not allowed to have different powers of α. This restriction reduces the possible Lagrangians down to $2 \cdot 3 \cdot 4 = 24$, a much more manageable number.

With this restriction, the effective Yukawa Lagrangian can be written down with

common higher dimensional operators factored as leading coefficients, yielding

$$\begin{aligned}\mathcal{L}^{\text{Yuk}}_{\text{quark}} = {} & y^u_{33}\overline{q^3_L}u^3_R\widetilde{H} \\ & + \left(\frac{H^\dagger H}{M^2}\right)^{1-n_1}\left(\frac{S^\dagger S}{M^2}\right)^{n_1}\Big(y^d_{33}\overline{q^3_L}d^3_R H + y^u_{22}\overline{q^2_L}u^2_R\widetilde{H} + y^u_{23}\overline{q^2_L}u^3_R\widetilde{H} + y^u_{32}\overline{q^3_L}u^2_R\widetilde{H}\Big) \\ & + \left(\frac{H^\dagger H}{M^2}\right)^{2-n_2}\left(\frac{S^\dagger S}{M^2}\right)^{n_2}\Big(y^d_{22}\overline{q^2_L}d^2_R H + y^d_{23}\overline{q^2_L}d^3_R H + y^d_{32}\overline{q^3_L}d^2_R H + y^u_{12}\overline{q^1_L}u^2_R\widetilde{H} \\ & \qquad + y^u_{21}\overline{q^2_L}u^1_R\widetilde{H} + y^u_{13}\overline{q^1_L}u^3_R\widetilde{H} + y^u_{31}\overline{q^3_L}u^1_R\widetilde{H}\Big) \\ & + \left(\frac{H^\dagger H}{M^2}\right)^{3-n_3}\left(\frac{S^\dagger S}{M^2}\right)^{n_3}\Big(y^d_{11}\overline{q^1_L}d^1_R H + y^d_{12}\overline{q^1_L}d^2_R H + y^d_{21}\overline{q^2_L}d^1_R H \\ & \qquad + y^d_{13}\overline{q^1_L}d^3_R H + y^d_{31}\overline{q^3_L}d^1_R H + y^u_{11}\overline{q^1_L}u^1_R\widetilde{H}\Big) + h.c.\end{aligned} \tag{3.39}$$

The operator exponents from Eq. (3.29) have been specified. Since n takes a fixed value according to the flavors of each coupling, it can be directly set ($n = 1, 2, 3$). Also, since $0 \leq n_S \leq n$, the exponent n_S can be specified as n_k such that $0 \leq n_k \leq k$ where $k \in \{1, 2, 3\}$.

One of the consequences of these higher dimensional operators is flavor changing neutral currents in the Higgs sector. This occurs because the effective Yukawa matrices and the effective mass matrices will not be proportional. The effective mass matrices will all be similar to Eq. (3.14) with extra factors of α. However, the effective Yukawa matrices will have extra numerical factors corresponding to the coefficients resulting from the binomial expansions of the operators after they acquire vevs. In Eqs. (3.36)–(3.38), factors with n or n_S will generally be different for each matrix element.

Generalized expressions for the quark masses can be found in terms of n_1, n_2, n_3, α, and ϵ using a biunitary transformation $M^{\psi'} = V_L^{\psi\dagger} M^\psi V_R^\psi$, where $\psi \in \{u, d\}$ so that M^ψ is either mass matrix from Eq. (3.36). The prime indicates the mass basis, so that the matrix $M^{\psi'}$ is the diagonal mass matrix.

The effective Yukawa matrices can also be found by $f^{h\psi'} = V_L^{\psi\dagger} f^{h\psi} V_R^\psi$, where

V_L^ψ, V_R^ψ are the unitary matrices that diagonalize M^ψ. Since the Yukawa matrices $f^{h\psi}, f^{s\psi}$ are not proportional to the mass matrices M^ψ, the Yukawa matrices in the mass basis $f^{h\psi'}, f^{s\psi'}$ will not be diagonal.

Expansions of the mass and Yukawa matrices were made in powers of ϵ. The masses and Yukawa couplings have been expanded to ϵ^6. The CKM matrix is also given up to ϵ^4. Calculations were made assuming coupling coefficients are real and symmetric ($y_{ij}^\psi = y_{ji}^\psi$). The Yukawa couplings and CKM matrix are in Appendix A. The masses are

$$M_{11}^{u'} \approx \left(\alpha^{2n_3} y_{11}^u - \alpha^{2(2n_2-n_1)} \frac{{y_{12}^u}^2}{y_{22}^u}\right) \epsilon^6, \tag{3.40a}$$

$$M_{22}^{u'} \approx \alpha^{2n_1} y_{22}^u \, \epsilon^2 - \alpha^{4n_1} \frac{{y_{23}^u}^2}{y_{33}^u} \, \epsilon^4 + \left(\alpha^{2(2n_2-n_1)} \frac{{y_{12}^u}^2}{y_{22}^u} + \alpha^{6n_1} \frac{y_{22}^u {y_{23}^u}^2}{{y_{33}^u}^2}\right) \epsilon^6, \tag{3.40b}$$

$$M_{33}^{u'} \approx y_{33}^u + \alpha^{4n_1} \frac{{y_{23}^u}^2}{y_{33}^u} \, \epsilon^4 + \alpha^{6n_1} \frac{y_{22}^u {y_{23}^u}^2}{{y_{33}^u}^2} \, \epsilon^6, \tag{3.40c}$$

$$M_{11}^{d'} \approx \alpha^{2n_3} y_{11}^d \, \epsilon^6, \tag{3.40d}$$

$$M_{22}^{d'} \approx \alpha^{2n_2} y_{22}^d \, \epsilon^4 - \alpha^{2(2n_2-n_1)} \frac{{y_{23}^d}^2}{y_{33}^d} \, \epsilon^6, \tag{3.40e}$$

$$M_{33}^{d'} \approx \alpha^{2n_1} y_{33}^d \, \epsilon^2 + \left(\alpha^{2(2n_2-n_1)} \frac{{y_{23}^d}^2}{y_{23}^d} - \alpha^{2(6n_2-3n_1-2n_3)} \frac{{y_{22}^d}^2 {y_{23}^d}^4}{{y_{13}^d}^2 {y_{33}^d}^3}\right) \epsilon^6. \tag{3.40f}$$

The Yukawa couplings $f^{h\psi}, f^{s\psi}$ are couplings of the quarks to the Higgs fields with both field types in the gauge basis. The Yukawa couplings $f^{h\psi'}, f^{s\psi'}$ are with the quarks in the mass basis; however, the Higgs fields are still in the gauge basis. To get the Yukawa couplings in the mass basis of both the quarks and the Higgs fields, the rotation of the Higgs fields still needs to be applied. Doing so yields the Yukawa couplings $f^{\phi_H\psi'}, f^{\phi_S\psi'}$ from the expressions

$$\frac{1}{\sqrt{2}} f_{ij}^{\phi_H\psi'} \overline{\psi_L'^i} \psi_R'^j \phi_H = \frac{1}{\sqrt{2}} \left(f_{ij}^{h\psi'} \cos\vartheta - f_{ij}^{s\psi'} \sin\vartheta\right) \overline{\psi_L'^i} \psi_R'^j \phi_H, \tag{3.41a}$$

$$\frac{1}{\sqrt{2}} f_{ij}^{\phi_S\psi'} \overline{\psi_L'^i} \psi_R'^j \phi_S = \frac{1}{\sqrt{2}} \left(f_{ij}^{h\psi'} \sin\vartheta + f_{ij}^{s\psi'} \cos\vartheta\right) \overline{\psi_L'^i} \psi_R'^j \phi_S. \tag{3.41b}$$

CHAPTER 4

MASS GENERATING MECHANISM

So far, the gauge symmetries of the SM have been extended by an additional $U(1)_S$ local symmetry. To explain the origin of the operators $H^\dagger H$ and $S^\dagger S$ in the Yukawa couplings, some additional $U(1)_{F_i}$ global symmetries will also be employed in the use of a Froggatt-Nielsen type mechanism. In the one model where none of the effective low energy interactions in the Lagrangian have a coefficient of $(S^\dagger S)^{n_S}$, the $U(1)_S$ symmetry is not included; it essentially decouples from the model and can be ignored.

Each $U(1)_{F_i}$ global symmetry has a flavor scalar boson F_i (called a flavon) that is charged only under its corresponding symmetry, and neutral with respect to all other symmetries. Because the $U(1)_{F_i}$ are global symmetries, there are no gauge bosons associated with them. It should be noted that even though there is no restriction being placed on the number of $U(1)_{F_i}$ symmetries, it is not necessary to have more than two.

The effective Yukawa couplings are created by interactions with new heavy exotic vector-like quarks, the new flavons F_i, and the Higgs bosons H and S. The new quark doublets will be denoted by Q, and the singlets by U and D. They have the same hypercharges as their SM counterparts q, u, and d.

It should be noted that unlike the SM quarks, which only come in right-handed singlets and left-handed doublets, the new heavy quarks occur in left-right pairs and behave vector-like with respect to the gauge groups of the SM and $U(1)_S$. The quantum numbers of a left-right pair will be identical except for the quantum number

of one $U(1)_{F_i}$ symmetry. This quantum number will differ by a value of one. When this symmetry breaks, the vev of the F_i gives mass to the new heavy quarks. The vev of each F_i is assumed to be around the TeV scale.

These extra fields are necessary in a Froggatt-Nielsen mechanism as each field occupies a unique position in the charge space of $U(1)_Y \times U(1)_S \times U(1)_{F_1} \times U(1)_{F_2} \times \cdots$. The flavons and the Higgs fields provide the interactions that link the quark fields to their neighbors in the charge space. A sequence of interactions is required to move between non-neighboring fields, such as the SM quarks.

Within a given model, the sequence of field interactions beginning and ending with SM particles was chosen so that there is only one sequence connecting any two SM quarks (assuming backward steps are not taken within the sequence). Although this is not strictly necessary, if distinctly different sequences of particle interactions were allowed into a model, then some models may have explicit terms in the Lagrangian with higher powers of $(H^\dagger H)^{n-n_S}(S^\dagger S)^{n_S}$ than are written down in Eq. (3.39).

In order to make different interaction sequences non-interacting with each other, it is necessary to space the non-interacting quark fields at least two quantum numbers away from each other in the charge space. This leads to a large number of quark fields being used as each interaction sequence path through this space must be long enough to go around many other fields and avoid unwanted interactions with other paths.

4.1 Couplings in the Lagrangian

The couplings of these heavy quarks in the Lagrangian take on a generalized form. Specifically, the couplings each particle has will depend on their charge assignments within a given model. The hermitian conjugate of each coupling will also be included in the Lagrangian. For the terms listed in Eqs. (4.1a)–(4.1c), no summation over the indices is implied. All of the coupling coefficients (f^{FQ}, f^{FU}, f^{FD}, f^{SQ}, f^{SU}, f^{SD},

f^{HU}, f^{HD}) are taken to be $\mathcal{O}(1)$ and occur in the following terms:

$$\left.\begin{array}{ccc} f_{ab}^{FQ}\overline{Q_L^a}Q_R^bF_i & f_{ab}^{FU}\overline{U_L^a}U_R^bF_i & f_{ab}^{FD}\overline{D_L^a}D_R^bF_i \\ f_{ab}^{FQ}\overline{Q_L^a}Q_R^bF_i^\dagger & f_{ab}^{FU}\overline{U_L^a}U_R^bF_i^\dagger & f_{ab}^{FD}\overline{D_L^a}D_R^bF_i^\dagger \end{array}\right\} \text{Flavon Couplings,} \tag{4.1a}$$

$$\left.\begin{array}{ccc} f_{ab}^{SQ}\overline{Q_L^a}Q_R^bS & f_{ab}^{SU}\overline{U_L^a}U_R^bS & f_{ab}^{SD}\overline{D_L^a}D_R^bS \\ f_{ab}^{SQ}\overline{Q_L^a}Q_R^bS^\dagger & f_{ab}^{SU}\overline{U_L^a}U_R^bS^\dagger & f_{ab}^{SD}\overline{D_L^a}D_R^bS^\dagger \end{array}\right\} \text{Higgs Singlet Couplings,} \tag{4.1b}$$

$$\left.\begin{array}{cc} f_{ab}^{HU}\overline{Q_L^a}U_R^b\widetilde{H} & f_{ab}^{HD}\overline{Q_L^a}D_R^bH \\ f_{ab}^{HU}\overline{Q_R^a}U_L^b\widetilde{H} & f_{ab}^{HD}\overline{Q_R^a}D_L^bH \end{array}\right\} \text{Higgs Doublet Couplings.} \tag{4.1c}$$

Every heavy quark will have one coupling from Eq. (4.1a) where $a = b$, as this will be a massive left-right pair when the flavon F breaks the flavor symmetry. Every heavy quark must also have at least one coupling from Eqs. (4.1a)–(4.1b) where $a \neq b$, or from Eq. (4.1c) where a and b are indexed over different quark types. For the few heavy quarks that directly couple to the SM quarks, the appropriate replacement should be made to the terms coming from Eqs. (4.1a)–(4.1c) (e.g. $\overline{Q_L^a}Q_R^b \mapsto \overline{q_L^a}Q_R^b$).

4.1.1 The effective Lagrangian

In all model variations, the Yukawa coupling $y_{33}^u\overline{q_L^3}u_R^3\widetilde{H}$ is the only one that involves only SM particles. All the other model variations have coefficients of $(H^\dagger H)^{n-n_S}(S^\dagger S)^{n_S}$ on terms which would otherwise be SM Yukawa couplings. These terms have dimension larger than four and come from a process of integrating out the heavy fermions from the tree level diagrams, which correspond with terms of the forms from Eqs. (4.1a)–(4.1c).

For example, consider the term $(H^\dagger H/M^2)y_{23}^u\overline{q_L^2}u_R^3\widetilde{H}$. This terms exists in 12 of the 24 variations of the effective Lagrangian. One possible heavy quark model has thirteen terms associated with this process. This process can be represented by the

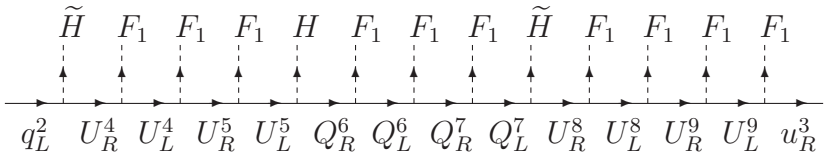

Figure 4.1: Feynman diagram linking q_L^2 to u_R^3 in an $H^\dagger H$ model.

Feynman diagram in Fig. 4.1. The necessary terms are

$$\begin{aligned} &f_{2,4}^{HU}\overline{q_L^2}U_R^4\widetilde{H} + f_{4,4}^{FU}\overline{U_R^4}U_L^4F_1 + f_{4,5}^{FU}\overline{U_L^4}U_R^5F_1 + f_{5,5}^{FU}\overline{U_R^5}U_L^5F_1 + f_{5,6}^{HU}\overline{U_L^5}Q_R^6H \\ &+ f_{6,6}^{FQ}\overline{Q_R^6}Q_L^6F_1 + f_{6,7}^{FQ}\overline{Q_L^6}Q_R^7F_1 + f_{7,7}^{FQ}\overline{Q_R^7}Q_L^7F_1 + f_{7,8}^{HU}\overline{Q_L^7}U_R^8\widetilde{H} \\ &+ f_{8,8}^{FU}\overline{U_R^8}U_L^8F_1 + f_{8,9}^{FU}\overline{U_L^8}U_R^9F_1 + f_{9,9}^{FU}\overline{U_R^9}U_L^9F_1 + f_{9,3}^{FU}\overline{U_L^9}u_R^3F_1 + h.c. \end{aligned} \tag{4.2}$$

This particular model choice exhibits only a single extra symmetry $U(1)_{F_1}$ in the given terms. The flavon symmetry breaks, and the flavons acquire a vev $\langle F_i\rangle$. The heavy fermions can be integrated out and an effective expression below the TeV scale is proportional to

$$f_{2,4}^{HU}f_{4,4}^{FU}f_{4,5}^{FU}f_{5,5}^{FU}f_{5,6}^{HU}f_{6,6}^{FQ}f_{6,7}^{FQ}f_{7,7}^{FQ}f_{7,8}^{HU}f_{8,8}^{FU}f_{8,9}^{FU}f_{9,9}^{FU}f_{9,3}^{FU}\left(\frac{\langle F_1\rangle}{M}\right)^{10}\frac{H^\dagger H}{M^2}\overline{q_L^2}u_R^3\widetilde{H} + h.c. \tag{4.3}$$

Thus for this particular model choice, the effective coupling parameter in the low energy Lagrangian is

$$y_{23}^u \sim f_{2,4}^{HU}f_{4,4}^{FU}f_{4,5}^{FU}f_{5,5}^{FU}f_{5,6}^{HU}f_{6,6}^{FQ}f_{6,7}^{FQ}f_{7,7}^{FQ}f_{7,8}^{HU}f_{8,8}^{FU}f_{8,9}^{FU}f_{9,9}^{FU}f_{9,3}^{FU}\left(\frac{\langle F_1\rangle}{M}\right)^{10}. \tag{4.4}$$

The couplings f are $\mathcal{O}(1)$. The vev of the flavons is the same order as the vector-like quark masses, $\langle F_1\rangle \sim M$. This means y^u can also be $\mathcal{O}(1)$, consistent with the assumption in the effective Lagrangian.

For a comparison, consider the 12 effective Lagrangians that have the same term, except with $H^\dagger H \mapsto S^\dagger S$. Some possible model choices may again have thirteen interaction terms. The Feynman diagram in Fig. 4.2 is similar, but there are noticeable

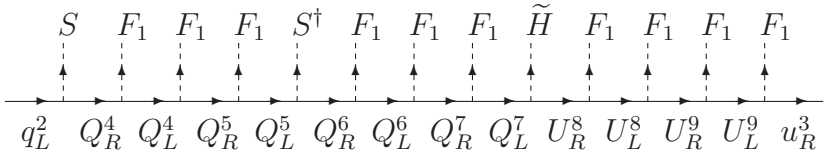

Figure 4.2: Feynman diagram linking q_L^2 to u_R^3 in an $S^\dagger S$ model.

differences in the first five interactions. The terms are

$$\begin{aligned} &f_{2,4}^{SQ}\overline{q_L^2}Q_R^4 S + f_{4,4}^{FQ}\overline{Q_R^4}Q_L^4 F_1 + f_{4,5}^{FQ}\overline{Q_L^4}Q_R^5 F_1 + f_{5,5}^{FQ}\overline{Q_R^5}Q_L^5 F_1 + f_{5,6}^{SQ}\overline{Q_L^5}Q_R^6 S^\dagger \\ &+ f_{6,5}^{FQ}\overline{Q_R^6}Q_L^6 F_1 + f_{6,7}^{FQ}\overline{Q_L^6}Q_R^7 F_1 + f_{7,7}^{FQ}\overline{Q_R^7}Q_L^7 F_1 + f_{7,8}^{HU}\overline{Q_L^7}U_R^8 \widetilde{H} \\ &+ f_{8,8}^{FU}\overline{U_R^8}U_L^8 F_1 + f_{8,9}^{FU}\overline{U_L^8}U_R^9 F_1 + f_{9,9}^{FU}\overline{U_R^9}U_L^9 F_1 + f_{9,3}^{FU}\overline{U_L^9}u_R^3 F_1 + h.c. \end{aligned} \tag{4.5}$$

This expression is similar to the previous case, and likewise when the heavy fermions are integrated out, the effective expression below the TeV scale looks similar, with

$$f_{2,4}^{SQ} f_{4,4}^{FQ} f_{4,5}^{FQ} f_{5,5}^{FQ} f_{5,6}^{SQ} f_{6,5}^{FQ} f_{6,7}^{FQ} f_{7,7}^{FQ} f_{7,8}^{HU} f_{8,8}^{FU} f_{8,9}^{FU} f_{9,9}^{FU} f_{9,3}^{FU} \left(\frac{\langle F_1\rangle}{M}\right)^{10} \frac{S^\dagger S}{M^2}\overline{q_L^2}u_R^3\widetilde{H} + h.c. \tag{4.6}$$

As before, the effective coupling parameter in the low energy Lagrangian can be pulled out, and yields

$$y_{23}^u \sim f_{2,4}^{SQ} f_{4,4}^{FQ} f_{4,5}^{FQ} f_{5,5}^{FQ} f_{5,6}^{SQ} f_{6,5}^{FQ} f_{6,7}^{FQ} f_{7,7}^{FQ} f_{7,8}^{HU} f_{8,8}^{FU} f_{8,9}^{FU} f_{9,9}^{FU} f_{9,3}^{FU} \left(\frac{\langle F_1\rangle}{M}\right)^{10}. \tag{4.7}$$

And once again, y_{23}^u can be $\mathcal{O}(1)$.

4.2 Charge assignments for specific models

4.2.1 Effective Lagrangian with only powers of $S^\dagger S$

In the effective Lagrangian where all the interactions of dimension greater than four only have powers of $S^\dagger S$, the $U(1)_S$ symmetry only needs to be accompanied by a single $U(1)_F$ symmetry. With only these two extra symmetries, one possible model has a set of 166 heavy quarks (18 U_L^a, 18 U_R^a, 29 D_L^a, 29 D_R^a, 36 Q_L^a, 36 Q_R^a). The quantum numbers of the SM quarks, Higgs doublet, Higgs singlet, and the vector

Table 4.1: Charge assignments of the SM quarks, Higgs doublet, Higgs singlet, and new vector boson for an effective Lagrangian with powers of $S^\dagger S$.

Fields	$U(1)_S$	$U(1)_F$	Fields	$U(1)_S$	$U(1)_F$	Fields	$U(1)_S$	$U(1)_F$
q_L^3	0	0	u_R^3	0	0	d_R^3	0	4
q_L^2	0	16	u_R^2	0	4	d_R^2	0	10
q_L^1	0	24	u_R^1	0	10	d_R^1	0	32
H	0	0	F	0	1			
S	1	0						

boson are in Table 4.1. The quantum numbers of the heavy quarks can be found in Table B.1.

4.2.2 Effective Lagrangian with only powers of $H^\dagger H$

In the effective Lagrangian where there are no interactions with the S, the $U(1)_S$ symmetry is effectively eliminated. Some possible choices of fields for a model use only two $U(1)_{F_i}$ symmetries. As indicated previously, this means there will be two new flavon scalars F_1 and F_2. An explicit choice can be made that consists of 124 heavy quarks (17 U_L^a, 17 U_R^a, 20 D_L^a, 20 D_R^a, 20 Q_L^a, 20 Q_R^a). The quantum numbers of the SM quarks, Higgs doublet, and the vector bosons are in Table 4.2. The heavy quarks have their quantum numbers listed in Table B.3.

4.2.3 Generalized model

The two previous models were constructed independently from each other. Each of the other 22 models can also be constructed independently from each other. However, constructing a model and assigning appropriate charges to the heavy quarks for each effective Lagrangian doesn't need to be done 24 times. It is possible to construct a generalized model that will match any of the effective Lagrangians by simply changing

Table 4.2: Charge assignments of the SM quarks, Higgs doublet, and new vector bosons for an effective Lagrangian with powers of $H^\dagger H$.

Fields	$U(1)_{F_1}$	$U(1)_{F_2}$	Fields	$U(1)_{F_1}$	$U(1)_{F_2}$	Fields	$U(1)_{F_1}$	$U(1)_{F_2}$
q_L^3	0	0	u_R^3	0	0	d_R^3	5	-5
q_L^2	-2	0	u_R^2	2	6	d_R^2	5	3
q_L^1	-4	-2	u_R^1	5	3	d_R^1	-6	4
H	0	0	F_1	1	0			
			F_2	0	1			

specific groups of particles.

An example of this change was already done in Eqns. (4.2) and (4.5). In those expressions, the fields U_R^4, U_L^4, U_R^5, and U_L^5 were replaced with Q_R^4, Q_L^4, Q_R^5, and Q_L^5; and the corresponding interactions with H were replaced by interactions with S. In terms of their quantum numbers, the change in hypercharge of the $U(1)_Y$ symmetry at either end of this four step sequence was replaced by a change in the charge of the $U(1)_S$ symmetry.

The generalized model presented here uses two $U(1)_{F_i}$ symmetries and has 282 heavy quarks. The charge assignments of the fields under these symmetries can be found in Tables 4.3 and B.4–B.6.

As presented, Tables B.4–B.6 are for the effective Lagrangian with only powers of $H^\dagger H$. To adjust the Table to fit any of the other variations of the Lagrangian, replace an appropriate set of fields with a different set of fields. The choice of replacements is also, in most cases, not unique. A particular choice of replacements is given in Tables B.7–B.12.

It should be noted, in the replacement tables the numbering superscript is changed to avoid possible duplication of names. For example, the replacement $U_L^{20} \mapsto Q_L^{90}$ is made instead of $U_L^{20} \mapsto Q_L^{20}$ because there already exists a quark with the name Q_L^{20}.

Table 4.3: Charge assignments of the SM quarks, Higgs doublet, Higgs singlet, and the new vector bosons, for a generalized model.

Fields	$U(1)_S$	$U(1)_{F_1}$	$U(1)_{F_2}$	Fields	$U(1)_S$	$U(1)_{F_1}$	$U(1)_{F_2}$
q_L^3	0	5	12	d_R^3	0	7	18
q_L^2	0	5	2	d_R^2	0	13	20
q_L^1	0	6	29	d_R^1	0	0	17
u_R^3	0	5	12	H	0	0	0
u_R^2	0	11	14	S	1	0	0
u_R^1	0	13	20	F_1	0	1	0
				F_2	0	0	1

4.3 Charged leptons

So far, the mass hierarchy of the quarks has been addressed, but the hierarchy of the leptons has not been mentioned. Fortunately, the same approach of using vector-like fermions—heavy exotic leptons—can be used. A mass matrix like those from Eqn. (3.14) can be constructed for the charged leptons.

It turns out, the matrix M^e can have the same ϵ texture as M^d. Thus generally, the mass matrix and the Yukawa couplings have the form

$$M_{ij}^e = \alpha^{2n_S}\epsilon^{2n} y_{ij}^e \frac{v_H}{\sqrt{2}}, \tag{4.8}$$

$$f_{ij}^{he} = (2(n-n_S)+1)\alpha^{2n_S}\epsilon^{2n} y_{ij}^e, \tag{4.9}$$

$$f_{ij}^{se} = 2n_S\alpha^{2n_S-1}\epsilon^{2n} y_{ij}^e. \tag{4.10}$$

Again, the values of n and n_S may vary between matrix elements.

Because it has the same powers of ϵ as the down-type quark sector, it is not always necessary to find a set of vector-like leptons from scratch. If a set of vector-like quarks

is known, then some simple replacements can be made with

$$D \mapsto E, \qquad Q \mapsto L, \qquad U \mapsto N, \tag{4.11}$$

where E and N are vector-like singlet counterparts to e and ν, and L is the vector-like lepton doublet. Then remove the vector-like leptons that are unnecessary in order to eliminate the unwanted interactions with the light neutrinos.

4.4 Chapter summary

Presented here is a scheme under which the charged fermion mass hierarchy of the SM can be understood with couplings with massive vector-like fermions. The effective Yukawa couplings are generated by the breaking of global flavor symmetries $U(1)_{F_i}$ at the TeV scale. It should be noted, as an effective model, it may not be valid above the breaking scale. At that point, another mechanism may take over, or the theory may be embedded in a larger symmetry group.

CHAPTER 5

GENERAL PHENOMENOLOGY

The specific phenomenology of each of the 24 models is shared by differing subgroups of the 24 models. They can be distinguished by looking at two different types of signals: Higgs decay signatures and flavor changing neutral current (FCNC) processes.

5.1 Higgs decays

In the low Higgs mass range of the SM (114–125 Gev) the dominant mode of Higgs decay is to two bottom quarks $\phi_H \to b\bar{b}$. The branching ratio for this decay is almost 100%. This is undesirable from an experimental point of view because these signals are difficult to disentangle from a large QCD background. In 12 of the 24 models, the branching ratio of this decay can be altered significantly. These 12 models are distinguished by the $\phi_H \to b\bar{b}$ coupling coming from $S^\dagger S$ in the Lagrangian. For all of these models, the coupling is

$$y^d_{33}(\alpha \cos\vartheta - 2\sin\vartheta)\epsilon^2\alpha/\sqrt{2}. \tag{5.1}$$

Taking $\alpha \sim 1$ and $\vartheta \sim 26^\circ$, this coupling can be reduced significantly. As a result there is an enhancement of signals in other modes that are easier to see. For example the $\phi_H \to \gamma\gamma$ signal can be enhanced by a factor of 10 as seen in [25, 29, 30]. Varying the angle ϑ drastically alters the branching ratio of the Higgs. If there is no mixing, $\vartheta \sim 0^\circ$, the structure of Higgs decays is virtually indistinguishable from the SM.

In the other 12 models, $\phi_H \to b\bar{b}$ is controlled by $H^\dagger H$ in the Lagrangian. In these models the coupling of $\phi_H \to b\bar{b}$ is $3\epsilon^2 y^d_{33}\cos\vartheta$. This causes an enhancement

of $9\cos^2\vartheta$. The $\phi_H \to \gamma\gamma$ signal is largely unchanged. The dominant diagrams for this process have $W^\pm$ and top quarks running in the loop. Because the singlet Higgs does not couple directly to these particles, the $\phi_H \to \gamma\gamma$ signal will only change by a factor of $\cos^2\vartheta$. Because $\phi_H \to b\bar{b}$ is enhanced by a factor of 9, while $\phi_H \to \gamma\gamma$ stays the same, the $\gamma\gamma$ signal is effectively reduced by a factor of 9 [23].

5.2 Meson decay: $B_s^0 \to \mu^+\mu^-$

In all 24 models this process is mediated by ϕ_S and ϕ_H exchange. Amongst the 24 models there are 3 different categories of amplitudes for this process, controlled dominantly by the second power operators $(H^\dagger H)^2$, $(S^\dagger S)^2$, and $(H^\dagger H)(S^\dagger S)$. The first power operators $H^\dagger H$ and $S^\dagger S$ have a less significant influence. The amplitudes for ϕ_H and ϕ_S exchange, arranged by first and second power operators, are:

$$H^\dagger H, (H^\dagger H)^2: \quad A_{\phi_H} \sim -5\epsilon^8 y^e_{22} y^d_{23} \cos^2\vartheta / m^2_{\phi_H} \tag{5.2a}$$

$$A_{\phi_S} \sim -5\epsilon^8 y^e_{22} y^e_{23} \sin^2\vartheta / m^2_{\phi_S} \tag{5.2b}$$

$$H^\dagger H, (H^\dagger H)(S^\dagger S): \quad A_{\phi_H} \sim \alpha^2\epsilon^8 y^e_{22} y^d_{23} \sin\vartheta(3\alpha\cos\vartheta - 2\sin\vartheta)/m^2_{\phi_H} \tag{5.2c}$$

$$A_{\phi_S} \sim -\alpha^2\epsilon^8 y^e_{22} y^d_{23} \cos\vartheta(3\alpha\sin\vartheta + 2\cos\vartheta)/m^2_{\phi_S} \tag{5.2d}$$

$$H^\dagger H, (S^\dagger S)^2: \quad A_{\phi_H} \sim \alpha^6\epsilon^8 y^e_{22} y^d_{23} (\alpha^2\cos^2\vartheta - 8\sin^2\vartheta - \alpha\sin 2\vartheta)/m^2_{\phi_H} \tag{5.2e}$$

$$A_{\phi_S} \sim \alpha^6\epsilon^8 y^e_{22} y^d_{23} (\alpha^2\sin^2\vartheta - 8\cos^2\vartheta + \alpha\sin 2\vartheta)/m^2_{\phi_S} \tag{5.2f}$$

$$S^\dagger S, (H^\dagger H)^2: \quad A_{\phi_H} \sim -5\epsilon^8 y^e_{22} y^d_{23} \cos\vartheta(2\alpha\cos\vartheta + \sin\vartheta)/\alpha m^2_{\phi_H} \tag{5.2g}$$

$$A_{\phi_S} \sim -5\epsilon^8 y^e_{22} y^d_{23} \sin\vartheta(2\alpha\sin\vartheta - \cos\vartheta)/\alpha m^2_{\phi_S} \tag{5.2h}$$

$$S^\dagger S, (H^\dagger H)(S^\dagger S): \quad A_{\phi_H} \sim \alpha^3\epsilon^8 y^e_{22} y^d_{23} \cos\vartheta(2\sin\vartheta - 3\alpha\cos\vartheta)/m^2_{\phi_H} \tag{5.2i}$$

$$A_{\phi_S} \sim -\alpha^3\epsilon^8 y^e_{22} y^d_{23} \sin\vartheta(2\cos\vartheta + 3\alpha\sin\vartheta)/m^2_{\phi_S} \tag{5.2j}$$

$$S^\dagger S, (S^\dagger S)^2: \quad A_{\phi_H} \sim \alpha^6\epsilon^8 y^e_{22} y^d_{23} \sin\vartheta(\alpha\cos\vartheta - 4\sin\vartheta)/m^2_{\phi_H} \tag{5.2k}$$

$$A_{\phi_S} \sim -\alpha^6\epsilon^8 y^e_{22} y^d_{23} \cos\vartheta(\alpha\sin\vartheta + 4\cos\vartheta)/m^2_{\phi_S} \tag{5.2l}$$

While there are differences in the form of each amplitude, they are all proportional to ϵ^8. This means the branching ratio of $\sim 10^{-9}$ is still within $< 4.7 \times 10^{-8}$, the experimental limit [25].

5.3 Top quark decay: $t \to c\phi_H$

Similar to $\phi_H \to b\bar{b}$, the decay $t \to c\phi_H$ is controlled by either $S^\dagger S$ or $H^\dagger H$. In the 12 $H^\dagger H$ models, the coupling of $t \to c\phi_H$ is $y^u_{23}\sqrt{2}\epsilon^2 \cos\vartheta$. The coupling of $t \to c\phi_S$ is $y^u_{23}\sqrt{2}\epsilon^2 \sin\vartheta$.

In the $S^\dagger S$ models the coupling of $t \to c\phi_H$ is $y^u_{23}\sqrt{2}\alpha\epsilon^2 \sin\vartheta$. The coupling of $t \to c\phi_S$ is $y^u_{23}\sqrt{2}\alpha\epsilon^2 \cos\vartheta$. These two diagrams add to produce the generic FCNC process $t \to cX$, which will be the same for both categories of models.

In all 24 models the coupling is proportional to $\sqrt{2}\epsilon^2$ which means that the branching ratio will be $\sim 8 \times 10^{-4}$. In the SM the branching ratio is $\sim 10^{-14}$ [31]. The LHC should be able to probe this range.

5.4 Double Higgs production

It is possible to pair produce the vector-like quarks of this model. The dominant decay mode (95%) is to a SM quark and a Higgs (e.g. $Q_L \to uh$). The Higgs will then decay to $b\bar{b}$. The signal for this process will be 4 b-jets and 2 hard jets. Taking the mass of the vector-like quarks to be 1 TeV, the production cross section for pair production at the LHC at 14 TeV is ~ 60 fb for each new quark [32]. Because there are more than 50 new quarks in each model, the total production cross section for all new quarks will be ~ 30 pb. We place kinematic cuts on the signal and background as follows: the invariant mass of the b-jets, $m_{bb} > 100$ GeV, the $p_T^{\text{jets}} > 100$ GeV and for the b-jets, $p_T^b > 30$ GeV. Using CalcHEP we find that imposing these cuts will reduce the branching ratio of the new quarks, such that $\text{BR}(Q_L \to uh) \sim 0.9$. If we take the b-tagging efficiency to be 50%, the signal is reduced by a factor of $\frac{1}{16}$. With

these cuts and 10 fb^{-1} of luminosity we would expect to see $\sim$ 30 events for each additional quark in the model.

The SM background for a six-b final state is calculated in Chapter 7. With the cuts imposed, the background is 60 fb. With a 100 GeV cut on each of the final state non-b-jets, we expect that the background for $4b + 2$ jets in the SM will be of similar order. With a few extra vector-like quarks from one of the models the signal should be much larger than the background and observable at the LHC with enough luminosity.

5.5 Chapter summary

The variations of the effective models have decays and exchange amplitudes that are different, based upon the interactions with Higgs doublet operator $H^\dagger H$ and the Higgs singlet operator $S^\dagger S$. Phenomena that distinguish between variations of the effective model have branching ratios that should fall within the observable limits of the LHC.

CHAPTER 6

MODEL WITH AN EXOTIC D-TYPE QUARK

Much of the previous chapters dealt with the impact the inclusion of an extra $U(1)_S$ symmetry can have on the SM and how it can be used to explain the variation in the Yukawa coupling magnitudes. The mechanism used to give the SM charged fermions their mass required the inclusion of heavy exotic quarks. However, the use of additional fields leads to the possibility of their detection at a collider with high enough energy.

Since the possible choices of which exotic quarks to include in the model is rather large, only one such exotic quark left-right pair will be considered, and will be referred to as D_L and D_R. They are color triplets and have the same hypercharge as the down-type quarks of the SM. However, they are both weak singlets, thus forming a vector-like pair, and the combination $D_L + D_R$ can be referred to as D. Under $U(1)_S$, the D has the opposite charge of the Higgs singlet S. Since the S has its charge normalized to 1, the D has a charge of -1.

The kinetic term of the Lagrangian for the D quark is given with the usual form of the covariant derivative, allowing for gauge interactions. The only type of gauge interactions it cannot directly have is through the $SU(2)_L$ group. Explicitly, it is

$$\overline{D} i \not{D} D = \overline{D} i \gamma^\mu \left(\partial_\mu - i g_C G_\mu + i g' \frac{1}{3} B_\mu + i g_S \frac{1}{2} {Z'}_\mu \right) D. \tag{6.1}$$

Below the breaking scale of any global $U(1)_{F_i}$ flavon symmetries, mass terms for D_L and D_R can be written down. Recalling Eq. (1.7), this is allowed because both are singlets under $SU(2)_L$ and have the same transformation properties ($V_L^\dagger V_R = 1$).

The mass terms are

$$\mathcal{L}^{\text{extra}}_{\text{mass}} = M_D \overline{D_L} D_R + M_D \overline{D_R} D_L. \tag{6.2}$$

Note that the new exotic vector-like quark D is like a new flavor, and it has color, hypercharge, and a $U(1)_S$ interaction. Without any other interaction, it will be stable. As none of the SM particles are charged under $U(1)_S$, the new symmetry will remain hidden from the SM, provided the gauge-kinetic-mixing terms are strongly suppressed. However, its gauge quantum numbers allow flavor changing Yukawa interactions with the down-type quarks and the singlet Higgs boson S with

$$\mathcal{L}^{\text{extra}}_{\text{Yukawa}} = f_{Dd^j} \overline{D_L} d^j_R S + h.c. \tag{6.3}$$

where D_L and D_R have the same hypercharge as d_R. Such a term in the Lagrangian leads to mixing between the SM down-type quarks with the new exotic vector-like quark D, giving rise to new decay modes for the heavy quark.

To understand the signatures of such an exotic quark at experiments, various mixings need to be considered which lead to the effective interaction of these exotics to SM particles and are responsible for their decays. We have already considered the mixing in the scalar sector of the model, which has interesting consequences for Higgs searches. We also find that by allowing the Yukawa interaction given in Eq. (6.3), there will be mixing between the down-type quarks with the new exotic quark D once the scalar S gets a vev. The mixing between the down-type quarks with the exotic D quark gives rise to additional EW decay modes for the heavy quark. The Z' also has additional interactions which lead to interesting decay modes.

For simplicity, we assume that only f_{Db} (the coupling between the D and the bottom quark) is non-zero in Eq. (6.3) while the other Yukawa coefficients are negligibly small. In the context of the charge space of the $U(1)_{F_i}$ symmetries, this is easily accommodated by a large enough separation between SM quark fields. This would

imply that the exotic quark mixes with the bottom quark. Thus when the EW symmetry breaks, it indirectly affects the top-bottom vertex (V_{tb} in the CKM matrix), as well as inducing a coupling between the exotic D quark with the top quark. The mixing can be parameterized in terms of two mixing angles θ_L and θ_R which represent the mixing angles of the b_L and b_R with D_L and D_R respectively. Expressing the gauge eigenstates for the mixing quarks as b^0 and D^0, the mass matrix in the (b^0, D^0) basis is given by

$$\mathcal{M} = \begin{pmatrix} f_b\, v_H/\sqrt{2} & 0 \\ f_{Db}\, v_S/\sqrt{2} & M_D \end{pmatrix}. \tag{6.4}$$

This matrix can be diagonalized with a bi-unitary transformation $\mathcal{M}_{\text{diag}} = \mathcal{R}_L \mathcal{M} \mathcal{R}_R^\dagger$, where $\mathcal{R}_L$ and $\mathcal{R}_R$ are unitary matrices which rotate the left-chiral and right-chiral gauge eigenstates to the mass eigenstates respectively. The interaction of the physical mass eigenstates (b, D) can then be obtained by writing the gauge basis states as

$$\begin{aligned} b_i^0 &= b_i \cos\theta_i + D_i \sin\theta_i, \\ D_i^0 &= -b_i \sin\theta_i + D_i \cos\theta_i, \end{aligned} \qquad \text{where } i = L, R. \tag{6.5}$$

The corresponding mixing angles for the left- and right-handed fields follow from the matrix $\mathcal{M}\mathcal{M}^\dagger$ and $\mathcal{M}^\dagger\mathcal{M}$ respectively and are given by

$$\tan 2\theta_L = \frac{-2\, f_{Db}\, f_b\, v_S\, v_H}{2M_D^2 + f_{Db}^2 v_S^2 - f_b^2 v_H^2}, \qquad \tan 2\theta_R = \frac{-2\sqrt{2}\, f_{Db}\, v_S\, M_D}{2M_D^2 - f_{Db}^2 v_S^2 - f_b^2 v_H^2}. \tag{6.6}$$

CHAPTER 7

PHENOMENOLOGY WITH AN EXOTIC D-TYPE QUARK

In hadronic colliders such as the LHC and Tevatron, the dominant signals arise from the pair productions of the exotic colored quarks, D and $\overline{D}$, and their subsequent decays (because D has hypercharge, the LEP2 bound of $\sim$ 100 GeV on its mass applies [33]). The other important production process is the pair productions of the exotic quark in association with the new $U(1)_S$ gauge boson, $D\overline{D}Z'$. It turns out that this is the only way the new gauge boson Z' can be produced on-shell at LHC because of its very suppressed or vanishing couplings to the SM particles in this model. In the following subsections we discuss the signals from the $D\overline{D}$ production. We also discuss the couplings of the extra gauge boson Z' with the SM particles.

7.1 Signals from $D\overline{D}$ productions

The heavy exotic quarks being colored particles will be produced copiously at the LHC through strong interactions. The major contribution, as in the case of top quarks, would come from the gluon induced subprocess ($\sim 80\%$). In Fig. 7.1 we plot the pair production cross section for the process

$$pp \longrightarrow D\overline{D} \tag{7.1}$$

at LHC for two different center-of-mass energies (7 TeV and 14 TeV).

The figure clearly shows that one can have quite large production cross section for such an exotic quark at the LHC and its signals should be observable through its decay products. We also include the most updated Tevatron bounds obtained by

CDF using 4.8 fb^{-1} data which rules out such exotic quarks with mass $m_D < 385$ GeV at 95% C.L. [35]. However, this bound assumes that the exotic bottom-type quark decays to tW with 100% probability. The bound gets diluted as the branching probability goes down, and in our case turns out to be ~ 300 GeV for our choice of model parameters. We have implemented the model into CalcHEP [36] to calculate the production cross sections as well as the two-body decays of the new particles in the model.

The heavy quark in the gauge eigenbasis couples directly to the Z' gauge boson

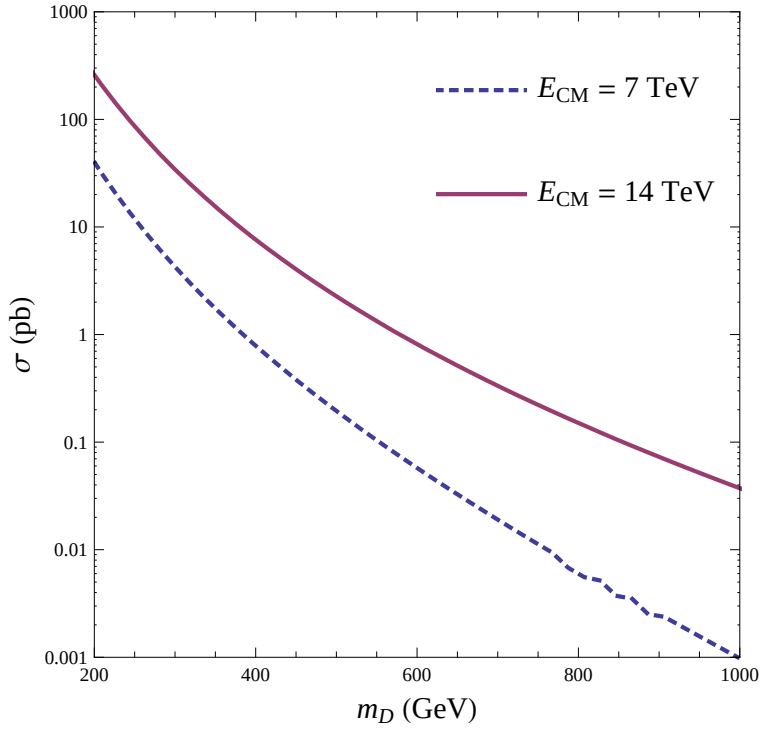

Figure 7.1: Pair production cross section for the exotic quarks at LHC as a function of its mass (m_D). We use the CTEQ6L1 parton distribution functions (PDF) [34] for the protons. We have set the scale $Q^2 = m_D^2$. We also include the cross section at the Tevatron experiment along with the observed data by CDF [35], excluding such an exotic quark of mass ≤ 385 GeV at 95% C.L.

through the $U(1)_S$ charge, with the gauge coupling strength g_S. However, its decay is more dependent on the mixing parameters resulting from its mixing with the b quark, leading to a much richer phenomenology. The heavy exotic itself is a mixed mass eigenstate and we list its couplings to the other particles of the model in Tables C.1–C.2.

The two body decay width for D of mass m_D in its rest frame is

$$\Gamma(D \to X_2 X_3) = \frac{1}{16\pi m_D} \lambda^{1/2} \left(1, \frac{m_{X_2}^2}{m_D^2}, \frac{m_{X_3}^2}{m_D^2}\right) \overline{|\mathcal{M}|^2}, \tag{7.2}$$

where the function $\lambda(x, y, z) = x^2 + y^2 + z^2 - 2(xy + yz + zx)$. Using the effective couplings given in Tables C.1–C.2, one can write down the explicit decay amplitudes for the exotic quarks decaying into vector (V) modes as

$$\begin{aligned} \overline{|\mathcal{M}|^2}(D \to \psi V) = K^2 \Bigg[& 3 \left(m_D^2 + m_\psi^2 - 2m_V^2 + \frac{(m_D^2 - m_\psi^2)^2}{m_V^2} \right) (c_V^2 + c_A^2) \\ & -18 m_D m_\psi (c_V^2 - c_A^2) \Bigg] , \end{aligned} \tag{7.3a}$$

and scalar (Φ) modes as

$$\overline{|\mathcal{M}|^2}(D \to \psi \Phi) = K^2 \left[3 \left(m_D^2 + m_\psi^2 - m_\Phi^2 \right) (c_S^2 + c_P^2) + 6 m_D m_\psi (c_S^2 - c_P^2) \right] . \tag{7.3b}$$

The parameters c_V, c_A, c_S, and c_P respectively refer to vector, axial, scalar, and pseudoscalar interactions. The parameter K is an overall factor common to all the interaction types in each equation.

We can now estimate the decay probabilities of the heavy exotic D quark. To highlight distinct scenarios, we choose two different sets of input values for the free parameters as representative points in the model listed in Table 7.1. Note that the input parameters for the model also affect some EW observables, e.g. the Z boson decay width or the mass limits for Higgs boson and other heavy exotics that appear in our model. We have checked that the input parameters given in Table 7.1 are allowed and do not contradict any existing experimental bounds [33]. In Fig. 7.2 we

Table 7.1: Representative points in the model parameter space and the relevant mass spectrum used in the analysis.

Parameters	Set I	Set II
$(\lambda_H, \lambda_S, \lambda_{HS})$	$(0.11, 0.16, 0.005)$	$(0.2, 0.05, 0.1)$
v_S	1000 GeV	800 GeV
f_{Db}	0.15	0.05
m_{ϕ_H}	115 GeV	127 GeV
m_{ϕ_S}	566 GeV	268 GeV
$m_{Z'}$	1000 GeV	800 GeV

present the decay branching ratios of the heavy quark D as a function of its mass m_D for the representative points I & II given in Table 7.1.

The curves in Fig. 7.2(a) represent Point-I from Table 7.1. When D is lighter than $m_t + m_W$ then it always decays to $Z\,b$ through mixing if its coupling to the lighter Higgs boson is very suppressed. This would happen when the lighter scalar state is dominantly an $SU(2)_L$ doublet. The $t\,W^-$ mode starts picking up and becomes comparable to the $Z\,b$ mode for heavier D. The decay mode $t\,W^-$ is common in 4th-generation models and theories with top or bottom partners [37, 38, 39, 40] and results in multi-lepton signals.

The curves in Fig. 7.2(b) represent Point-II, where the choice of parameters give a very suppressed mixing angle θ_L. The couplings of $Z\,b$ and $t\,W$ to the exotic quark are proportional to $\sin\theta_L$ and hence also get suppressed. As soon as the scalar modes become kinematically accessible, they completely dominate the decay properties of the exotic quark.

We find if the Z' boson is light, then as soon as the $D \to Z'b$ mode opens up, the remaining modes drop out very quickly for Point-I while for Point-II it becomes comparable to the scalar mode for very large mass m_D. It is worth pointing out

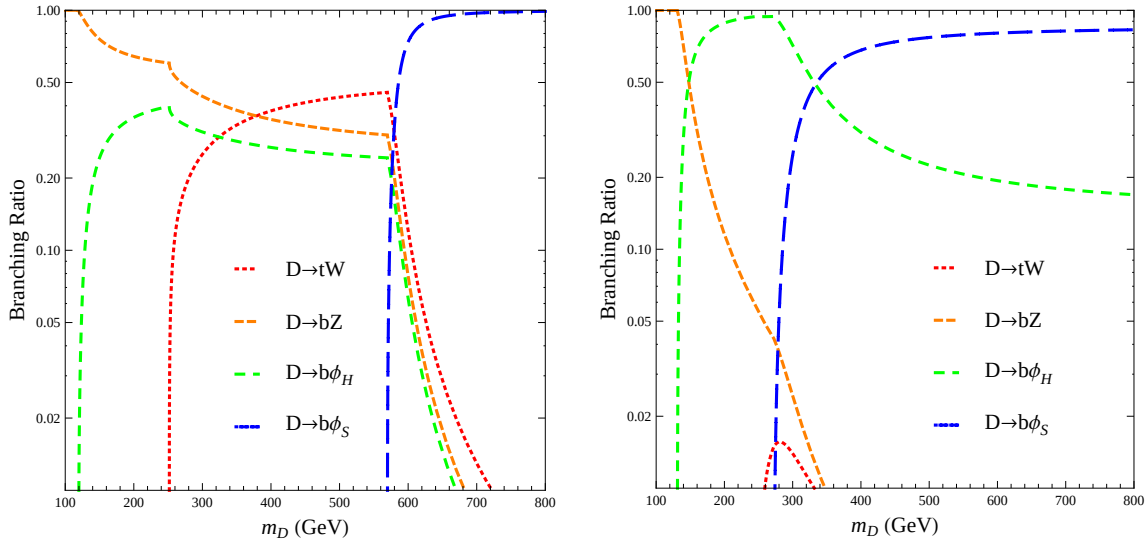

(a) Parameter Set I (b) Parameter Set II

Figure 7.2: Illustrating the decay probabilities of D as a function of its mass m_D.

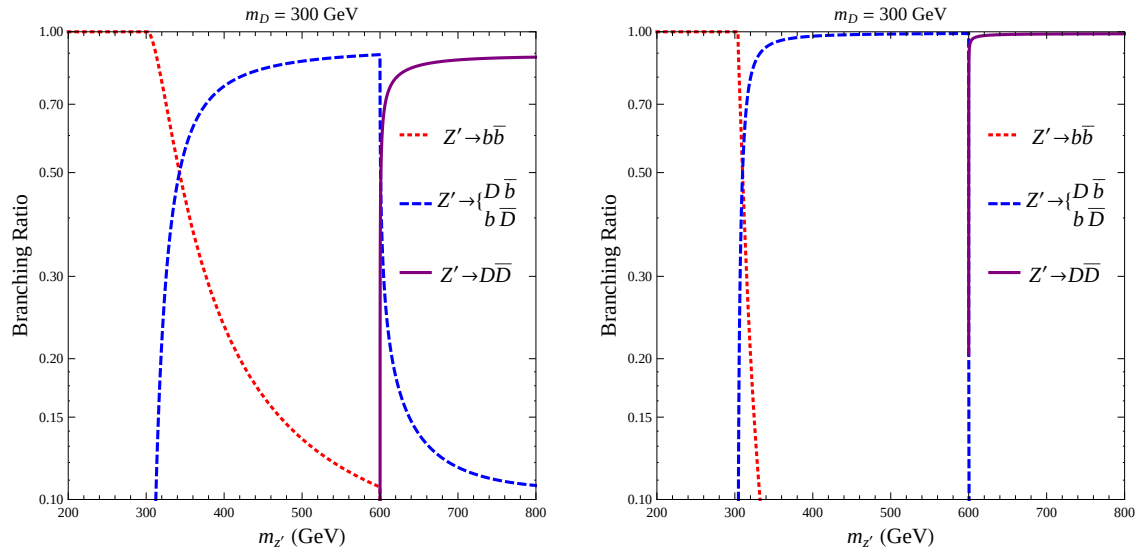

(a) Parameter Set I (b) Parameter Set II

Figure 7.3: Illustrating the decay probabilities of Z' as a function of its mass $m_{Z'}$.

here that the dominant decay mode for the Z' when $m_{Z'} < m_D$ is to $b\bar{b}$ with 100% branching probability. However for Z' heavier than D, the dominant decay of Z' is to $D\bar{b}$ and $\overline{D}b$ as shown in Fig. 7.3; and as soon as $m_{Z'} > 2\ m_D$ it decays dominantly to

Table 7.2: Branching Ratios for various Higgs decay modes for parameter sets I and II.

	Branching Ratios			Branching Ratios	
Decays	I	II	Decays	I	II
$\phi_H \to b\bar{b}$	0.672	0.510	$\phi_S \to \phi_H\phi_H$	0.25	0.27
$\phi_H \to c\bar{c}$	0.031	0.024	$\phi_S \to W^+W^-$	0.42	0.51
$\phi_H \to \tau^+\tau^-$	0.093	0.072	$\phi_S \to ZZ$	0.20	0.22
$\phi_H \to gg$	0.104	0.096	$\phi_S \to t\bar{t}$	0.13	–
$\phi_H \to WW^*$	0.088	0.266			

$\overline{D}D$ with maximum probability. We should also point out that the Z' phenomenology in our model is quite different from other models with $U(1)$ extension of the SM. As there exists no coupling between any SM fermion pair (other than b quark) or with the EW gauge bosons (no kinetic mixing), it is not possible to produce this particle directly through exchange of SM particles at LEP or Tevatron and so the strong constraints that exist on the mass of similar Z' exotics through the effective four-fermion operators [41] do not apply in our case and neither do the search limits from the Tevatron experiments [42]. Thus the Z' in our model can be light but remains invisible in the existing experimental data. We will however not discuss the Z' signals any further and only focus on the signals arising from the production of the exotic D quarks in the model. To understand the full decay chain of the D quark to final state particles we also list the decay probabilities of the scalars ϕ_H and ϕ_S in Table 7.2 for the two representative points I & II.

Thus the above decay patterns suggest that one can have the following interesting

final states from the decay of the exotic quarks:

$$pp \to D\overline{D} \to \begin{cases} \to b\bar{b} + 2Z & & \\ \to t\bar{t} + W^+W^- & & \\ \to t\bar{b} + ZW^- & & \\ \to b\bar{b} + 2\phi_H & \to b\bar{b} + 2(W^+W^-) & \\ \to b\bar{b} + 2\phi_H & \to 3(b\bar{b}) & \\ \to b\bar{b} + \phi_H\phi_S & \to b\bar{b} + 3\phi_H & \to 4(b\bar{b}) \\ \to b\bar{b} + 2\phi_S & \to b\bar{b} + 4\phi_H & \to 5(b\bar{b}) \end{cases} \tag{7.4}$$

where the first four suggest multi-lepton and multi-jet final states with two or more b-jets, while the remaining give more exotic signatures like N b-jet final states where N can be as large as 10. Note that the above decays only illustrate some of the possible decay chains and we have not listed other possible combinations of the D decays which can also lead to similar final states.

In Table 7.3 we list the probabilities for the decay modes for a few specific values of the D quark mass. We also show the corresponding cross sections for the pair production of these exotics at LHC for the center of mass energies of $\sqrt{s} = 7$ TeV and $\sqrt{s} = 14$ TeV. The decays suggest a large multiplicity of b quarks in the final state. It turns out that six-b final states for the signal are very promising. However, there exists no estimate for this final state in the literature, arising from the SM. We present below a leading-order (LO) estimate of the cross section for the six-b SM background from QCD for LHC energies.

7.2 Calculation of six-b final states from QCD

The six-b final state is interesting, independent of our particular model. The presence of six b-jets allow the jets to be tagged. All other six-jet final states involve mixtures of light quarks and gluons, and one cannot separate light jets from gluon jets. There-

Table 7.3: Cross sections and branching probabilities for specific mass values of D quark for the representative points I and II.

			Branching Ratios							
m_D	$\sigma(D\bar{D})$(pb)		$D \to tW$		$D \to bZ$		$D \to b\phi_H$		$D \to b\phi_S$	
	7 TeV	14 TeV	I	II	I	II	I	II	I	II
250	12.15	87.760	0	0	0.603	0.055	0.397	0.945	0	0
300	4.265	34.368	0.251	0.014	0.438	0.024	0.311	0.715	0	0.247
400	0.791	7.692	0.381	0.005	0.351	0.005	0.268	0.308	0	0.681
500	0.194	2.270	0.434	0.003	0.316	0.002	0.250	0.225	0	0.770
600	0.059	0.820	0.121	0.002	0.078	0.001	0.063	0.194	0.738	0.803

fore the six-b final state itself presents an interesting test of QCD. Furthermore by computing the full matrix element, we can test the validity of the differential cross section by looking at differential observables. While we only use the six-b cross section as a background to our signal, this is the first time such a six-b cross section in QCD has been estimated, and this also is an important result of this paper.

Any six-final state process is a challenge to compute. The phase space is 14 dimensional (excluding the two additional integrations over the initial parton fluxes). There are thousands of diagrams, and thousands of distinct color configurations. While six-jet final states are produced every day by Monte Carlo generators such as Pythia [43] and Herwig [44], the mechanism they use creates additional jets from an initial $2 \to 2$ or $2 \to 3$ process via a showering procedure that resums leading logarithms, splitting an extra gluon from the hard final state partons.

As is well known, the showering procedure cannot produce the correct correlations among three or more hard jets, nor can it compute the total cross section for three or more hard jets. It assumes that each parton is independent of all the others. For a single radiation it is strictly correct in the limit that the extra radiation is soft and/or

collinear with the initial parton. However, for multiple radiations it ignores the QCD connection among the radiations, assuming that each radiation factorizes from the others. There is also quantum mechanical interference in different radiations which result in the same final state that is ignored.

This means that one should not examine in detail observables such as the angles between jets, invariant masses of jet pairs, or the thrust, when one hard jet came from the showering procedure. This showering technique is however extremely useful as long as one is not sensitive to the details of correlations in the differential cross section, as this method is computationally simpler than a full matrix element calculation.

Therefore, to have an accurate Monte Carlo with six jets in the final state, one must compute the full matrix element, which automatically includes all color flows and interference. This is accurate to approximately the 10% level, at which point NLO loop corrections become important. Note that due to the b quark mass, there is no soft radiation which benefits significantly from the usual Sudakov logarithm resummation. The b mass acts as a regulator, relegating this cross section strictly into the "hard" regime, in which the matrix element is valid. Even if all six b quarks are at rest, the energy in the final state is 30 GeV, and any virtual gluon must have a virtuality $q^2 \sim m_b^2$.

For this calculation we have chosen the tool MadEvent, which is an event generator built upon the matrix element generator MadGraph [45]. We have modified these tools to be able to cope with thousands of diagrams and thousands of color configurations. Computing five-final state and six-final state QCD processes has a number of challenges, all of which are technical rather than physics-based. MadEvent is in principle capable of computing any process with any number of final state particles, however several internal restrictions[1] caused previous versions to fail on processes

[1]MadGraph internally writes several arrays of size $N_D \times N_D$ and $N_{Cf} \times N_{Cf}$ into the Fortran matrix element output, where N_D (N_{Cf}) is the number of diagrams (color configurations). For

such as a six-b final state. Although the program is equipped to handle the large color configurations, some input/output statements restrict this computation to a smaller number of color flow configurations which makes it incapable of calculating the six-b final states at a hadron machine like the LHC. These input/output statements have been repaired to permit larger color flow configurations so that the six-b cross section in the SM from QCD can be calculated for the LHC.

7.3 Signal and background analysis

A simple minded estimate of the cross section using $\sigma \times BR$ shows that the final states which would be of interest at the LHC would involve at least two b-jets in the final state. Besides the two hard b-jets, one expects charged leptons in the final state coming from the decays of the weak gauge bosons. It is also worth noting that when the D quark decays to the Higgs bosons, one would get a large multiplicity of b-jets in the final states as the Higgs with $m_{\phi_H} < 2m_W$ dominantly decays to b-jets. To select our events for the final states given in Table 7.4, we have imposed the following kinematic cuts:

- All b-jets must have a $p_T^b > 20$ GeV and lie within the rapidity gap of $|\eta^b| < 3.0$.
- All charged leptons ($\ell = e, \mu$) must have a $p_T^\ell > 20$ GeV and lie within the rapidity gap of $|\eta^\ell| < 2.5$.

$N_{Cf} \sim N_D \sim 1000$, this results in 1 MB fortran files that cause optimizing compilers (even with optimizations turned off) to use approximately 1000 times the size of the array in compiling it. Thus, the compiler uses $\mathcal{O}(1$ GB) of memory just to compile the process. As modern 32-bit computers can address at most 4 GB of memory, a process with $N_D \sim 1000$ and/or $N_{Cf} \sim 1000$ is at the limit of being able to be compiled at all. These arrays contain many zeroes, and their presence at compile-time drastically improves performance since optimizing compilers can pre-compute many results, and prevent the computation of irrelevant results. However, for extremely large processes, one can simply read in these arrays. A 1 MB array is not very large after all. This enables the computation of even larger processes, at the expense of increased run-time.

- The final states also must satisfy $\Delta R_{bb} > 0.7$, $\Delta R_{b\ell} > 0.4$, and $\Delta R_{\ell\ell} > 0.2$ where $\Delta R_{ij} = \sqrt{(\Delta\eta_{ij})^2 + (\Delta\phi_{ij})^2}$.

- All b-jet pairs must have a minimum invariant mass $M_{bb} > 10$ GeV.

In Table 7.4 we present the cross-sections for the signal for two different mass values of the exotic D quark after passing through the above mentioned kinematic cuts. As expected, the favored final states are dependent on the high b-jet multiplicity. At the hadron collider such as LHC, one favors final states with leptons. However b-jets can also be triggered upon and identified and thus can prove to be useful in isolating new physics signals such as ours which involve at least two or more b-jets. Looking at Table 7.4 we find that we get a good signal rate for the inclusive $6b + X$ final state. The SM background for multi-b final state is quite large [46]. However no estimate of a six-b final state exists in the literature, which we find relevant for our signal. We have used the MadGraph+MadEvent package to estimate the leading order partonic cross section for the six-b final state at LHC. With the above mentioned kinematic cuts, we find that for LHC energy of $\sqrt{s} = 14$ TeV, the SM background for six-b final state is ~ 70 fb and falls to less than 10 fb for the $\sqrt{s} = 7$ TeV option. This implies that the signal in our model is much larger than the SM background even for larger mass values of the exotic D quark. The other signals which are worth looking for in this model is one or two charged leptons with varying b-jet multiplicities. We have listed the interesting ones in Table 7.4. The final state with $2\ell+4b+X$ also stands out against the SM background, where one gets the SM cross sections to be quite small as it is already $\alpha_{\rm EW}/\alpha_{\rm strong}$ suppressed compared to the six-b cross section. The SM background is much larger for the final states $\ell+nb+X$ where $n = 2$ and $2\ell+2b+X$, where the significant SM background results from the $t\bar{t}$ production. For the final states $\ell + nb + X$ one can get rid of the huge $t\bar{t}$ background by demanding $n \geq 3$. This helps in improving the significance of the signal, even though we also lose a large fraction of the signal events in the process. For the other final state, we find that at

Table 7.4: Illustrating the final state cross sections after the decay of D quarks. All cross sections are in units of femtobarn (fb).

	$m_D = 300$ GeV				$m_D = 500$ GeV			
Final	$\sqrt{s} = 7$ TeV		$\sqrt{s} = 14$ TeV		$\sqrt{s} = 7$ TeV		$\sqrt{s} = 14$ TeV	
States	I	II	I	II	I	II	I	II
$6b + X$	181.92	718.79	1394.32	5521.23	4.94	10.79	531.10	115.02
$4b + 2\ell + X$	51.07	24.36	384.24	183.73	1.85	2.06	20.33	22.20
$2b + 2\ell + X$	146.53	14.95	1127.15	117.08	8.71	6.61	11.77	75.56
$nb + \ell + X$ $(n \geq 2)$	452.50	188.22	3559.94	1465.42	32.17	27.88	43.37	313.96

leading order, at LHC with pp collision energy of $\sqrt{s} = 7$ TeV, the $2\ell + 2b + X$ SM background is ~ 3.3 pb. As the leading two b-jets in our signal come from the decays of the heavy exotic D quark, we put a stronger p_T cut of 100 GeV. This reduces the signal by two-thirds. However the SM background is reduced by more than an order of magnitude, and becomes ~ 232 fb for $\sqrt{s} = 7$ TeV collisions while it is ~ 1.63 pb for $\sqrt{s} = 14$ TeV which does look promising for the signal with large enough luminosities at the LHC. We must point out that we have not incorporated any efficiency factors for our final state particles. Most notably, all numerical estimates involving b-jets for signal as well as the SM background will have to be scaled with the b-tagging efficiency of around 50 to 60% expected at the LHC [47].

7.4 Chapter summary

In this work, we have proposed a new extension of the SM, by introducing a hidden $U(1)$ symmetry. The difference with the previously studied $U(1)$ symmetries is that all the SM particles are singlets under our proposed new $U(1)_S$, and hence hidden.

Such a symmetry may be present at the TeV scale, and may manifest at the LHC giving new signals observable at the LHC. The model incorporates a new EW singlet Higgs, as well as new vector-like charge $-1/3$ quarks.

The new massive vector boson Z' resulting from the broken hidden $U(1)_S$ symmetry does not couple to the SM fields directly and may be hidden in all experimental data due to the very small mixing parameters making its production cross section too small to observe. However, if once produced it can be observed through its decays. We leave its detailed phenomenological study for future work and have focused on the exotic colored fermion in the model.

We have studied the pair productions of these new quarks and their subsequent decays. The dominant final states include multiple b-jets with high p_T or b-jets plus charged leptons with high p_T and missing energy, and stands out beyond the SM background. The most distinctive final state signal is six-b with high p_T and no missing energy. A lot of effort has been put in both for the ATLAS and CMS detectors to improve the b-tagging efficiency. So the calculation for this six-b final state is also of great importance in the SM, and has not yet been calculated. We have calculated this six-b signal in our model, and have also estimated the SM expectation using MadGraph and MadEvent. We found that the signal in our model stands well above that expected from the SM.

CHAPTER 8

NEUTRINO MASSES FROM FINE-TUNING

In the SM, there are no right-handed neutrinos ν_R. This prevents a Yukawa term from being written down (i.e. $\overline{l_L} f^\nu \nu_R \widetilde{H}$ is not allowed in SM). Consequently, the neutrinos are predicted to be massless. However, experiments over the past decade have established the existence of tiny neutrino masses [48, 49, 50, 51, 52, 53, 54]. It has been shown that the mixing angles between the neutrinos are relatively large when compared to the quark mixing angles. And because the neutrinos are electrically neutral, there exists the possibility the neutrinos may be Majorana spinors, unlike all the other fundamental fermions which are Dirac spinors. And it still cannot be determined if they have a normal mass hierarchy or an inverted hierarchy.

The most popular idea proposed so far for understanding the tiny neutrino mass is the famous see-saw mechanism [55, 56, 57, 58, 59]. One postulates the existence of a very massive SM singlet right-handed neutrino with Majorana mass M_R of order of $\sim 10^{14}$ GeV. The Yukawa coupling of the left-handed (LH) neutrino to this heavy right-handed (RH) neutrino then gives a Dirac mass of the order of the charged lepton masses m_l, which comes from the first term of the effective mass terms

$$m_l \overline{\nu_L} N_R + \frac{M_R}{2} N_R^{\mathrm{T}} C^{-1} N_R + h.c. \tag{8.1}$$

As a result, the LH neutrino obtains a mass of the order of m_l^2/M_R, as can be seen by an expansion of the mass eigenvalues:

$$\begin{pmatrix} 0 & m_l \\ m_l & M_R \end{pmatrix} \rightarrow \frac{1}{2}\left(M_R \pm \sqrt{M_R^2 + 4m_l^2}\right) \approx \begin{cases} -\frac{m_l^2}{M_R} + \mathcal{O}(m_l^4/M_R^3) \\ M_R + \mathcal{O}(m_l^2/M_R) \end{cases} . \tag{8.2}$$

The see-saw mechanism does not naturally lead to small values of the experimentally observed neutrino masses, but it does accommodate them with appropriately large values of M_R. Although there are several indirect benefits for the existence of massive RH neutrinos, there is no direct experimental evidence for such heavy particles. The mass scale is so high that no connection can be made with the physics to be explored at the high energy colliders such as the Tevatron and the LHC. It is important to explore other possibilities to explain the tiny neutrino masses.

Recent astrophysical observation requires a tiny but non-zero value of the cosmological constant ($\Lambda^{1/4} \simeq 10^{-4}$ eV). This value is surprisingly close to the value of the light neutrino masses required from the neutrino oscillation experiments ($\simeq 10^{-2}$ to 10^{-1} eV). It has been exceedingly difficult to derive such a tiny value for the cosmological constant, and there is some acceptance that it may be fine-tuned. The idea of the Higgs mass also being fine-tuned has been explored, leading to the so-called "Split Supersymmetry" [60] with interesting implications at the TeV scale that can be explored at the LHC. With neutrino masses being in the same ballpark as the cosmological constant, it is not unreasonable to assume that their values are also fine-tuned. The objective in this project is to adopt this philosophy, build a concrete model realizing this scenario, and explore its phenomenological implications, especially for the LHC.

In this work, we present a model in which the light neutrinos get their masses from the usual see-saw mechanism, except the RH neutrino masses are at the EW scale. The neutrino Dirac masses get contributions from two different Higgs doublets with their vevs at the EW scale. The neutrino masses are small, but not because of tiny Yukawa couplings or tiny vevs of the new Higgs doublets [61, 62]. In fact, we take the Yukawa couplings to be of order one. The smallness of the light neutrino masses are due to a cancelation in the Dirac neutrino mass matrix, making $m_{\rm Dirac} \sim \mathcal{O}(10^{-4})$ GeV and giving rise to light neutrino masses $m_\nu \sim m_{\rm Dirac}^2/M$ where M is

the RH Majorana neutrino mass. Thus with M in the EW scale, we get the light neutrino masses in the correct range of 10^{-2} to 10^{-1} eV.

This chapter explores a combination of the see-saw mechanism with fine-tuning to produce tiny masses for the LH neutrinos. It also yields massive RH neutrinos, but their masses are in the TeV scale. Unlike the previous chapters, a $U(1)$ symmetry is not employed. Instead a discrete Z_2 symmetry is used.

8.1 Model

8.1.1 The fields under a Z_2 symmetry

The model is based on the SM gauge symmetry, $SU(3)_C \times SU(2)_L \times U(1)_Y$, supplemented by a discrete Z_2 symmetry. In addition to the SM fermions and the Higgs doublet H, we introduce three RH neutrinos N_{Ri} $(i = 1, 2, 3)$ and two additional Higgs doublets H_1, H_2 with vevs at the EW scale. All the SM particles are even under the Z_2 symmetry, while the three RH neutrinos and the two new Higgs doublets are odd under Z_2. The Z_2 symmetry is softly broken by the bilinear Higgs terms in the potential. With this symmetry, the Yukawa interactions from the SM remain unchanged:

$$\mathcal{L}_{\rm SM}^{\rm Yuk} = \overline{q_L} f^u u_R \widetilde{H} + \overline{q_L} f^d d_R H + \overline{l_L} f^e e_R H + h.c. \tag{8.3}$$

Here the fermion fields span the three generations (indices are suppressed), and f^u, f^d, and f^e are the three Yukawa coupling matrices of the SM. New terms in the Lagrangian allowed by the odd fields include

$$\mathcal{L}_{\rm new}^{\rm Yuk} = \overline{l_L} f^{1\nu} N_R \widetilde{H}_1 + \overline{l_L} f^{2\nu} N_R \widetilde{H}_2 + h.c., \tag{8.4}$$

$$\mathcal{L}_{\rm Maj} = \frac{1}{2} M_{\rm Maj} N_R^T C^{-1} N_R, \tag{8.5}$$

where $f^{1\nu}$ and $f^{2\nu}$ are new Yukawa coupling matrices and $M_{\rm Maj}$ is the Majorana mass matrix (again, generation indices are suppressed).

When the new Higgs fields H_1, H_2 acquire vevs v_1, v_2, the resulting 3×3 Dirac mass matrix is

$$m_{\text{Dirac}} = \frac{1}{\sqrt{2}} \left(f^{1\nu} v_1 + f^{2\nu} v_2 \right). \tag{8.6}$$

Arranging the three LH and the three RH neutrinos in a six component vector, the full 6×6 neutrino mass matrix is

$$M^{\text{Full}} = \begin{pmatrix} 0 & m_{\text{Dirac}} \\ (m_{\text{Dirac}})^{\text{T}} & M_{\text{Maj}} \end{pmatrix}. \tag{8.7}$$

For the mass scales in which $m_{\text{Dirac}} \ll M_{\text{Maj}}$, the 3×3 light neutrino mass matrix is given by

$$m_{\nu}^{\text{light}} = -m_{\text{Dirac}} M_{\text{Maj}}^{-1} (m_{\text{Dirac}})^{\text{T}}. \tag{8.8}$$

Note that experimentally, masses of the light neutrinos are in the 10^{-1} eV range. Thus with M_{Maj} in the TeV scale, the matrix m_{Dirac} needs to be in the scale of 10^{-4} GeV. With the vevs v_1, v_2 in the EW scale, we can get m_{Dirac} in the 10^{-4} GeV scale by assuming the Yukawa couplings to be very tiny, of order 10^{-6}. Such a choice, similar to the usual see-saw, will not have any interesting implications for neutrino physics in the TeV scale. Instead, we assume that the Yukawa couplings $f^{1\nu}$, $f^{2\nu}$ are of order one, and these Yukawa couplings and vevs v_1, v_1 are fined-tuned to get m_{Dirac} on the order of 10^{-4} GeV. As we will see, this gives interesting implications for neutrino physics at the TeV scale, and can be explored at the LHC.

8.1.2 Higgs potential

In addition to the usual SM Higgs H, two other Higgs doublets H_1, H_2 are required in this model. The only fermions these two new Higgs doublets couple to are the neutrinos, and this is imposed using the Z_2 symmetry. It is the cancelation of contributions to the Dirac neutrino mass from these two new doublets that enable the use of fine-tuning.

We assume that the Z_2 symmetry is softly broken by the bilinear terms in the Higgs Potential. This will allow these two new Higgs doublets to mix with the SM Higgs doublet, and as we will see, this will produce entirely new signals for the SM Higgs boson decays. The Higgs potential is given by

$$\mathcal{V} = \mathcal{V}^{(2)\text{even}} + \mathcal{V}^{(2)\text{odd}} + \mathcal{V}^{(4)\text{even}}, \tag{8.9a}$$

$$\mathcal{V}^{(2)\text{even}} = \mu_H^2 H^\dagger H + \mu_1^2 H_1^\dagger H_1 + \mu_2^2 H_2^\dagger H_2 + \mu_{12}^2 (H_1^\dagger H_2 + H_2^\dagger H_1), \tag{8.9b}$$

$$\mathcal{V}^{(2)\text{odd}} = \mu_{H1}^2 (H^\dagger H_1 + H_1^\dagger H) + \mu_{H2}^2 (H^\dagger H_2 + H_2^\dagger H), \tag{8.9c}$$

$$\begin{aligned}
\mathcal{V}^{(4)\text{even}} = {} & \lambda (H^\dagger H)^2 + \lambda_1 (H_1^\dagger H_1)^2 + \lambda_2 (H_2^\dagger H_2)^2 \\
& + \lambda_{1122} (H_1^\dagger H_1)(H_2^\dagger H_2) + \lambda_{HH12} (H^\dagger H) \left(H_1^\dagger H_2 + H_2^\dagger H_1 \right) \\
& + \lambda_{HH22} (H^\dagger H)(H_2^\dagger H_2) + \lambda_{1112} (H_1^\dagger H_1) \left(H_1^\dagger H_2 + H_2^\dagger H_1 \right) \\
& + \lambda_{HH11} (H^\dagger H)(H_1^\dagger H_1) + \lambda_{2212} (H_2^\dagger H_2) \left(H_1^\dagger H_2 + H_2^\dagger H_1 \right) \\
& + \lambda_{12} (H_1^\dagger H_2)^2 + \lambda_{H1} (H^\dagger H_1)^2 + \lambda_{H2} (H^\dagger H_2)^2 \\
& + \lambda_{H1H2} \left(H^\dagger H_1 + H_1^\dagger H \right) \left(H^\dagger H_2 + H_2^\dagger H \right).
\end{aligned} \tag{8.9d}$$

Note that the odd part of the potential breaks the Z_2 symmetry softly, and as a result, SM Higgs bosons can mix with the two new Higgs doublets. This will have interesting implications for the SM Higgs boson decays.

Since there are three Higgs doublets, after EW symmetry breaking, there will remain a pair of charged Higgs ($H^\pm, H'^\pm$), three neutral scalar Higgses (h', H_1', H_2'), and two neutral pseudoscalar Higgses (A_1', A_2'). Due to the breaking of the Z_2 symmetry, there is mixing within each of these three groups of Higgses (but not between groups). We denote the mass eigenstates of the three neutral Higgses by h, H_{10}, and H_{20}.

8.1.3 Mixing between the light and heavy neutrinos

In our model, we are considering a scenario in which the three RH handed neutrinos have masses in the EW scale having order one Yukawa couplings with the light LH neutrinos. They mix with the light neutrinos, and thus will participate in the gauge

interactions. The LEP experiment has searched for such RH neutrinos. Before we discuss these constraints, let us first consider the mixing between the light neutrinos and the RH neutrinos. Using the observed values of the light neutrino masses and mixings, we can make a reasonable estimate of the mixing between the LH and RH neutrinos. We use the normal hierarchy for the light neutrino masses with the values

$$m_{\nu\text{Eigenvalues}}^{\text{light}} = \text{Diag}(m_{\nu_1}, m_{\nu_2}, m_{\nu_3}) = \text{Diag}(0, 8.71, 49.3) \times 10^{-12} \text{ GeV}. \tag{8.10}$$

The mixing matrix $R_{\nu\nu}$ follows the standard parametrization. The angles θ_{12} and θ_{23} are the central values from experiment, and θ_{13} is the maximal value allowed by current experiment. Thus we have

$$(\theta_{12}, \theta_{23}, \theta_{13}) = (0.601, 0.642, 0.226), \tag{8.11}$$

$$R_{\nu\nu} = \begin{pmatrix} 0.804 & 0.551 & 0.223 \\ -0.563 & 0.585 & 0.584 \\ 0.190 & -0.595 & 0.781 \end{pmatrix}. \tag{8.12}$$

The three possible CP-violating phases are assumed to be zero. From the above mass eigenvalues and the mixing matrix, we can calculate the light neutrino mass matrix using

$$(R_{\nu\nu})^{\text{T}} m_{\nu}^{\text{light}} R_{\nu\nu} = m_{\nu\text{Eigenvalues}}^{\text{light}}. \tag{8.13}$$

For simplicity, we assume that the 3×3 Majorana mass matrix M_{Maj} to be proportional to the unit matrix,

$$M_{\text{Maj}} = \text{Diag}(M, M, M). \tag{8.14}$$

As a consequence of this choice for M_{Maj} and having a symmetric m_{Dirac}, the mixing matrix among only the generations of heavy neutrinos is equivalent to the mixing matrix among only the generations of light neutrinos (i.e. $R_{NN} = R_{\nu\nu}$). Using the

Table 8.1: Solution values for the matrix $m_{\rm Dirac}$.

(GeV)	Set 1	Set 2
m_{11}	-1.25×10^{-5}	-5.43×10^{-6}
m_{12}	-1.87×10^{-5}	-2.80×10^{-7}
m_{13}	-2.67×10^{-6}	2.20×10^{-5}
m_{22}	-3.42×10^{-5}	1.40×10^{-5}
m_{23}	-2.20×10^{-5}	4.25×10^{-5}
m_{33}	-5.36×10^{-5}	3.27×10^{-5}

values from Eq. (8.12) and choosing $M = 100$ GeV, we can now calculate numerically the 3×3 Dirac neutrino mass matrix from the equation

$$m_\nu^{\rm light} = -m_{\rm Dirac} M_{\rm Maj}^{-1} m_{\rm Dirac}^{\rm T}. \tag{8.15}$$

There are four sets of real solutions for $m_{\rm Dirac}$. Only two sets of solutions are presented in Table 8.1. The other two are just the negatives of these two sets. Using the solutions for $m_{\rm Dirac}$ and $M_{\rm Maj}$, we can now use the full 6×6 neutrino mass matrix $M^{\rm Full}$ and calculate the full mixing matrix Q and the mixing angles between the heavy and light neutrinos. They are given by

$$M^{\rm Full} = \begin{pmatrix} 0_{3\times3} & m_{\rm Dirac} \\ (m_{\rm Dirac})^{\rm T} & M_{\rm Maj} \end{pmatrix}, \qquad Q^{-1} M^{\rm Full} Q = M^{\rm Full}_{\rm Eigenvalues}. \tag{8.16}$$

The parametrization of Q is

$$Q = \begin{pmatrix} C_{\nu\nu} & C_{\nu N} \\ C_{N\nu} & C_{NN} \end{pmatrix} \begin{pmatrix} 1_{3\times3} & 0 \\ 0 & R_{NN} \end{pmatrix} \begin{pmatrix} R_{\nu\nu} & 0 \\ 0 & 1_{3\times3} \end{pmatrix} = \begin{pmatrix} C_{\nu\nu}R_{\nu\nu} & C_{\nu N}R_{NN} \\ C_{N\nu}R_{\nu\nu} & C_{NN}R_{NN} \end{pmatrix}. \tag{8.17}$$

The rotation matrices C_{ij} between light and heavy neutrinos are arranged as

$$\begin{pmatrix} C_{\nu\nu} & C_{\nu N} \\ C_{N\nu} & C_{NN} \end{pmatrix} = (C_{36}C_{35}C_{34})(C_{26}C_{25}C_{24})(C_{16}C_{15}C_{14}), \tag{8.18}$$

and each C_{ij} depends on the mixing angle θ_{ij}. The values $i = 1, 2, 3$ are for the three generations of LH neutrinos, and the values $j = 4, 5, 6$ are for the three generations of RH neutrinos.

For solution set 1, the full rotation matrix is

$$Q \approx \begin{pmatrix} \begin{matrix} 0.80 & 0.55 & 0.22 \\ -0.56 & 0.59 & 0.58 \\ 0.19 & -0.60 & 0.78 \end{matrix} & \begin{pmatrix} 3.1 \times 10^{-3} & 1.6 & 1.6 \\ 3.513 \times 10^{-3} & 1.7 & 4.1 \\ -2.5 \times 10^{-3} & -1.8 & 5.5 \end{pmatrix} \times 10^{-7} \\ \begin{pmatrix} 1.1 \times 10^{-4} & -1.6 & -1.6 \\ 1.3 \times 10^{-4} & -1.7 & -4.1 \\ -8.8 \times 10^{-5} & 1.8 & -5.5 \end{pmatrix} \times 10^{-7} & \begin{matrix} 0.81 & 0.55 & 0.22 \\ -0.56 & 0.59 & 0.58 \\ 0.19 & -0.60 & 0.78 \end{matrix} \end{pmatrix}. \tag{8.19}$$

For solution set 2, the full rotation matrix is

$$Q \approx \begin{pmatrix} \begin{matrix} 0.80 & 0.55 & 0.22 \\ -0.56 & 0.59 & 0.58 \\ 0.19 & -0.60 & 0.78 \end{matrix} & \begin{pmatrix} 4.1 \times 10^{-3} & 1.6 & -1.6 \\ 3.9 \times 10^{-3} & 1.7 & -4.1 \\ -5.7 \times 10^{-3} & -1.8 & -5.5 \end{pmatrix} \times 10^{-7} \\ \begin{pmatrix} -8.9 \times 10^{-4} & -1.6 & 1.6 \\ -7.9 \times 10^{-4} & -1.7 & 4.1 \\ 1.4 \times 10^{-3} & 1.8 & 5.5 \end{pmatrix} \times 10^{-7} & \begin{matrix} 0.80 & 0.55 & 0.22 \\ -0.56 & 0.590 & 0.58 \\ 0.19 & -0.60 & 0.78 \end{matrix} \end{pmatrix}. \tag{8.20}$$

As can be seen on Table 8.2, the mixing between the heavy and light neutrinos is extremely small.

8.2 Phenomenological implications

In this section, we discuss the phenomenological implications of our model. We are considering RH neutrinos at the EW scale. Their mass can be below the W boson mass. Thus they can be searched for at LEP, Tevatron, and the LHC. First we discuss the constraints that already exist from the search at LEP.

Table 8.2: Mixing angles between the light neutrinos (subscripts $1, 2, 3$) and the heavy neutrinos (subscripts $4, 5, 6$).

$(\times 10^{-7})$	θ_{14}	θ_{15}	θ_{16}	θ_{24}	θ_{25}	θ_{26}	θ_{34}	θ_{35}	θ_{36}
Set 1	1.2	1.9	0.26	1.9	3.4	2.2	0.26	2.2	5.3
Set 2	0.55	0.36	-2.2	0.034	-1.4	-4.2	-2.2	-4.2	-3.2

8.2.1 LEP constraints

Searches for N_R have been conducted at LEP in the channel $e^+e^- \to Z \to N_R\nu_L$, with N_R subsequently decaying to W^+e^- or $Z\nu$. This experiment puts limits on the mixing angle θ between the heavy and the light neutrinos [63] with

$$\sin^2\theta < 10^{-4} \qquad \text{for } 3 \text{ GeV } < M_N < 80 \text{ GeV}, \tag{8.21}$$

$$\sin^2\theta < 0.1 \qquad \text{for } M_N > 80 \text{ GeV}. \tag{8.22}$$

As we discussed in the previous section, the mixing angles θ between the light and heavy neutrinos are extremely small, ranging between $\sim 10^{-6}$ to 10^{-8}. Thus in our model, LEP constraints allow small masses for the heavy Majorana neutrinos.

8.2.2 Higgs decays and Higgs signals

In our model, the Yukawa couplings between the LH neutrinos, the RH neutrinos, and the new Higgs fields H_1, H_2 are of order one. The SM Higgs H mixes with the new Higgses, and these mixings are naturally large. Thus for $M_N < M_h$, the SM Higgs will dominantly decay to a ν and N_R as soon as this decay mode becomes kinematically allowed, because the coupling for this decay mode is much larger than the usually dominant $\bar{b}b$ mode or even the WW mode. The branching ratios for the various Higgs decay modes are shown in Fig. 8.1 for $M_N = 80$ GeV for the Yukawa couplings $f^{1\nu} + f^{2\nu} = 1$. As can be seen from the plot, as soon as the decay mode $h \to \nu N_R$ becomes kinematically allowed, this mode dominates over the usual $\bar{b}b$

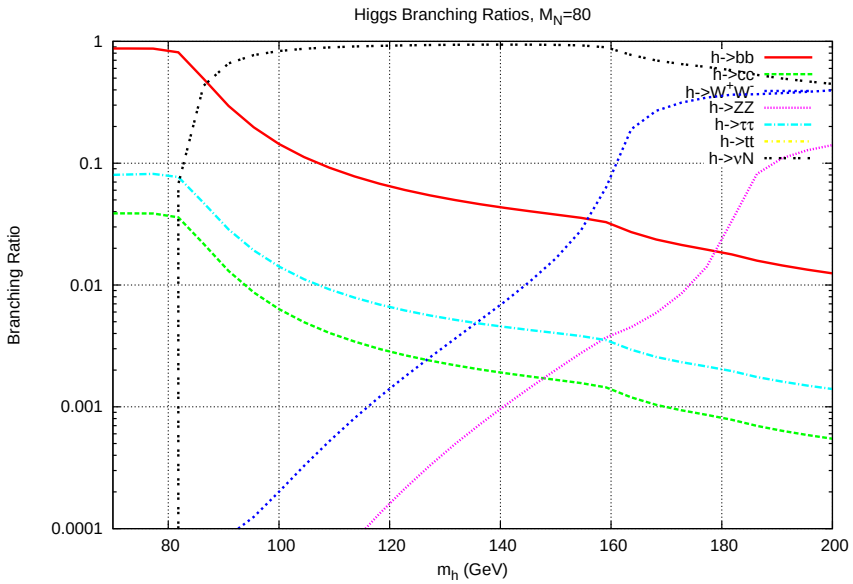

Figure 8.1: Branching ratios of $h \to 2x$ with $f^{1\nu} + f^{2\nu} = 1$.

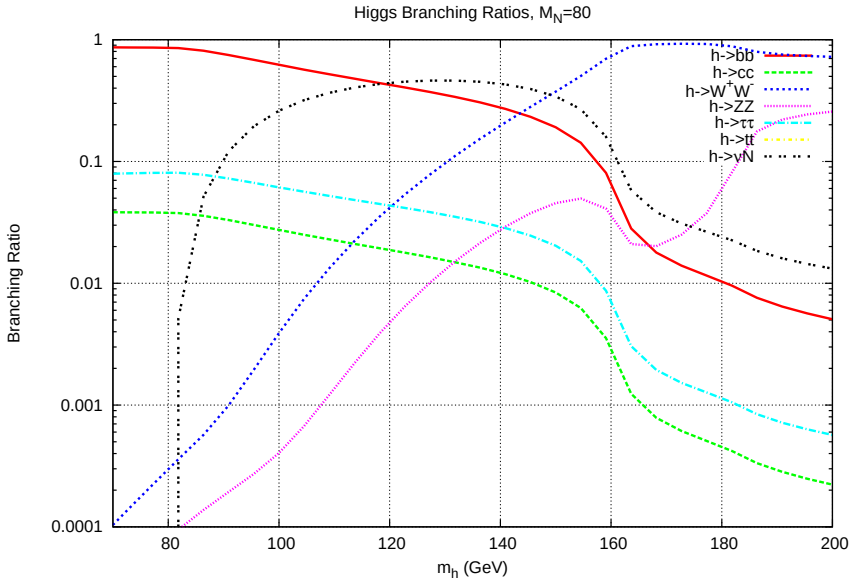

Figure 8.2: Branching ratios of $h \to 2x$ with $f^{1\nu} + f^{2\nu} = \frac{1}{14}$

mode, and is larger than the usually dominant WW mode, even beyond the WW threshold. Thus in this model, the SM Higgs decay mode is greatly altered. A second plot is shown for Yukawa couplings summing to 1/14 in Fig. 8.2.

At Hadron colliders, the SM model Higgs is dominantly produced via gluon fusion

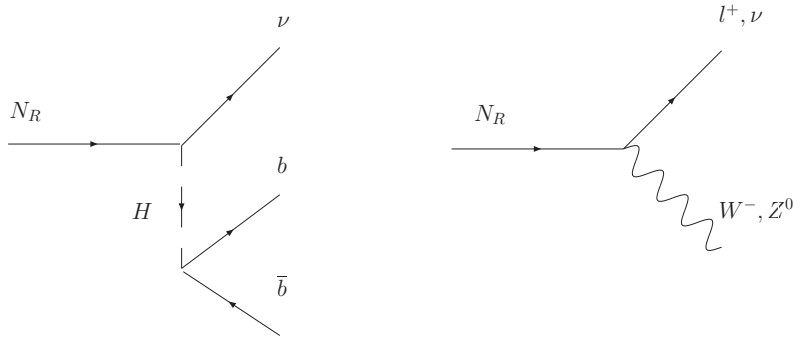

Figure 8.3: Two of the allow decay modes of N_R

with a top quark in the loop. In this model, because of the mixing of H with H_1 and H_2, the lightest mass neutral scalar Higgs decays dominantly as $h \to \nu N_R$. The final state signal will depend on the decay modes of N_R. Two of the allowed decay modes of N_R are shown in Fig. 8.3. The 3-body decay mode $N_R \to \nu\bar{b}b$ is completely dominant over the 2-body decay mode lW or νZ. This is because the 2-body decay is suppressed by the tiny mixing angle $\theta \sim 10^{-6}$ or smaller. Thus the final state signals for the Higgs bosons at the LHC are $\overline{\nu}\nu\bar{b}b$. Collider signals will include large missing energy and 2 hard b-jets.

Using MadGraph, we generated events for $pp \to \overline{\nu}\nu\bar{b}b$ in the SM for LHC (at 7 TeV and 14 TeV) and Tevatron. Using the cuts $\not{E}_T > 30$ GeV and $p_T^b > 20$ GeV for each b-jet, we find the cross section to be ~ 13 pb for the LHC at 14 TeV. This provides a reasonable estimate of the background. The cross section for Higgs production at the LHC at 14 TeV is $\sim$ 50 pb for a 120 GeV Higgs. The branching ratios for a large mass range of the Higgs boson in our model are dominated by $\text{BR}(h \to \nu N_R) \sim 100\%$. Thus prior to any cuts on the signal, this mode is observable at the LHC, and stands out over the SM background. A summary for different energies is given in Table 8.3. The Higgs production at the Tevatron is taken from

Table 8.3: Collider Searches for $m_h = 120$ GeV.

Collider	$\sqrt{s}$	Background	Signal
LHC	14 TeV	13 pb	50 pb
LHC	7 TeV	2.4 pb	30 pb
Tevatron	2 TeV	240 pb	1 pb

Ref. [64], and the LHC from Ref. [65].

8.2.3 $ZH \to \nu\bar{\nu}b\bar{b}$ search at Tevatron

The D0 Collaboration at the Tevatron has searched for the SM Higgs boson in the $ZH \to \nu\bar{\nu}b\bar{b}$ channel using 5.2 fb^{-1} of data [66]. With both b's being tagged and a $\not{E}_T > 40$ GeV and $p_T > 20$ GeV for the b-jets, they expect about 5 events for the ZH mode. However there is a large SM background arising mainly from W+jets, Z+jets, and $t\bar{t}$. The estimated background with these cuts is about 538 ± 93 events, while they observe 514 events. Thus the SM signal from ZH production for this $\nu\bar{\nu}b\bar{b}$ mode is not observable with the current Tevatron data. However in our model, depending on BR($h \to \nu N_R$), this signal is much larger and may be observable, especially as luminosity accumulates in the coming year. Other possibilities for our model are that the RH neutrinos could decay via a charged Higgs.

8.2.4 N_R decays via charged Higgs

For a sufficiently light $m_{H^\pm} < 250$ GeV, the decay $N_R \to \nu_\tau \tau^+ \tau^-$ via a charged Higgs becomes important (see Fig. 8.4). Taking the Yukawa couplings to be order one, and the mixing to be maximal between the three Higgs doublets, the decay rates for the N_R decays are shown in Table 8.4. Taking the tau $p_T > 20$ GeV and $\not{E}_T > 30$ GeV, the cross section for $p\bar{p} \to \nu\bar{\nu}\tau^+\tau^-$ at the Tevatron is 45 fb (123 pb at the LHC for 7 TeV collisions). This background is much smaller than the $pp \to \bar{b}b\nu\bar{\nu}$ background,

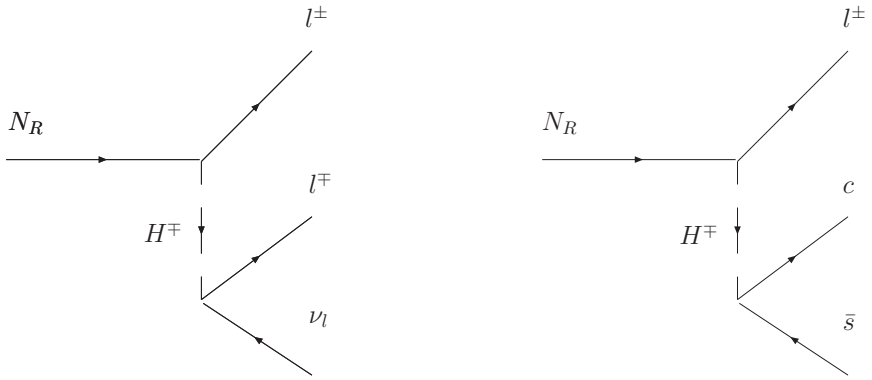

Figure 8.4: Decay modes of N_R through a charged Higgs $H^{\pm}$.

Table 8.4: Decay Rates of N_R for $M_N = 80$ GeV, $M_h = 120$ GeV.

Decay Mode	$\Gamma(N_R \to 3x)$ (GeV)	$m_{H^{\pm}}$ (GeV)	BR
$N_R \to \nu b\bar{b}$	1.56×10^{-9}	200	43.8%
$N_R \to \nu_\tau \tau^+ \tau^-$	1.32×10^{-9}	200	37.0%
$N_R \to \tau c\bar{s}$ (or $\bar{c}s$)	5.80×10^{-10}	200	16.3%
$N_R \to \nu c\bar{c}$	6.60×10^{-11}	200	1.85%
$N_R \to \nu_\mu \mu^+ \mu^-$	4.00×10^{-11}	200	1.12%
$N_R \to \nu b\bar{b}$	1.56×10^{-9}	250	63.6%
$N_R \to \nu_\tau \tau^+ \tau^-$	5.62×10^{-10}	250	22.9%
$N_R \to \tau^- c\bar{s}$ (or $\tau^+ \bar{c}s$)	2.26×10^{-10}	250	9.21%
$N_R \to \nu c\bar{c}$	6.60×10^{-11}	250	2.69%
$N_R \to \nu_\mu \mu^+ \mu^-$	2.45×10^{-11}	250	1.65%

as it is a leptonic (not QCD) process. This signature, two high p_T taus plus missing energy, may be easier to see.

8.3 Chapter summary

We have proposed a new approach for understanding of the tininess of the light neutrino masses. We extend the SM gauge symmetry by a discrete Z_2 symmetry, and

the particle content by adding three right handed neutrinos and two additional Higgs doublets. These new Higgs doublets couple only to the neutrinos. The tiny neutrino masses are generated via the see-saw mechanism with the right handed neutrino mass matrix at the EW scale, and the Dirac neutrino mass matrix at the 10^{-4} GeV scale. The Dirac neutrino mass matrix gets contributions from the two new EW Higgs doublets with vevs at the EW scale. The Yukawa couplings are of order one, and the two EW contributions are fine-tuned to create the Dirac neutrino mass matrix at the 10^{-4} GeV level. The model links neutrino physics to collider physics at the TeV scale. The SM Higgs decays are drastically altered. For a wide range of the Higgs mass, it decays dominantly to $\nu_L N_R$ giving rise to the final state $\bar{\nu}\nu\bar{b}b$, or $\bar{\nu}\nu\tau^+\tau^-$. This can be tested at the LHC and possibly at the Tevatron.

BIBLIOGRAPHY

[1] S. Weinberg, Phys. Rev. Lett. **19**, 1264 (1967).

[2] A. Salam, in *Proceedings of 8th Nobel Symposium, Lerum, Sweden, 19-25 May 1968*, pp 367-377.

[3] B. N. Grossmann, Z. Murdock and S. Nandi, arXiv:1011.5256 [hep-ph].

[4] B. N. Grossmann, B. McElrath, S. Nandi and S. K. Rai, Phys. Rev. D **82**, 055021 (2010) [arXiv:1006.5019 [hep-ph]].

[5] B. N. Grossmann, Z. Murdock and S. Nandi, Phys. Lett. B **693**, 274 (2010) [arXiv:1005.4953 [hep-ph]].

[6] N. Arkani-Hamed, S. Dimopoulos and G. R. Dvali, Phys. Lett. B **429**, 263 (1998) [arXiv:hep-ph/9803315].

[7] I. Antoniadis, N. Arkani-Hamed, S. Dimopoulos and G. R. Dvali, Phys. Lett. B **436**, 257 (1998) [arXiv:hep-ph/9804398].

[8] Z. Bern, T. Dennen, Y. t. Huang and M. Kiermaier, Phys. Rev. D **82**, 065003 (2010) [arXiv:1004.0693 [hep-th]].

[9] H. Davoudiasl, R. Kitano, T. Li and H. Murayama, Phys. Lett. B **609**, 117 (2005) [arXiv:hep-ph/0405097].

[10] I. Gogoladze, Y. Mimura and S. Nandi, Phys. Lett. B **562**, 307 (2003) [arXiv:hep-ph/0302176].

[11] J. H. Heo, Phys. Rev. D **80**, 033001 (2009) [arXiv:0811.0298 [hep-ph]].

[12] P. Langacker, arXiv:0911.4294 [hep-ph].

[13] J. L. Hewett and T. G. Rizzo, Phys. Rept. **183**, 193 (1989).

[14] D. J. Muller and S. Nandi, Phys. Lett. B **383**, 345 (1996) [arXiv:hep-ph/9602390].

[15] E. Malkawi, T. M. P. Tait and C. P. Yuan, Phys. Lett. B **385**, 304 (1996) [arXiv:hep-ph/9603349].

[16] R. S. Chivukula, E. H. Simmons and J. Terning, Phys. Rev. D **53**, 5258 (1996) [arXiv:hep-ph/9506427].

[17] J. C. Pati and A. Salam, Phys. Rev. D **10**, 275 (1974) [Erratum-ibid. D **11**, 703 (1975)].

[18] T. Han, P. Langacker and B. McElrath, Phys. Rev. D **70**, 115006 (2004) [arXiv:hep-ph/0405244].

[19] B. A. Dobrescu and P. J. Fox, JHEP **0808**, 100 (2008) [arXiv:0805.0822 [hep-ph]].

[20] B. S. Balakrishna, Phys. Rev. Lett. **60**, 1602 (1988).

[21] B. S. Balakrishna, A. L. Kagan and R. N. Mohapatra, Phys. Lett. B **205**, 345 (1988).

[22] B. S. Balakrishna and R. N. Mohapatra, Phys. Lett. B **216**, 349 (1989).

[23] K. S. Babu and S. Nandi, Phys. Rev. D **62**, 033002 (2000) [arXiv:hep-ph/9907213].

[24] G. F. Giudice and O. Lebedev, Phys. Lett. B **665**, 79 (2008) [arXiv:0804.1753 [hep-ph]].

[25] J. D. Lykken, Z. Murdock and S. Nandi, Phys. Rev. D **79**, 075014 (2009) [arXiv:0812.1826 [hep-ph]].

[26] C. D. Froggatt and H. B. Nielsen, Nucl. Phys. B **147**, 277 (1979).

[27] W. M. Yao *et al.* [Particle Data Group], J. Phys. G **33**, 1 (2006).

[28] P. Langacker, Rev. Mod. Phys. **81**, 1199 (2009) [arXiv:0801.1345 [hep-ph]].

[29] S. Mrenna and J. D. Wells, Phys. Rev. D **63**, 015006 (2001) [arXiv:hep-ph/0001226].

[30] A. Melnitchouk [D0 Collaboration], Int. J. Mod. Phys. A **20**, 3305 (2005) [arXiv:hep-ex/0501067].

[31] J. A. Aguilar-Saavedra and G. C. Branco, Phys. Lett. B **495**, 347 (2000) [arXiv:hep-ph/0004190].

[32] M. Cacciari, S. Frixione, M. L. Mangano, P. Nason and G. Ridolfi, JHEP **0809**, 127 (2008) [arXiv:0804.2800 [hep-ph]].

[33] C. Amsler *et al.* [Particle Data Group], Phys. Lett. B **667**, 1 (2008).

[34] J. Pumplin, A. Belyaev, J. Huston, D. Stump and W. K. Tung, JHEP **0602**, 032 (2006) [arXiv:0512167 [hep-ph]].

[35] L. Scodellaro (CDF Collaborations and D0 Collaboration), in *Proceedings of the International Conference on High Energy Physics, Paris, 2010* (unpublished)

[36] A. Pukhov, "CalcHEP 2.3: MSSM, structure functions, event generation, batchs, and generation of matrix elements for other packages" [arXiv:hep-ph/0412191].

[37] R. Contino and G. Servant, JHEP **0806**, 026 (2008) [arXiv:0801.1679 [hep-ph]].

[38] J. A. Aguilar-Saavedra, JHEP **0911**, 030 (2009) [arXiv:0907.3155 [hep-ph]].

[39] T. Han, Z. Si, K. M. Zurek and M. J. Strassler, JHEP **0807**, 008 (2008) [arXiv:0712.2041 [hep-ph]].

[40] W. F. Chang, J. N. Ng and J. M. S. Wu, Phys. Rev. D **75**, 115016 (2007) [arXiv:hep-ph/0701254].

[41] J. Erler, P. Langacker, S. Munir and E. R. Pena, JHEP **0908**, 017 (2009) [arXiv:0906.2435 [hep-ph]].

[42] T. Aaltonen *et al.* [CDF Collaboration], Phys. Rev. Lett. **102**, 091805 (2009) [arXiv:0811.0053 [hep-ex]].

[43] T. Sjostrand, S. Mrenna and P. Z. Skands, JHEP **0605**, 026 (2006) [arXiv:hep-ph/0603175].

[44] G. Corcella *et al.*, "HERWIG 6.5 Release Note" [arXiv:hep-ph/0210213].

[45] T. Stelzer and W. F. Long, Comput. Phys. Commun. **81**, 357 (1994) [arXiv:hep-ph/9401258].

[46] H. Baer, V. Barger, A. Lessa and X. Tata, JHEP **0909**, 063 (2009) [arXiv:0907.1922 [hep-ph]].

[47] I. R. Tomalin [CMS Collaboration], J. Phys. Conf. Ser. **110**, 092033 (2008).

[48] S. N. Ahmed *et al.* [SNO Collaboration], Phys. Rev. Lett. **92**, 181301 (2004) [arXiv:nucl-ex/0309004].

[49] Q. R. Ahmad *et al.* [SNO Collaboration], Phys. Rev. Lett. **89**, 011301 (2002) [arXiv:nucl-ex/0204008].

[50] S. Fukuda *et al.* [Super-Kamiokande Collaboration], Phys. Lett. B **539**, 179 (2002) [arXiv:hep-ex/0205075].

[51] M. B. Smy *et al.* [Super-Kamiokande Collaboration], Phys. Rev. D **69**, 011104 (2004) [arXiv:hep-ex/0309011].

[52] Y. Ashie *et al.* [Super-Kamiokande Collaboration], Phys. Rev. Lett. **93**, 101801 (2004) [arXiv:hep-ex/0404034].

[53] Y. Ashie *et al.* [Super-Kamiokande Collaboration], Phys. Rev. D **71**, 112005 (2005) [arXiv:hep-ex/0501064].

[54] R. N. Mohapatra *et al.*, Rept. Prog. Phys. **70**, 1757 (2007) [arXiv:hep-ph/0510213].

[55] P. Minkowski, Phys. Lett. B **67**, 421 (1977).

[56] M. Gell-Mann, P. Ramond, and R. Slansky, Supergravity (P. van Nieuwenhuizen et al. eds.), North Holland, Amsterdam, 1980, p. 315; Print-80-0576 (CERN).

[57] T. Yanagida, in *Proceedings of the Workshop on the Unified Theory and the Baryon Number in the Universe* (O. Sawada and A. Sugamoto, eds.), KEK, Tsukuba, Japan, 13-14 Feb 1979, p. 95.

[58] S. L. Glashow, NATO Adv. Study Inst. Ser. B Phys. **59**, 687 (1980).

[59] R. N. Mohapatra and G. Senjanovic, Phys. Rev. Lett. **44**, 912 (1980).

[60] N. Arkani-Hamed and S. Dimopoulos, JHEP **0506**, 073 (2005) [arXiv:hep-th/0405159].

[61] S. Gabriel and S. Nandi, Phys. Lett. B **655**, 141 (2007) [arXiv:hep-ph/0610253].

[62] S. Gabriel, B. Mukhopadhyaya, S. Nandi and S. K. Rai, Phys. Lett. B **669**, 180 (2008) [arXiv:0804.1112 [hep-ph]].

[63] P. Achard *et al.* [L3 Collaboration], Phys. Lett. B **517**, 67 (2001) [arXiv:hep-ex/0107014].

[64] J. Baglio and A. Djouadi, JHEP **1010**, 064 (2010) [arXiv:1003.4266 [hep-ph]].

[65] F. Stockli and R. Suarez,
http://wwweth.cern.ch/HiggsCrossSections/HiggsCrossSection.html

[66] V. M. Abazov *et al.* [D0 Collaboration], Phys. Rev. Lett. **104**, 071801 (2010) [arXiv:0912.5285 [hep-ex]].

[67] S. Nandi and Z. Tavartkiladze, Phys. Lett. B **672**, 240 (2009) [arXiv:0804.1996 [hep-ph]].

[68] F. Maltoni and T. Stelzer, JHEP **0302**, 027 (2003) [arXiv:0208156 [hep-ph]].

[69] G. Bertone, D. Hooper and J. Silk, Phys. Rept. **405**, 279 (2005) [arXiv:hep-ph/0404175].

[70] T. j. Li and S. Nandi, Phys. Lett. B **617**, 112 (2005) [arXiv:hep-ph/0408160].

[71] S. Gopalakrishna, S. Jung and J. D. Wells, Phys. Rev. D **78**, 055002 (2008) [arXiv:0801.3456 [hep-ph]].

[72] V. Barger, H. E. Logan and G. Shaughnessy, Phys. Rev. D **79**, 115018 (2009) [arXiv:0902.0170 [hep-ph]].

[73] G. Bhattacharyya, G. C. Branco and S. Nandi, Phys. Rev. D **77**, 117701 (2008) [arXiv:0712.2693 [hep-ph]].

[74] M. Apollonio *et al.* [CHOOZ Collaboration], Phys. Lett. B **420**, 397 (1998) [arXiv:hep-ex/9711002].

APPENDIX A

MATRIX ELEMENT EXPANSIONS

All the expansions in this were done assuming the couplings y^u_{ij}, y^d_{ij} are symmetric and real positive numbers.

The $\overline{u}uh$-Yukawa couplings in the u-mass eigenbasis are $f^{hu'} = V_L^{u\dagger} f^{hu} V_R^u$.

$$f^{hu'}_{11} \approx \left((4n_2 - 2n_1 - 7)\alpha^{2(2n_2-n_1)} \frac{{y^u_{12}}^2}{y^u_{22}} + (7-2n_3)\alpha^{2n_3} y^u_{11} \right) \epsilon^6 \tag{A.1a}$$

$$f^{hu'}_{12} \approx 2(n_2 - n_1 - 1)\alpha^{2n_2} y^u_{12}\, \epsilon^4 + 2\alpha^{2(n_1+n_2)} y^u_{23} \left((2-n_2)\frac{y^u_{13}}{y^u_{33}} + (n_1-1)\frac{y^u_{12}y^u_{23}}{y^u_{22}y^u_{33}} \right) \epsilon^6 \tag{A.1b}$$

$$\begin{aligned} f^{hu'}_{13} \approx{}& 2\alpha^{2n_2} \left((2-n_2) y^u_{13} + (n_1-1)\frac{y^u_{12}y^u_{23}}{y^u_{22}} \right) \epsilon^4 \\ &+ 2\alpha^{2(n_1+n_2)} y^u_{23} \left((1+n_1-n_2)\frac{y^u_{12}}{y^u_{33}} + (1-n_1)\frac{y^u_{13}y^u_{23}}{y^u_{22}y^u_{33}} + (n_1-1)\frac{y^u_{12}{y^u_{23}}^2}{{y^u_{22}}^2 y^u_{33}} \right) \epsilon^6 \end{aligned} \tag{A.1c}$$

$$\begin{aligned} f^{hu'}_{22} \approx{}& (3-2n_1)\alpha^{2n_1} y^u_{22}\, \epsilon^2 + (4n_1-5)\alpha^{4n_1} \frac{{y^u_{23}}^2}{y^u_{33}}\, \epsilon^4 \\ &+ \left((6n_1-7)\alpha^{6n_1} \frac{y^u_{22}{y^u_{23}}^2}{{y^u_{33}}^2} + (7+2n_1-4n_2)\alpha^{2(2n_2-n_1)} \frac{{y^u_{12}}^2}{y^u_{22}} \right) \epsilon^6 \end{aligned} \tag{A.1d}$$

$$\begin{aligned} f^{hu'}_{23} \approx{}& 2(n_1-1)\alpha^{2n_1} y^u_{23}\, \epsilon^2 + 2(n_1-1)\alpha^{4n_1} \frac{y^u_{22}y^u_{23}}{y^u_{33}}\, \epsilon^4 \\ &+ \left(2(n_1-1)\alpha^{6n_1} y^u_{23} \frac{{y^u_{22}}^2 - 2{y^u_{23}}^2}{{y^u_{33}}^2} \right. \\ &\qquad \left. + \alpha^{2(2n_2-n_1)} \frac{y^u_{12}}{y^u_{22}} \left(2(n_2-2) y^u_{13} + (1-n_1)\frac{y^u_{12}y^u_{23}}{y^u_{22}} \right) \right) \epsilon^6 \end{aligned} \tag{A.1e}$$

$$f^{hu'}_{33} \approx y^u_{33} + (5-4n_1)\alpha^{4n_1} \frac{{y^u_{23}}^2}{y^u_{33}}\, \epsilon^4 + (7-6n_1)\alpha^{6n_1} \frac{y^u_{22}{y^u_{23}}^2}{{y^u_{33}}^2}\, \epsilon^6 \tag{A.1f}$$

The $\overline{u}us$-Yukawa couplings in the u-mass eigenbasis are $f^{su'} = V_L^{u\dagger} f^{su} V_R^u$.

$$f_{11}^{su'} \approx 2\left((n_1-2n_2)\alpha^{2(2n_2-n_1)-1}\frac{{y_{12}^u}^2}{y_{22}^u} + n_3\alpha^{2n_3-1}y_{11}^u\right)\ \epsilon^6 \tag{A.2a}$$

$$f_{12}^{su'} \approx 2(n_1-n_2)\alpha^{2n_2-1}y_{12}^u\ \epsilon^4 + 2\alpha^{2(n_1+n_2)-1}y_{23}^u\frac{n_2y_{13}^uy_{22}^u - n_1y_{12}^uy_{23}^u}{y_{22}^uy_{33}^u}\ \epsilon^6 \tag{A.2b}$$

$$\begin{aligned} f_{13}^{su'} \approx{}& 2\alpha^{2n_2-1}\frac{n_2y_{13}^uy_{22}^u - n_1y_{12}^uy_{23}^u}{y_{22}^u}\ \epsilon^4 \\ &+ 2\alpha^{2(n_1+n_2)-1}y_{23}^u\left((n_2-n_1)\frac{y_{12}^u}{y_{33}^u} + n_1\frac{y_{13}^uy_{23}^u}{y_{22}^uy_{33}^u} - n_1\frac{y_{12}^u{y_{23}^u}^2}{{y_{22}^u}^2y_{33}^u}\right)\ \epsilon^6 \end{aligned} \tag{A.2c}$$

$$\begin{aligned} f_{22}^{su'} \approx{}& 2n_1\alpha^{2n_1-1}y_{22}^u\ \epsilon^2 - 4n_1\alpha^{4n_1-1}\frac{{y_{23}^u}^2}{y_{33}^u}\ \epsilon^4 \\ &+ \left(-6n_1\alpha^{6n_1-1}\frac{y_{22}^u{y_{23}^u}^2}{{y_{33}^u}^2} + 2(2n_2-n_1)\alpha^{4n_2-2n_1-1}\frac{{y_{12}^u}^2}{y_{22}^u}\right)\ \epsilon^6 \end{aligned} \tag{A.2d}$$

$$\begin{aligned} f_{23}^{su'} \approx{}& -2n_1\alpha^{2n_1-1}y_{23}^u\ \epsilon^2 - 2n_1\alpha^{4n_1-1}\frac{y_{22}^uy_{23}^u}{y_{33}^u}\ \epsilon^4 \\ &+ \left(2n_1\alpha^{6n_1-1}y_{23}^u\frac{2{y_{23}^u}^2 - {y_{22}^u}^2}{{y_{33}^u}^2} + \alpha^{4n_2-2n_1-1}y_{12}^u\frac{n_1y_{12}^uy_{23}^u - 2n_2y_{13}^uy_{22}^u}{{y_{22}^u}^2}\right)\ \epsilon^6 \end{aligned} \tag{A.2e}$$

$$f_{33}^{su'} \approx 4n_1\alpha^{4n_1-1}\frac{{y_{23}^u}^2}{y_{33}^u}\ \epsilon^4 + 6n_1\alpha^{6n_1-1}\frac{y_{22}^u{y_{23}^u}^2}{{y_{33}^u}^2}\ \epsilon^6 \tag{A.2f}$$

The $\overline{d}dh$-Yukawa couplings in the d-mass eigenbasis are $f^{hd'} = V_L^{d\dagger} f^{hd} V_R^d$.

$$f_{11}^{hd'} \approx (7-2n_3)\alpha^{2n_3}y_{11}^d\ \epsilon^6 \tag{A.3a}$$

$$f_{12}^{hd'} \approx 2(n_3-n_2-1)\alpha^{2n_3}y_{12}^d\ \epsilon^6 \tag{A.3b}$$

$$f_{13}^{hd'} \approx 2\alpha^{2n_3}\left((2+n_1-n_3)y_{13}^d + (n_2-n_1-1)\frac{y_{12}^dy_{23}^d}{y_{22}^d}\right)\ \epsilon^6 \tag{A.3c}$$

$$f_{22}^{hd'} \approx (5-2n_2)\alpha^{2n_2}y_{22}^d\ \epsilon^4 + (4n_2-2n_1-7)\alpha^{2(2n_2-n_1)}\frac{{y_{23}^d}^2}{y_{33}^d}\ \epsilon^6 \tag{A.3d}$$

$$f_{23}^{hd'} \approx 2(n_2-n_1-1)\alpha^{2n_2}y_{23}^d\ \epsilon^4 + 2(n_2-n_1-1)\alpha^{2(2n_2-n_2)}\frac{y_{22}^dy_{23}^d}{y_{33}^d}\ \epsilon^6 \tag{A.3e}$$

$$\begin{aligned} f_{33}^{hd'} \approx{}& (3-2n_1)\alpha^{2n_1}y_{33}^d\ \epsilon^2 \\ &+ \left((7+2n_1-4n_2)\alpha^{2(2n_2-n_1)}\frac{{y_{23}^d}^2}{y_{33}^d} + (2n_1-3)\alpha^{2(6n_2-3n_1-2n_3)}\frac{{y_{22}^d}^2{y_{23}^d}^4}{{y_{13}^d}^2{y_{33}^d}^3}\right)\ \epsilon^6 \end{aligned} \tag{A.3f}$$

The $\bar{d}ds$-Yukawa couplings in the d-mass eigenbasis are $f^{sd'} = V_L^{d\dagger} f^{sd} V_R^d$.

$$f_{11}^{sd'} \approx 2n_3\alpha^{2n_3-1} y_{11}^d \ \epsilon^6 \tag{A.4a}$$

$$f_{12}^{sd'} \approx 2(n_2-n_3)\alpha^{2n_3-1} y_{12}^d \ \epsilon^6 \tag{A.4b}$$

$$f_{13}^{sd'} \approx 2\alpha^{2n_3-1}\left((n_3-n_1)y_{13}^d + (n_1-n_2)\frac{y_{12}^d y_{23}^d}{y_{22}^d}\right) \ \epsilon^6 \tag{A.4c}$$

$$f_{22}^{sd'} \approx 2n_2\alpha^{2n_2-1} y_{22}^d \ \epsilon^4 + 2(n_1-2n_2)\alpha^{4n_2-2n_1-1}\frac{{y_{23}^d}^2}{y_{33}^d} \ \epsilon^6 \tag{A.4d}$$

$$f_{23}^{sd'} \approx 2(n_1-n_2)\alpha^{2n_2-1} y_{23}^d \ \epsilon^4 + 2(n_1-n_2)\alpha^{4n_2-2n_1-1}\frac{y_{22}^d y_{23}^d}{y_{33}^d} \ \epsilon^6 \tag{A.4e}$$

$$\begin{aligned} f_{33}^{sd'} \approx{}& 2n_1\alpha^{2n_1-1} y_{33}^d \ \epsilon^2 \\ &+ 2\left((2n_2-n_1)\alpha^{4n_2-2n_1-1}\frac{{y_{23}^d}^2}{y_{33}^d} - n_1\alpha^{12n_2-6n_1-4n_3-1}\frac{{y_{22}^d}^2 {y_{23}^d}^4}{{y_{13}^d}^2 {y_{33}^d}^3}\right) \ \epsilon^6 \end{aligned} \tag{A.4f}$$

The Cabbio-Kobayashi-Maskawa matrix is $V^{\rm CKM} = V_L^{u\dagger} V_L^d$.

$$V_{11}^{\rm CKM} \approx 1 - \left(\frac{\alpha^{4(n_2-n_1)}}{2}\frac{{y_{12}^u}^2}{{y_{22}^u}^2} + \frac{\alpha^{4(n_3-n_2)}}{2}\frac{{y_{12}^d}^2}{{y_{22}^d}^2} - \alpha^{2(n_3-n_1)}\frac{y_{12}^d y_{12}^u}{y_{22}^d y_{22}^u}\right)\epsilon^4 \tag{A.5a}$$

$$\begin{aligned} V_{21}^{\rm CKM} \approx{}& \left(\alpha^{2(n_3-n_2)}\frac{y_{12}^d}{y_{22}^d} - \alpha^{2(n_2-n_1)}\frac{y_{12}^u}{y_{22}^u}\right) \ \epsilon^2 \\ &+ \left(\alpha^{2(4n_1-n_2)}{y_{23}^u}^2\frac{{y_{23}^u}^2 - {y_{22}^u}^2}{y_{12}^u {y_{33}^u}^3} - \alpha^{2n_2}\frac{y_{13}^u y_{23}^u}{y_{22}^u y_{33}^u}\right. \\ &\left. + \alpha^{2(n_3-n_1)} y_{23}^d \frac{y_{12}^d y_{23}^d - y_{13}^d y_{22}^d}{{y_{22}^d}^2 y_{33}^d} + \alpha^{4(n_3-n_2)}\frac{y_{11}^d y_{12}^d}{{y_{22}^d}^2}\right) \ \epsilon^4 \end{aligned} \tag{A.5b}$$

$$\begin{aligned} V_{31}^{\rm CKM} \approx{}& \left(\alpha^{4(2n_1-n_2)}{y_{23}^u}^2\frac{{y_{23}^u}^2 - {y_{22}^u}^2}{y_{13}^u {y_{33}^u}^3} + \alpha^{2(n_3-n_1)}\frac{y_{12}^d y_{23}^d - y_{13}^d y_{22}^d}{y_{22}^d y_{23}^d}\right. \\ &\left. - \alpha^{2(n_3-n_2+n_1)}\frac{y_{12}^d y_{23}^u}{y_{22}^d y_{33}^u}\right) \ \epsilon^4 \end{aligned} \tag{A.5c}$$

$$\begin{aligned} V_{12}^{\rm CKM} \approx{}& \left(\alpha^{2(n_2-n_1)}\frac{y_{12}^u}{y_{22}^u} - \alpha^{2(3n_2-2n_1-n_3)}\frac{y_{22}^d {y_{23}^d}^2}{y_{12}^d {y_{33}^d}^2}\right) \ \epsilon^2 \\ &+ \left(\alpha^{2n_2} y_{23}^u \frac{y_{12}^u y_{23}^u - y_{13}^u y_{22}^u}{{y_{22}^u}^2 y_{33}^u}\right. \\ &\left. + \alpha^{2(4n_2-3n_1-n_3)}{y_{23}^d}^2 \ \frac{y_{12}^d({y_{23}^d}^2 - {y_{22}^d}^2) - y_{13}^d y_{22}^d y_{23}^d}{{y_{12}^d}^2 {y_{33}^d}^3}\right) \ \epsilon^4 \end{aligned} \tag{A.5d}$$

$$V_{22}^{\rm CKM} \approx 1 - \left(\alpha^{4n_1} \frac{{y_{23}^u}^2}{2{y_{33}^u}^2} - \alpha^{2n_2} \frac{y_{23}^d y_{23}^u}{y_{33}^d y_{33}^u} + \alpha^{4(n_2-n_1)} \frac{{y_{33}^d}^2 {y_{12}^u}^2 + {y_{23}^d}^2 {y_{22}^u}^2}{2{y_{33}^d}^2 {y_{22}^u}^2} + \alpha^{4(3n_2-2n_1-n_3)} \frac{{y_{22}^d}^2 {y_{23}^d}^4}{2{y_{12}^d}^2 {y_{33}^d}^4} - \alpha^{2(4n_2-3n_1-n_3)} \frac{y_{22}^d {y_{23}^d}^2 y_{12}^u}{y_{12}^d {y_{33}^d}^2 y_{22}^u} \right) \epsilon^4 \tag{A.5e}$$

$$V_{32}^{\rm CKM} \approx \left(\alpha^{2(n_2-n_1)} \frac{y_{23}^d}{y_{33}^d} - \alpha^{2n_1} \frac{y_{23}^u}{y_{33}^u} \right) \epsilon^2 + \left(\alpha^{4(n_2-n_1)} \frac{y_{22}^d y_{23}^d}{{y_{33}^d}^2} - \alpha^{4n_1} \frac{y_{22}^u y_{23}^u}{{y_{33}^u}^2} \right) \epsilon^4 \tag{A.5f}$$

$$V_{13}^{\rm CKM} \approx -\alpha^{2(3n_2-2n_1-n_3)} \frac{y_{22}^d {y_{23}^d}^2}{y_{13}^d {y_{33}^d}^2} \epsilon^2 + \left(\alpha^{2n_2} \frac{y_{12}^u y_{23}^u - y_{13}^u y_{22}^u}{y_{22}^u y_{33}^u} - \alpha^{4(n_2-n_1)} \frac{y_{23}^d y_{12}^u}{y_{33}^d y_{22}^u} - \alpha^{2(4n_2-3n_1-n_3)} {y_{12}^d}^2 \frac{y_{13}^d ({y_{22}^d}^2 - {y_{23}^d}^2) - y_{12}^d y_{22}^d y_{23}^d}{{y_{13}^d}^2 {y_{33}^d}^3} \right) \epsilon^4 \tag{A.5g}$$

$$V_{23}^{\rm CKM} \approx \left(\alpha^{2n_1} \frac{y_{23}^u}{y_{33}^u} - \alpha^{2(n_2-n_1)} \frac{y_{23}^d}{y_{33}^d} \right) \epsilon^2 + \left(\alpha^{4n_1} \frac{y_{22}^u y_{23}^u}{{y_{33}^u}^2} - \alpha^{4(n_2-n_1)} \frac{y_{22}^d y_{23}^d}{{y_{33}^d}^2} + \alpha^{2(4n_2-3n_1-n_3)} \frac{y_{22}^d {y_{23}^d}^2 y_{12}^u}{y_{13}^d {y_{33}^d}^2 y_{22}^u} \right) \epsilon^4 \tag{A.5h}$$

$$V_{33}^{\rm CKM} \approx 1 - \left(\alpha^{4n_1} \frac{{y_{23}^u}^2}{2{y_{33}^u}^2} - \alpha^{2n_2} \frac{y_{23}^d y_{23}^u}{y_{33}^d y_{33}^u} + \alpha^{4(n_2-n_1)} \frac{{y_{23}^d}^2}{2{y_{33}^d}^2} + \alpha^{4(3n_2-2n_1-n_3)} \frac{{y_{22}^d}^2 {y_{23}^d}^4}{2{y_{13}^d}^2 {y_{33}^d}^4} \right) \epsilon^4 \tag{A.5i}$$

APPENDIX B

TABLES OF CHARGE ASSIGNMENTS

Table B.1: Charge assignments of the heavy Q quarks for a model having an effective Lagrangian with only powers of $S^\dagger S$.

Fields	$U(1)_S$	$U(1)_F$	Fields	$U(1)_S$	$U(1)_F$	Fields	$U(1)_S$	$U(1)_F$
$Q^1_{L,R}$	3	29, 28	$Q^{13}_{L,R}$	1	23, 24	$Q^{25}_{L,R}$	-2	4, 3
$Q^2_{L,R}$	2	6, 7	$Q^{14}_{L,R}$	1	27, 26	$Q^{26}_{L,R}$	-2	18, 17
$Q^3_{L,R}$	2	16, 17	$Q^{15}_{L,R}$	0	4, 3	$Q^{27}_{L,R}$	-2	20, 19
$Q^4_{L,R}$	2	18, 19	$Q^{16}_{L,R}$	0	26, 25	$Q^{28}_{L,R}$	-2	24, 23
$Q^5_{L,R}$	2	20, 21	$Q^{17}_{L,R}$	0	30, 29	$Q^{29}_{L,R}$	-2	26, 25
$Q^6_{L,R}$	2	22, 23	$Q^{18}_{L,R}$	0	32, 31	$Q^{30}_{L,R}$	-2	28, 27
$Q^7_{L,R}$	2	28, 27	$Q^{19}_{L,R}$	-1	1, 0	$Q^{31}_{L,R}$	-3	5, 4
$Q^8_{L,R}$	1	7, 8	$Q^{20}_{L,R}$	-1	3, 2	$Q^{32}_{L,R}$	-3	7, 6
$Q^9_{L,R}$	1	9, 10	$Q^{21}_{L,R}$	-1	17, 16	$Q^{33}_{L,R}$	-3	9, 8
$Q^{10}_{L,R}$	1	11, 12	$Q^{22}_{L,R}$	-1	21, 20	$Q^{34}_{L,R}$	-3	11, 10
$Q^{11}_{L,R}$	1	13, 14	$Q^{23}_{L,R}$	-1	23, 22	$Q^{35}_{L,R}$	-3	13, 12
$Q^{12}_{L,R}$	1	15, 16	$Q^{24}_{L,R}$	-1	29, 28	$Q^{36}_{L,R}$	-3	15, 14

Table B.2: Charge assignments of the heavy U and D quarks for a model having an effective Lagrangian with only powers of $S^\dagger S$.

Fields	$U(1)_S$	$U(1)_F$	Fields	$U(1)_S$	$U(1)_F$	Fields	$U(1)_S$	$U(1)_F$
$U^1_{L,R}$	1	1, 0	$U^7_{L,R}$	0	8, 9	$U^{13}_{L,R}$	-1	11, 10
$U^2_{L,R}$	1	3, 2	$U^8_{L,R}$	0	16, 15	$U^{14}_{L,R}$	-1	15, 14
$U^3_{L,R}$	1	5, 4	$U^9_{L,R}$	0	18, 17	$U^{15}_{L,R}$	-2	4, 5
$U^4_{L,R}$	1	7, 6	$U^{10}_{L,R}$	0	22, 21	$U^{16}_{L,R}$	-2	6, 7
$U^5_{L,R}$	1	19, 18	$U^{11}_{L,R}$	0	24, 23	$U^{17}_{L,R}$	-2	12, 11
$U^6_{L,R}$	1	21, 20	$U^{12}_{L,R}$	-1	7, 8	$U^{18}_{L,R}$	-2	14, 13
$D^1_{L,R}$	3	29, 30	$D^{11}_{L,R}$	0	22, 21	$D^{21}_{L,R}$	-2	30, 31
$D^2_{L,R}$	2	6, 5	$D^{12}_{L,R}$	0	24, 23	$D^{22}_{L,R}$	-3	15, 16
$D^3_{L,R}$	2	30, 31	$D^{13}_{L,R}$	-1	7, 8	$D^{23}_{L,R}$	-3	17, 18
$D^4_{L,R}$	1	5, 4	$D^{14}_{L,R}$	-1	11, 10	$D^{24}_{L,R}$	-3	19, 20
$D^5_{L,R}$	1	19, 18	$D^{15}_{L,R}$	-1	15, 14	$D^{25}_{L,R}$	-3	21, 22
$D^6_{L,R}$	1	21, 20	$D^{16}_{L,R}$	-1	31, 32	$D^{26}_{L,R}$	-3	23, 24
$D^7_{L,R}$	1	31, 32	$D^{17}_{L,R}$	-2	4, 5	$D^{27}_{L,R}$	-3	25, 26
$D^8_{L,R}$	0	8, 9	$D^{18}_{L,R}$	-2	6, 7	$D^{28}_{L,R}$	-3	27, 28
$D^9_{L,R}$	0	16, 15	$D^{19}_{L,R}$	-2	12, 11	$D^{29}_{L,R}$	-3	29, 30
$D^{10}_{L,R}$	0	18, 17	$D^{20}_{L,R}$	-2	14, 13			

Table B.3: Charge assignments of the heavy Q, U, and D quarks for a model having an effective Lagrangian with only powers of $H^\dagger H$.

Fields	$U(1)_{F_1}$	$U(1)_{F_2}$	Fields	$U(1)_{F_1}$	$U(1)_{F_2}$	Fields	$U(1)_{F_1}$	$U(1)_{F_2}$
$Q^1_{L,R}$	5, 4	−5,−5	$Q^8_{L,R}$	1, 0	−3,−3	$Q^{15}_{L,R}$	−3,−4	−1,−1
$Q^2_{L,R}$	5, 4	3, 3	$Q^9_{L,R}$	0, 1	4, 4	$Q^{16}_{L,R}$	−3,−3	1, 0
$Q^3_{L,R}$	3, 2	−5,−5	$Q^{10}_{L,R}$	0,−1	6, 6	$Q^{17}_{L,R}$	−4,−3	6, 6
$Q^4_{L,R}$	3, 3	−1, 0	$Q^{11}_{L,R}$	−1,−1	−1,−2	$Q^{18}_{L,R}$	−4, −4	−4,−3
$Q^5_{L,R}$	3, 3	3, 4	$Q^{12}_{L,R}$	−1,−2	−5,−5	$Q^{19}_{L,R}$	−5,−5	1, 0
$Q^6_{L,R}$	2, 1	6, 6	$Q^{13}_{L,R}$	−1,−1	1, 0	$Q^{20}_{L,R}$	−6,−5	4, 4
$Q^7_{L,R}$	1, 1	1, 0	$Q^{14}_{4L,R}$	−2, −3	4, 4			
$U^1_{L,R}$	2, 3	−1,−1	$U^7_{L,R}$	−1,−1	2, 1	$U^{13}_{L,R}$	−3,−3	4, 3
$U^2_{L,R}$	0, 1	−1,−1	$U^8_{L,R}$	−1,−1	4, 3	$U^{14}_{L,R}$	−5,−4	−2,−2
$U^3_{L,R}$	1, 1	2, 1	$U^9_{L,R}$	−1,−1	6, 5	$U^{15}_{L,R}$	−5,−4	6, 6
$U^4_{L,R}$	1, 1	4, 3	$U^{10}_{L,R}$	−2,−2	−3,−2	$U^{16}_{L,R}$	−5,−5	0,−1
$U^5_{L,R}$	−1,−1	−4,−5	$U^{11}_{L,R}$	−2,−2	−1, 0	$U^{17}_{L,R}$	−5,−5	4, 5
$U^6_{L,R}$	0,−1	−3,−3	$U^{12}_{L,R}$	−3,−3	2, 1			
$D^1_{L,R}$	3, 3	0, 1	$D^8_{L,R}$	0, 0	−1, 0	$D^{15}_{L,R}$	−3,−2	6, 6
$D^2_{L,R}$	3, 3	4, 5	$D^9_{L,R}$	1, 0	2, 0	$D^{16}_{L,R}$	−2,−3	−5,−5
$D^3_{L,R}$	3, 2	2, 2	$D^{10}_{L,R}$	−1, 0	4, 4	$D^{17}_{L,R}$	−4,−4	−5,−4
$D^4_{L,R}$	3, 2	6, 6	$D^{11}_{L,R}$	−1,−2	−2,−2	$D^{18}_{L,R}$	−3,−4	−2,−2
$D^5_{L,R}$	2, 1	−5,−5	$D^{12}_{L,R}$	−2,−2	1, 0	$D^{19}_{L,R}$	−3,−4	2, 2
$D^6_{L,R}$	1, 1	−4,−3	$D^{13}_{L,R}$	−1,−2	2, 2	$D^{20}_{L,R}$	−5,−5	2, 1
$D^7_{L,R}$	1, 1	−2,−1	$D^{14}_{L,R}$	−2,−2	5, 4			

Table B.4: Charge assignments for the heavy quark doublets Q to be used in a generalized model. The given values are for the case where all coefficients are of the form $(H^\dagger H)^n$. See Tables B.7–B.12 to make the necessary changes for the different Lagrangians.

Fields	$U(1)_{F_1}$	$U(1)_{F_2}$	Fields	$U(1)_{F_1}$	$U(1)_{F_2}$	Fields	$U(1)_{F_1}$	$U(1)_{F_2}$
$Q^1_{L,R}$	0, 0	3, 2	$Q^{22}_{L,R}$	2, 3	29, 29	$Q^{41}_{L,R}$	7, 7	18, 17
$Q^2_{L,R}$	0, 0	5, 4	$Q^{23}_{L,R}$	3, 4	2, 2	$Q^{42}_{L,R}$	7, 6	2, 2
$Q^3_{L,R}$	0, 0	9, 8	$Q^{24}_{L,R}$	3, 4	12, 12	$Q^{43}_{L,R}$	7, 6	12, 12
$Q^4_{L,R}$	0, 0	11, 10	$Q^{25}_{L,R}$	4, 5	29, 29	$Q^{44}_{L,R}$	8, 7	3, 3
$Q^5_{L,R}$	0, 0	15, 14	$Q^{26}_{L,R}$	5, 5	0, 1	$Q^{45}_{L,R}$	7, 7	4, 5
$Q^6_{L,R}$	0, 0	17, 16	$Q^{27}_{L,R}$	7, 6	0, 0	$Q^{46}_{L,R}$	7, 7	6, 7
$Q^7_{L,R}$	2, 2	1, 2	$Q^{28}_{L,R}$	9, 8	0, 0	$Q^{47}_{L,R}$	7, 7	8, 9
$Q^8_{L,R}$	2, 2	3, 4	$Q^{29}_{L,R}$	11, 10	0, 0	$Q^{48}_{L,R}$	7, 7	10, 11
$Q^9_{L,R}$	2, 2	5, 6	$Q^{20}_{L,R}$	13, 12	0, 0	$Q^{49}_{L,R}$	10, 9	3, 3
$Q^{10}_{L,R}$	2, 2	7, 8	$Q^{30}_{L,R}$	15, 14	0, 0	$Q^{50}_{L,R}$	11, 11	4, 4
$Q^{11}_{L,R}$	2, 2	9, 10	$Q^{31}_{L,R}$	15, 15	2, 1	$Q^{51}_{L,R}$	11, 11	6, 5
$Q^{12}_{L,R}$	2, 2	11, 12	$Q^{32}_{L,R}$	15, 15	4, 3	$Q^{52}_{L,R}$	13, 12	4, 4
$Q^{13}_{L,R}$	2, 2	13, 14	$Q^{33}_{L,R}$	15, 15	6, 5	$Q^{53}_{L,R}$	13, 13	6, 5
$Q^{14}_{L,R}$	2, 2	15, 16	$Q^{34}_{L,R}$	5, 5	5, 6	$Q^{54}_{L,R}$	6, 6	31, 30
$Q^{15}_{L,R}$	2, 2	17, 18	$Q^{35}_{L,R}$	5, 5	8, 7	$Q^{55}_{L,R}$	7, 7	22, 23
$Q^{16}_{L,R}$	2, 2	19, 20	$Q^{36}_{L,R}$	5, 5	14, 15	$Q^{56}_{L,R}$	7, 8	24, 24
$Q^{17}_{L,R}$	2, 2	21, 22	$Q^{37}_{L,R}$	5, 5	16, 17	$Q^{57}_{L,R}$	7, 7	26, 27
$Q^{18}_{L,R}$	2, 2	23, 24	$Q^{38}_{L,R}$	5, 5	20, 21	$Q^{58}_{L,R}$	8, 9	26, 26
$Q^{19}_{L,R}$	2, 2	25, 26	$Q^{39}_{L,R}$	5, 5	22, 23	$Q^{59}_{L,R}$	8, 7	29, 29
$Q^{20}_{L,R}$	2, 2	27, 28	$Q^{40}_{L,R}$	7, 7	16, 15	Cont. on Table B.5		

Table B.5: Charge assignments for the heavy quark doublets Q to be used in a generalized model. The given values are for the case where all coefficients are of the form $(H^\dagger H)^n$. See Tables B.7–B.12 to make the necessary changes for the different Lagrangians.

Fields	$U(1)_{F_1}$	$U(1)_{F_2}$	Fields	$U(1)_{F_1}$	$U(1)_{F_2}$	Fields	$U(1)_{F_1}$	$U(1)_{F_2}$
Cont. from Table B.4			$Q^{67}_{L,R}$	9, 9	16, 15	$Q^{75}_{L,R}$	13, 13	12, 11
$Q^{60}_{L,R}$	10, 9	29, 29	$Q^{68}_{L,R}$	9, 9	18, 17	$Q^{76}_{L,R}$	13, 13	14, 13
$Q^{61}_{L,R}$	8, 7	33, 33	$Q^{69}_{L,R}$	11, 11	12, 11	$Q^{77}_{L,R}$	13, 13	18, 17
$Q^{62}_{L,R}$	10, 9	33, 33	$Q^{70}_{L,R}$	11, 11	14, 13	$Q^{78}_{L,R}$	13, 13	20, 19
$Q^{63}_{L,R}$	7, 8	20, 20	$Q^{71}_{L,R}$	11, 11	18, 19	$Q^{79}_{L,R}$	13, 13	24, 25
$Q^{64}_{L,R}$	9, 9	20, 21	$Q^{72}_{L,R}$	11, 11	20, 21	$Q^{80}_{L,R}$	13, 13	26, 27
$Q^{65}_{L,R}$	9, 9	10, 9	$Q^{73}_{L,R}$	11, 11	24, 25	$Q^{81}_{L,R}$	13, 13	30, 31
$Q^{66}_{L,R}$	9, 9	12, 11	$Q^{74}_{L,R}$	11, 11	26, 27	$Q^{82}_{L,R}$	13, 13	32, 33

Table B.6: Charge assignments for the heavy quark singlets U, D to be used in a generalized model. The given values are for the case where all coefficients are of the form $(H^\dagger H)^n$. See Tables B.7–B.12 to make the necessary changes for the different Lagrangians.

Fields	$U(1)_{F_1}$	$U(1)_{F_2}$	Fields	$U(1)_{F_1}$	$U(1)_{F_2}$	Fields	$U(1)_{F_1}$	$U(1)_{F_2}$
$U^1_{L,R}$	0, 0	2,1	$U^{12}_{L,R}$	5, 5	17, 18	$U^{23}_{L,R}$	11, 10	33, 33
$U^2_{L,R}$	1, 2	1, 1	$U^{13}_{L,R}$	5, 5	19, 20	$U^{24}_{L,R}$	13, 12	33, 33
$U^3_{L,R}$	0, 0	6, 5	$U^{14}_{L,R}$	5, 5	23, 24	$U^{25}_{L,R}$	13, 13	7, 6
$U^4_{L,R}$	0, 0	8, 7	$U^{15}_{L,R}$	5, 5	25, 26	$U^{26}_{L,R}$	13, 13	9, 8
$U^5_{L,R}$	0, 0	12, 11	$U^{16}_{L,R}$	5, 6	27, 27	$U^{27}_{L,R}$	13, 13	11, 10
$U^6_{L,R}$	0, 0	14, 13	$U^{17}_{L,R}$	6, 6	28, 29	$U^{28}_{L,R}$	13, 13	27, 28
$U^7_{L,R}$	5, 5	3, 2	$U^{18}_{L,R}$	11, 11	7, 6	$U^{29}_{L,R}$	13, 13	29, 30
$U^8_{L,R}$	5, 5	5, 4	$U^{19}_{L,R}$	11, 11	9, 8	$U^{30}_{L,R}$	13, 13	21, 22
$U^9_{L,R}$	5, 5	9, 8	$U^{20}_{L,R}$	11, 11	11, 10	$U^{31}_{L,R}$	13, 13	23, 24
$U^{10}_{L,R}$	5, 5	11, 10	$U^{21}_{L,R}$	11, 11	15, 16			
$U^{11}_{L,R}$	5, 5	13, 14	$U^{22}_{L,R}$	11, 11	17, 18			
$D^1_{L,R}$	5, 5	12, 13	$D^{11}_{L,R}$	9, 9	21, 22	$D^{21}_{L,R}$	11, 11	21, 22
$D^2_{L,R}$	6, 7	13, 13	$D^{12}_{L,R}$	8, 9	24, 24	$D^{22}_{L,R}$	11, 11	23, 24
$D^3_{L,R}$	7, 7	14, 15	$D^{13}_{L,R}$	9, 9	25, 26	$D^{23}_{L,R}$	11, 10	29, 29
$D^4_{L,R}$	6, 6	32, 31	$D^{14}_{L,R}$	9, 9	13, 12	$D^{24}_{L,R}$	11, 11	27, 28
$D^5_{L,R}$	7, 6	33, 33	$D^{15}_{L,R}$	9, 9	15, 14	$D^{25}_{L,R}$	13, 13	15, 14
$D^6_{L,R}$	7, 7	19, 20	$D^{16}_{L,R}$	9, 9	9, 8	$D^{26}_{L,R}$	13, 13	17, 16
$D^7_{L,R}$	7, 6	27, 27	$D^{17}_{L,R}$	10, 11	8, 8	$D^{27}_{L,R}$	13, 13	21, 22
$D^8_{L,R}$	6, 6	28, 29	$D^{18}_{L,R}$	12, 13	8, 8	$D^{28}_{L,R}$	13, 13	23, 34
$D^9_{L,R}$	8, 9	18, 18	$D^{19}_{L,R}$	14, 15	8, 8			
$D^{10}_{L,R}$	8, 7	22, 22	$D^{20}_{L,R}$	15, 15	7, 6			

Table B.7: Replacements made to Tables B.4–B.6 when changing the single power coefficient $(H^\dagger H)$ to $(S^\dagger S)$. The quantum numbers for the $U(1)_{F_1}$ and $U(1)_{F_2}$ symmetries do not change.

Fields	$U(1)_S$		Fields	$U(1)_S$
$D^1_{L,R}$	0	$\rightarrow$	$Q^{83}_{L,R}$	1
$D^2_{L,R}$	0	$\rightarrow$	$Q^{84}_{L,R}$	1
$D^3_{L,R}$	0	$\rightarrow$	$Q^{85}_{L,R}$	1
$U^7_{L,R}$	0	$\rightarrow$	$Q^{86}_{L,R}$	1
$U^8_{L,R}$	0	$\rightarrow$	$Q^{87}_{L,R}$	1
$U^{18}_{L,R}$	0	$\rightarrow$	$Q^{88}_{L,R}$	1
$U^{19}_{L,R}$	0	$\rightarrow$	$Q^{89}_{L,R}$	1
$U^{20}_{L,R}$	0	$\rightarrow$	$Q^{90}_{L,R}$	1

Table B.8: Replacements made to Tables B.4–B.6 when changing the second power coefficient $(H^\dagger H)^2$ to $(H^\dagger H)(S^\dagger S)$. The quantum numbers for the $U(1)_{F_1}$ and $U(1)_{F_2}$ symmetries do not change.

Fields	$U(1)_S$		Fields	$U(1)_S$
$U^{25}_{L,R}$	0	$\to$	$Q^{91}_{L,R}$	1
$U^{26}_{L,R}$	0	$\to$	$Q^{92}_{L,R}$	1
$U^{27}_{L,R}$	0	$\to$	$Q^{93}_{L,R}$	1
$U^{14}_{L,R}$	0	$\to$	$Q^{94}_{L,R}$	1
$U^{15}_{L,R}$	0	$\to$	$Q^{95}_{L,R}$	1
$U^{16}_{L,R}$	0	$\to$	$Q^{96}_{L,R}$	1
$U^{17}_{L,R}$	0	$\to$	$Q^{97}_{L,R}$	1
$D^{21}_{L,R}$	0	$\to$	$Q^{98}_{L,R}$	1
$D^{22}_{L,R}$	0	$\to$	$Q^{99}_{L,R}$	1
$Q^{65}_{L,R}$	0	$\to$	$D^{29}_{L,R}$	1
$Q^{66}_{L,R}$	0	$\to$	$D^{30}_{L,R}$	1

Table B.9: Replacements made to Tables B.4–B.6 when changing the second power coefficient $(H^\dagger H)^2$ to $(S^\dagger S)^2$. The replacements from Table B.8 must also be made with these replacements. The quantum numbers for the $U(1)_{F_1}$ and $U(1)_{F_2}$ symmetries do not change.

Fields	$U(1)_S$		Fields	$U(1)_S$
$D^{25}_{L,R}$	0	$\rightarrow$	$Q^{100}_{L,R}$	1
$D^{26}_{L,R}$	0	$\rightarrow$	$Q^{101}_{L,R}$	1
$U^{12}_{L,R}$	0	$\rightarrow$	$Q^{102}_{L,R}$	1
$U^{13}_{L,R}$	0	$\rightarrow$	$Q^{103}_{L,R}$	1
$D^{23}_{L,R}$	0	$\rightarrow$	$Q^{104}_{L,R}$	1
$D^{24}_{L,R}$	0	$\rightarrow$	$Q^{105}_{L,R}$	1
$Q^{67}_{L,R}$	0	$\rightarrow$	$D^{31}_{L,R}$	1
$Q^{68}_{L,R}$	0	$\rightarrow$	$D^{32}_{L,R}$	1

Table B.10: Replacements made to Tables B.4–B.6 when changing the third power coefficient $(H^\dagger H)^3$ to $(H^\dagger H)^2(S^\dagger S)$. The quantum numbers for the $U(1)_{F_1}$ and $U(1)_{F_2}$ symmetries do not change.

Fields	$U(1)_S$		Fields	$U(1)_S$
$U^{1}_{L,R}$	0	$\rightarrow$	$Q^{106}_{L,R}$	1
$U^{2}_{L,R}$	0	$\rightarrow$	$Q^{107}_{L,R}$	1
$D^{4}_{L,R}$	0	$\rightarrow$	$Q^{108}_{L,R}$	1
$D^{5}_{L,R}$	0	$\rightarrow$	$Q^{109}_{L,R}$	1
$Q^{57}_{L,R}$	0	$\rightarrow$	$D^{33}_{L,R}$	1
$Q^{58}_{L,R}$	0	$\rightarrow$	$D^{34}_{L,R}$	1

Table B.11: Replacements made to Tables B.4–B.6 when changing the third power coefficient $(H^\dagger H)^3$ to $(H^\dagger H)(S^\dagger S)^2$. The replacements from Table B.10 must also be made with these replacements. The quantum numbers for the $U(1)_{F_1}$ and $U(1)_{F_2}$ symmetries do not change.

Fields	$U(1)_S$		Fields	$U(1)_S$
$U^3_{L,R}$	0	$\rightarrow$	$Q^{110}_{L,R}$	1
$U^4_{L,R}$	0	$\rightarrow$	$Q^{111}_{L,R}$	1
$U^{23}_{L,R}$	0	$\rightarrow$	$Q^{112}_{L,R}$	1
$U^{24}_{L,R}$	0	$\rightarrow$	$Q^{113}_{L,R}$	1
$Q^{55}_{L,R}$	0	$\rightarrow$	$D^{35}_{L,R}$	1
$Q^{56}_{L,R}$	0	$\rightarrow$	$D^{36}_{L,R}$	1

Table B.12: Replacements made to Tables B.4–B.6 when changing the third power coefficient $(H^\dagger H)^3$ to $(S^\dagger S)^3$. The replacements from Tables B.10 and B.11 must also be made with these replacements. The quantum numbers for the $U(1)_{F_1}$ and $U(1)_{F_2}$ symmetries do not change.

Fields	$U(1)_S$		Fields	$U(1)_S$
$U^5_{L,R}$	0	$\rightarrow$	$Q^{114}_{L,R}$	1
$U^6_{L,R}$	0	$\rightarrow$	$Q^{115}_{L,R}$	1
$U^{28}_{L,R}$	0	$\rightarrow$	$Q^{116}_{L,R}$	1
$U^{29}_{L,R}$	0	$\rightarrow$	$Q^{117}_{L,R}$	1
$Q^{63}_{L,R}$	0	$\rightarrow$	$D^{37}_{L,R}$	1
$Q^{64}_{L,R}$	0	$\rightarrow$	$D^{38}_{L,R}$	1

APPENDIX C

TABLES OF EFFECTIVE COUPLINGS

In Tables C.1–C.2, the fields are all in the mass eigenstate. The electric charge is $e = g \sin\theta_W = g' \cos\theta_W$. The charge under $U(1)_S$ for the vector-like D quark is Y_S, and the value used in calculations is $Y_S = -1$.

Table C.1: The effective coupling of the exotic D quark with the other particles in the model. The electromagnetic coupling with photon and the strong coupling with gluon is the same as any down-type quark in the SM. Couplings are of the form $K\gamma^\mu(c_V - c_A\gamma^5)$.

	K	c_V	c_A
$\bar{b}bZ_\mu$	$\dfrac{e}{12\sin 2\theta_W}$	$4\cos 2\theta_W + 3\cos 2\theta_L - 1$	$3(1+\cos 2\theta_L)$
$\overline{D}DZ_\mu$	$\dfrac{e}{12\sin 2\theta_W}$	$4\cos 2\theta_W - 3\cos 2\theta_L - 1$	$3(1-\cos 2\theta_L)$
$\bar{b}DZ_\mu$	$\dfrac{-e}{4}\dfrac{\sin 2\theta_L}{\sin 2\theta_W}$	1	1
$\bar{b}bZ'_\mu$	$\dfrac{g_S Y_S}{4}$	$\cos 2\theta_L + \cos 2\theta_R - 2$	$\cos 2\theta_L - \cos 2\theta_R$
$\overline{D}DZ'_\mu$	$\dfrac{-g_S Y_S}{4}$	$\cos 2\theta_L + \cos 2\theta_R + 2$	$\cos 2\theta_L - \cos 2\theta_R$
$\bar{b}DZ'_\mu$	$\dfrac{-g_S Y_S}{4}$	$\sin 2\theta_L + \sin 2\theta_R$	$\sin 2\theta_L - \sin 2\theta_R$
$\bar{t}b\ W^+_\mu$	$\dfrac{-e\cos\theta_L}{2\sqrt{2}\sin\theta_W}$	1	1
$\bar{t}D\ W^+_\mu$	$\dfrac{e\sin\theta_L}{2\sqrt{2}\sin\theta_W}$	1	1

Table C.2: The effective coupling of the exotic D quark with the other particles in the model. The electromagnetic coupling with photon and the strong coupling with gluon is the same as any down-type quark in the SM. Couplings are of the form $K(c_S - c_P\gamma^5)$.

	K	c_S	c_P
$\bar{b}b\phi_H$	$\frac{\cos\theta_R}{\sqrt{2}}$	$f_b \cos\vartheta \cos\theta_L + f_{Db} \sin\vartheta \sin\theta_L$	0
$\overline{D}D\phi_H$	$\frac{\sin\theta_R}{\sqrt{2}}$	$f_b \cos\vartheta \sin\theta_L - f_{Db} \sin\vartheta \cos\theta_L$	0
$\bar{b}b\phi_S$	$\frac{-\cos\theta_R}{\sqrt{2}}$	$f_b \sin\vartheta \cos\theta_L - f_{Db} \cos\vartheta \sin\theta_L$	0
$\overline{D}D\phi_S$	$\frac{-\sin\theta_R}{\sqrt{2}}$	$f_b \sin\vartheta \sin\theta_L + f_{Db} \cos\vartheta \cos\theta_L$	0
$\bar{b}D\phi_H$	$\frac{1}{2\sqrt{2}}$	$f_{Db} \sin\vartheta \cos(\theta_L + \theta_R)$ $- f_b \cos\vartheta \sin(\theta_L + \theta_R)$	$f_{Db} \sin\vartheta \cos(\theta_L - \theta_R)$ $- f_b \cos\vartheta \sin(\theta_L - \theta_R)$
$\bar{b}D\phi_S$	$\frac{1}{2\sqrt{2}}$	$f_{Db} \cos\vartheta \cos(\theta_L + \theta_R)$ $+ f_b \sin\vartheta \sin(\theta_L + \theta_R)$	$f_{Db} \cos\vartheta \cos(\theta_L - \theta_R)$ $+ f_b \sin\vartheta \sin(\theta_L - \theta_R)$

VITA

Benjamin Nathanial Grossmann

Candidate for the Degree of

Doctor of Philosophy

Dissertation: FERMION MASSES AND NEW SYMMETRIES BEYOND THE STANDARD MODEL

Major Field: Physics

Biographical:

Personal Data: Born in Windsor, Missouri, USA on December 3, 1978.

Education:

Received the B.S. degree from Montana State University, Bozeman, Montana, USA, 2003 in Physics

Completed the requirements for the degree of Doctor of Philosophy with a major in Physics at Oklahoma State University in December, 2010.

Publications:

B. N. Grossmann, B. McElrath, S. Nandi, S. K. Rai, Phys. Rev. D **82**, 055021 (2010) [arXiv:1006.5019[hep-ph]]

B. N. Grossmann, M. Murdock, S. Nandi, Phys. Rev. Lett. B **693**, 274 (2010) [arXiv:1005.4953[hep-ph]]

Awards:

2006 AAPT Outstanding Teaching Assistant Award

Name: Benjamin Nathanial Grossmann Date of Degree: December, 2010

Institution: Oklahoma State University Location: Stillwater, Oklahoma

Title of Study: FERMION MASSES AND NEW SYMMETRIES BEYOND THE STANDARD MODEL

Pages in Study: 91 Candidate for the Degree of Doctor of Philosophy

Major Field: Physics

The Standard Model (SM) lacks a satisfactory explanation for the large hierarchy of the fermion masses. The use of extra symmetries is used to create a mechanism to explain this hierarchy.

An additional local $U(1)_S$ symmetry is appended to the SM along with an electroweak singlet Higgs boson that has a vacuum expectation value at the electroweak scale. Unlike many other models, the SM fields are neutral under this extra symmetry. Using a Froggatt-Nielsen type mechanism, the mass hierarchy is explained through the interaction of the SM quarks. They do not directly interact with each other, but with additional heavy vector-like quarks that have masses at the TeV scale.

How the Higgs singlet contributes to the generation of the mass hierarchy is generalized across a set of 24 model variation. Some of the phenomenology of Higgs interactions with SM fields by Higgs decays and flavor changing neutral currents are also explored.

The direct interaction of a heavy vector-like quark with a SM quark (the bottom quark) is also examined. The signal rates of this heavy vector-like quark and the SM background are calculated for the dominant signals at the high-energy hadron colliders, multilepton and multi-b-jet final states. For a wide range of masses, the signals are above the background at the LHC.

The neutrino masses are addressed by a different symmetry. Imposing a Z_2 symmetry, the SM neutrinos have interactions with two new Higgs fields and heavy right-handed neutrinos with masses in electroweak scale. The smallness of the left-handed neutrino masses is the result of a combination of fine tuning between the two new Yukawa couplings and using the see-saw mechanism. The proposed scenario gives interesting new Higgs decay signals and can be tested at the LHC.

ADVISOR'S APPROVAL: Dr. Satyanarayan Nandi